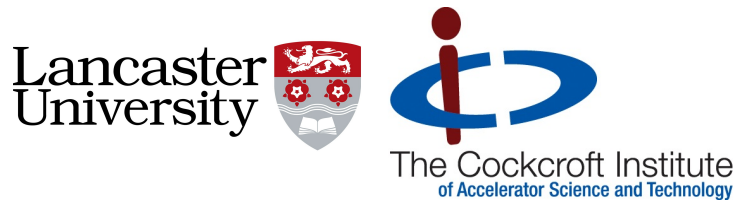


# An Exploration of the Effects of Radiation Reaction on Waves Propagating Through a Warm Plasma

Anthony Carr

MPhys Physics, Astrophysics and Cosmology (Lancaster)



Physics

Department of Physics

Lancaster University

June, 2015

A thesis submitted to Lancaster University for the degree of Doctor of  
Philosophy in the Faculty of Science and Technology

*This thesis is dedicated to my mother.*

*For her endless love, support and encouragement.*

## Acknowledgements

I would first like to thank my supervisor Dr David Burton, for all his guidance and instruction throughout the last four years. His inexhaustible enthusiasm for the subject of this thesis has been the perfect remedy for any periods of weariness I encountered. My thanks also go to the wider Department of Physics, for accommodating me for all of these years, and to all of the staff that have helped me out along the way.

I would especially like to thank the Cockcroft Institute for providing the funding to make this PhD thesis possible, as well as for their many interesting lectures on topics in accelerator physics.

I would also like to thank Dr Stephen Flood for all the helpful discussions we have had and who, on many occasions, has served as a pressure relief valve for my frustrations with the computational aspects of this thesis.

# Preface

In this thesis we consider the implications of radiation reaction for the behaviour of electric and electromagnetic waves propagating through a plasma. A plasma contains a very large number of particles, and obtaining a description of the dynamical behaviour of each individual particle is impractical. In Section 2 we detail how one can model such a plasma by treating the plasma as a fluid, and rather than examining the individual particles we instead look at the bulk properties of the fluid. Such a model is based upon the equation that describes the motion of a single particle, hence we introduce this first in Section 1.

As such, Section 1 should be viewed as an introduction to the necessary background one needs in order to understand the subsequent sections. We begin by reviewing the Lorentz force equation, from which one can determine the motion of a charged point particle in the absence of radiation reaction. Finding solutions to this equation, and plotting the particle's subsequent trajectory not only allows us to introduce notation that will be used throughout this thesis, but is also a point of comparison that can be referred back to in the subsequent sections.

The concept of radiation reaction is first introduced in Section 1.1.2, where we learn that the Lorentz Force Law does not describe the motion of a charged particle completely. It is here that we describe the origin of radiation reaction, as well as introducing the Abraham-Lorentz-Dirac (ALD) equation, the first covariant equation derived that determines the motion of a particle when the effects of radiation reaction are included. Not only is this equation of great historical significance, but it is used in the derivation of the equations of motion of Section 2.2, and hence is pivotal to the work carried out within.

It is well known that not all solutions to the ALD equation are physically reasonable. Considering the importance of the ALD equation in this thesis, it is prudent to review this property, and we do so in Section 1.1.2.

Many alternative models to the ALD equation have been proposed in an attempt to eliminate these unwanted solutions. We must also attempt to eliminate such unwanted behaviours from our solutions, and so Section 1.1.3 reviews the approach used to generate the Landau-Lifshitz (LL)

equation. We carry out a similar procedure with our equations, and so a review of the LL equation is called for.

This completes the necessary background in radiation reaction, however we still need to introduce some fundamentals of a plasma. All of the work within this thesis is carried out within the warm fluid approximation, which we detail in Section 2.2. This allows us to use a perturbative approach when seeking solutions; we assume that the solution we seek is that of the cold fluid, plus a small correction term. As such, it is necessary to first review the properties of a cold plasma. We end the introductory section with an example of where experiments are currently taking place that involve electromagnetic waves travelling through plasma.

Section 2 reviews the creation of the model we use in our description of a plasma. In Section 2.2 we build upon a recently developed kinetic model of a collection of charged point particles that incorporates radiation reaction. From this model, we proceed to generate an infinite hierarchy of moment equations that describes our system. We subsequently introduce a new closure mechanism to this model, inspired by closure mechanisms associated with the warm fluid approximation, thus obtaining a finite system of equations. Although this kinetic model has been used previously to generate a system of moment equations, the method used to close them was ad hoc, and the solutions predicted by the fluid model did not match up with that predicted by the kinetic model itself. The closure mechanism we use is a simple extension of that of the warm fluid, and needs no additional assumptions regarding the nature of the system. Additionally we show that the results it predicts are identical to those derived directly from the kinetic theory upon which it is based. Hence, the finite system of moment equations we derive is new work.

The remainder of Section 2 is focussed on using this model to determine the bulk properties of such a fluid in equilibrium – solutions which we perturb around in subsequent sections – and also represents entirely new work.

In Sections 3 and 4 we use what we have learned in the previous sections to model small amplitude electric and electromagnetic waves propagating through the plasma. We examine the dispersion relations of such waves, as well as – when possible – how such waves modify the bulk properties of the plasma. Finally, in Section 5, we turn our attention to electric waves of arbitrarily

strong amplitude. Sections 3 - 5 represent entirely new work.

Aspects of this thesis have been published in reference [1].

# Contents

<b>1 Preliminaries</b>	<b>1</b>
1.1 The Motion of a Charged Particle . . . . .	1
1.1.1 The Lorentz Force . . . . .	1
1.1.2 Introducing Radiation Reaction . . . . .	6
1.1.3 The Landau-Lifshitz Equation . . . . .	10
1.2 Plasmas . . . . .	15
1.2.1 Plasma Oscillations . . . . .	15
1.2.2 Electromagnetic Waves . . . . .	17
1.2.3 Laser-Wakefield Accelerators . . . . .	18
<b>2 The Fluid Model</b>	<b>20</b>
2.1 A Kinetic Approach . . . . .	20
2.1.1 Derivation of the Vlasov Equation . . . . .	20
2.1.2 A Modified Vlasov Equation Including Radiation Reaction . . . . .	23
2.2 A Fluid Approach . . . . .	24
2.2.1 Cold Fluid . . . . .	28
2.2.2 Warm Fluid . . . . .	29
2.3 An Examination of a Magnetised Plasma in Equilibrium . . . . .	31
<b>3 An Examination of Electric Waves</b>	<b>38</b>
3.1 In an Unmagnetised Plasma . . . . .	38
3.2 In a Magnetised Plasma . . . . .	44
<b>4 An Examination of Electromagnetic Waves</b>	<b>46</b>
4.1 R Mode . . . . .	48
4.1.1 Analysis of the Dispersion Relation . . . . .	51
4.2 L Mode . . . . .	58
4.2.1 Analysis of the Dispersion Relation . . . . .	58

4.3	O Mode . . . . .	64
4.3.1	Analysis of the Dispersion Relation . . . . .	64
4.4	X Mode . . . . .	68
4.4.1	Analysis of the Dispersion Relation . . . . .	69
4.5	A Practical Application : Neutron Star Crusts . . . . .	77
4.5.1	What is a Neutron Star? . . . . .	78
4.5.2	Our Fluid Model Applied to a Neutron Star Crust . . . . .	79
<b>5</b>	<b>Radiation Reaction and Large Amplitude Waves</b>	<b>84</b>
<b>6</b>	<b>Conclusion and Future Work</b>	<b>93</b>
<b>A</b>	<b>Derivation of the Moment Equations</b>	<b>95</b>
A.1	Generation of the 1 <sup>st</sup> Moment Equation . . . . .	95
A.2	Generation of the 2 <sup>nd</sup> Moment Equation . . . . .	97
A.3	Generation of the 3 <sup>rd</sup> Moment Equation . . . . .	97
<b>B</b>	<b>Centred Moment Expansions</b>	<b>99</b>
<b>C</b>	<b>Electromagnetic Electron Wave Dispersion Relations</b>	<b>100</b>
<b>D</b>	<b>The System of Equations Describing a Non-Linear Wave</b>	<b>102</b>

# 1 Preliminaries

## 1.1 The Motion of a Charged Particle

### 1.1.1 The Lorentz Force

In the mid to late nineteenth century, arguably one of the most fundamental laws of electromagnetism was discovered[2]; how a charged particle moves when subjected to an applied field. There is some debate as to who first derived the equation, but it has come to be known as the Lorentz Force Law; for a particle of charge  $q$  and mass  $m$  it is given by[3]

$$\ddot{x}^a = -\frac{q}{m} F^a{}_b \dot{x}^b. \quad (1)$$

In the above, and throughout this thesis, we have used the Einstein summation convention[4]; Latin indices range over 0,1,2,3 and Greek indices range over 1,2,3. Latin indices are raised and lowered using the metric tensor  $[\eta_{ab}] = \text{diag}(-1, 1, 1, 1)$  whilst Greek indices are raised and lowered using the Kronecker delta. Overdots represent differentiation with respect to proper time  $\lambda$ , and the particle's 4-velocity  $x^a$  obeys the normalisation condition

$$\dot{x}^a \dot{x}_a = -1. \quad (2)$$

Additionally,  $F_{ab}$  is the component on the  $a$ th row and  $b$ th column of the matrix representation of the electromagnetic tensor;

$$[F_{ab}] = \begin{bmatrix} 0 & E_x & E_y & E_z \\ -E_x & 0 & -B_z & B_y \\ -E_y & B_z & 0 & -B_x \\ -E_z & -B_y & B_x & 0 \end{bmatrix}. \quad (3)$$

Using the metric tensor to raise indices, it is simple to show

$$[F^a_b] = \begin{bmatrix} 0 & -E_x & -E_y & -E_z \\ -E_x & 0 & -B_z & B_y \\ -E_y & B_z & 0 & -B_x \\ -E_z & -B_y & B_x & 0 \end{bmatrix}, \quad (4)$$

and

$$[F^{ab}] = \begin{bmatrix} 0 & -E_x & -E_y & -E_z \\ E_x & 0 & -B_z & B_y \\ E_y & B_z & 0 & -B_x \\ E_z & -B_y & B_x & 0 \end{bmatrix}. \quad (5)$$

In addition to the matrix representation shown above, the electromagnetic tensor  $F$  can be expressed with use of the wedge product<sup>1</sup>. This is a product used in exterior algebra; it is associative,

$$(dx \wedge dy) \wedge dz = dx \wedge (dy \wedge dz), \quad (6)$$

distributive

$$(dx + dy) \wedge dz = dx \wedge dz + dy \wedge dz, \quad (7)$$

and anti-commutative

$$dx \wedge dy = -dy \wedge dx. \quad (8)$$

The wedge product can be used as an alternative to the matrix representation of the components

---

<sup>1</sup>For a more detailed examination of the properties of the wedge product, see reference [7].

of a rank 2 anti-symmetric tensor as follows;

$$\begin{aligned}
F &= \frac{1}{2} F_{ab} dx^a \wedge dx^b \\
&= E_x dx^0 \wedge dx^1 + E_y dx^0 \wedge dx^2 + E_z dx^0 \wedge dx^3 \\
&\quad - B_z dx^1 \wedge dx^2 - B_y dx^3 \wedge dx^1 - B_x dx^2 \wedge dx^3,
\end{aligned} \tag{9}$$

where  $x^0 = t$ ,  $x^1 = x$ ,  $x^2 = y$  and  $x^3 = z$ .

Such notation is used throughout this thesis.

Given a prescribed set of sources, one can determine the behaviour of a charged particle in any type of electromagnetic field by solving the Lorentz force equation along with Maxwell's equations<sup>2</sup>[6]

$$\partial_a F^{ab} = J^b, \tag{10}$$

$$\partial_a (\varepsilon^{abcd} F_{cd}) = 0. \tag{11}$$

In the above,  $J^a = (\rho, \mathbf{j})$  is the 4-current with  $\rho$  and  $\mathbf{j}$  the charge and current densities respectively, and  $\varepsilon^{abcd}$  is the Levi-Civita alternating symbol with  $\varepsilon_{0123} = +1$ . Additionally we have used Heaviside-Lorentz units – and will throughout this thesis – with  $c = \varepsilon_0 = \mu_0 = 1$ .

## A Solution to the Lorentz Force Equation

Consider the effect an electromagnetic plane wave propagating though vacuum has on a single electron. If we choose our coordinate system such that the  $z$ -axis lies along the direction of propagation of the wave, we can use (9) to write the electromagnetic tensor as

$$F = E_x dx^0 \wedge dx^1 - B_y dx^3 \wedge dx^1 \tag{12}$$

$$= E \cos(kz - \omega t) dt \wedge dx - B \cos(kz - \omega t) dz \wedge dx \tag{13}$$

$$= [(E dt - B dz) \cos(kz - \omega t)] \wedge dx, \tag{14}$$

---

<sup>2</sup>For the paper in which Maxwell's equations were first published, the reader is referred to [5].

where  $E$  and  $B$  are the amplitudes of the electric and magnetic fields respectively.

Before attempting to obtain the behaviour of charged particles in such a field, it is useful to first simplify (14). The frequency  $\omega$  and wavenumber  $k$  of an electromagnetic wave propagating through vacuum are related by the dispersion relation[3]

$$\omega = k. \quad (15)$$

Thus, (14) can be rewritten as

$$F = [(E dt - B dz) \cos(k(z - t))] \wedge dx \quad (16)$$

$$= [(E dt - B dz) \cos(kv)] \wedge dx, \quad (17)$$

where we have used the substitution  $v = t - z$  and the property of the cosine function  $\cos(-a) = \cos(a)$ .

Additionally, we can relate  $E$  and  $B$  with use of (10). In the absence of any sources  $J^0 = J^1 = J^2 = J^3 = 0$  and thus

$$\partial_a F^{a1} = -\partial_t E_x - \partial_z B_y \quad (18)$$

$$= -E \sin(kv) + B \sin(kv) \quad (19)$$

$$= 0 \quad (20)$$

$$\Rightarrow E = B \quad (21)$$

Thus, we are able to further simplify (17);

$$F = [(E(dt - dz)) \cos(kv)] \wedge dx \quad (22)$$

$$= [(E dv) \cos(kv)] \wedge dx \quad (23)$$

$$= E \cos(kv) dv \wedge dx. \quad (24)$$

The above motivates us to introduce the coordinates  $(u, v, x, y)$ , where  $u$  and  $v$  are related to

the Cartesian coordinates  $(t, x, y, z)$  by  $u = t + z$  and  $v = t - z$ . Note that in this coordinate system the line element takes the form

$$ds^2 = -du dv + (dx)^2 + (dy)^2. \quad (25)$$

The electromagnetic tensor is given by

$$F = E \cos(v) dv \wedge dx, \quad (26)$$

where  $E$  is the constant amplitude of the wave, and we have set  $k = 1$  for simplicity.

Substituting (26) into (1) we find

$$\ddot{v} = 0, \quad (27)$$

$$\ddot{u} = 2 \frac{q}{m} E \dot{x} \cos v, \quad (28)$$

$$\ddot{x} = \frac{q}{m} E \dot{v} \cos v, \quad (29)$$

$$\ddot{y} = 0, \quad (30)$$

and the normalisation condition (2) gives

$$-\dot{u} \dot{v} + \dot{x}^2 + \dot{y}^2 = -1, \quad (31)$$

where (25) has been used.

If we choose a frame in which the electron is at rest at the origin  $(x = 0, y = 0, z = 0)$  at  $t = 0$ , we have the initial conditions  $u = 0$ ,  $v = 0$ ,  $\dot{x} = 0$  and  $\dot{y} = 0$ . Choosing the initial values of  $\dot{u}$  and  $\dot{v}$  is less intuitive, requiring use of the normalisation condition. Rearranging (31) for  $\dot{v}$ , and choosing  $\dot{u}(0) = 1$ , sets  $\dot{v}(0) = 1$ . Then, using the transformation  $z = \frac{u-v}{2}$ , it is simple to show that a solution to the above system is

$$x(\lambda) = \frac{qE}{m} (1 - \cos(\lambda)), \quad (32)$$

$$y(\lambda) = \frac{\lambda}{2}, \quad (33)$$

$$z(\lambda) = -\frac{1}{4} \frac{q^2 E^2}{m^2} (\sin(2\lambda) - 2\lambda). \quad (34)$$

The linear term in (34) is an example of  $E \times B$  drift[6]. If we transform to a frame which moves at the velocity given by the drift term, the electron will undergo *figure of eight* motion in the  $\hat{z} - \hat{x}$  plane, as seen in Figure<sup>3</sup> 1, which was generated using Maplesoft's Maple<sup>4</sup>. We will encounter this drift term again in Section 1.1.3.

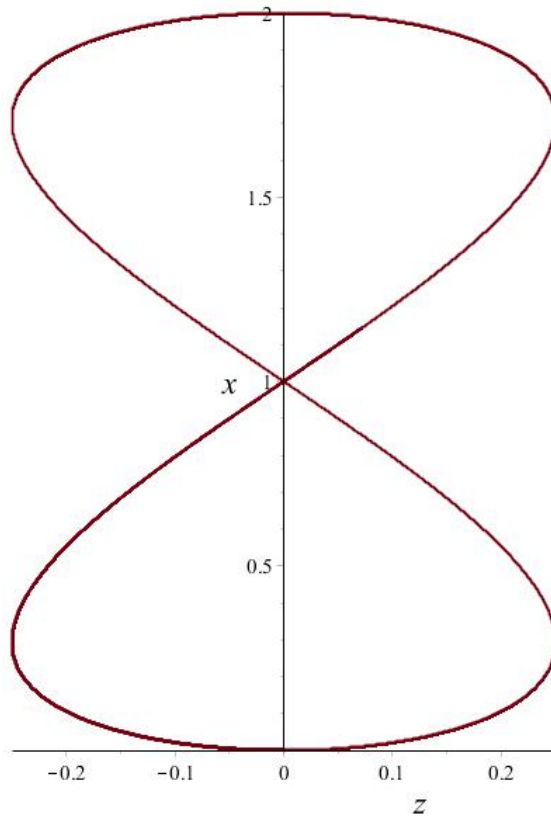


Figure 1: The trajectory of an electron in the  $\hat{z} - \hat{x}$  plane, predicted by the Lorentz force equation, under the influence of an electromagnetic wave.

---

<sup>3</sup>In order to generate the above plot we have set  $q = E = m = 1$ .

<sup>4</sup>Maple has been used extensively throughout this thesis, and has been used to generate all the plots within.

### 1.1.2 Introducing Radiation Reaction

Until the early 20th Century it was believed that (1) described the behaviour of a charged particle completely. However note that when a charged particle is accelerated it emits electromagnetic radiation[8]; this results in the particle losing some of its kinetic energy according to the Larmor formula[6]

$$\frac{dE}{dt} = \frac{q^2}{6\pi} \vec{a} \cdot \vec{a}. \quad (35)$$

Thus a charged particle will accelerate less than one would expect from (1), leading to the conclusion that there is a recoil force that acts back on the radiating particle. This force has come to be known as the *radiation reaction* force. In order to take this recoil into account, the Lorentz force equation must be modified. Such a modification was first carried out by Max Abraham in the non-relativistic regime in 1903[9] and was later generalised to the relativistic regime by Paul Dirac in 1938[10], leading to what is now known as the Abraham-Lorentz-Dirac (ALD) equation.

This phenomenon of radiation reaction is central to the work carried out within, and hence an examination of it in the context of single particle motion is useful before proceeding further.

Before we introduce the ALD equation however, it is helpful if we first introduce the characteristic time of the electron.

Consider the expression for the Coulomb field  $\mathfrak{E}$  of a point charge,

$$\mathfrak{E}(r) \propto \frac{1}{r^2}, \quad (36)$$

where  $r$  is the distance from the charge.

Such an expression becomes infinite at  $r = 0$ , which is clearly not a physical result. The reason is that it is incorrectly describing the origin of the field. In addition to neglecting quantum mechanics, it assumes that the particle is a classical point charge, when in reality such a particle must have a finite size. Suppose instead that the particle can be modelled as a spherical region of charge, with a radius determined by setting the Coulomb field of the particle equal to the rest mass of the particle, and solving for the radius  $r$ .

Carrying out this procedure for an electron, one obtains the *classical radius* of the electron; the time taken for light to cross this radius is known as the *characteristic time*  $\tau$  of the electron, where

$$\tau = \frac{q^2}{6\pi m} \approx 10^{-23} \text{ s.} \quad (37)$$

We can now introduce the ALD equation, which can be written in covariant form as

$$\ddot{x}^a = -\frac{q}{m} F^{ab} \dot{x}_b + \tau \Delta^a_b \ddot{x}^b, \quad (38)$$

where  $\Delta^a_b = \delta^a_b + \dot{x}^a \dot{x}_b$ . Note that the above contains the term  $\ddot{x}^a$ , therefore in order to find solutions we must know not only the position and velocity of the electron at one instant of time, but also its acceleration. Then the rate of change of acceleration can be found and the motion determined.

The ALD equation has some peculiar consequences[11][12] and these consequences are the primary motivation for the approximation procedure we discuss in Section 1.1.3. For this reason we will now examine these consequences in more detail.

### Runaway Solutions

Let us look at the behaviour of the charged particle in the absence of an applied field. Then (38) becomes

$$\ddot{x}^a - \tau(\ddot{x}^a + \dot{x}^a \dot{x}_b \ddot{x}^b) = 0. \quad (39)$$

Clearly, a possible solution of the above is  $\ddot{x}^a = 0$ . However this is not the only solution.

The normalisation condition demands

$$\dot{x}^a \dot{x}_a = -1, \quad (40)$$

which can be differentiated once to give

$$\dot{x}^a \ddot{x}_a = 0, \quad (41)$$

and a second time to give

$$\dot{x}^a \ddot{x}_a = -\ddot{x}^a \ddot{x}_a. \quad (42)$$

Equation (42) allows us to rewrite (39) as

$$\ddot{x}^a - \tau \left( \dot{x}^a - \dot{x}^a \ddot{x}^b \ddot{x}_b \right) = 0. \quad (43)$$

If we choose a frame in which the initial velocity  $\dot{x}^a$  and acceleration  $\ddot{x}^a$  four-vectors lie in the  $x-t$  plane, the subsequent motion must also lie in this plane. Equation (43) can then be written as

$$\ddot{t} - \frac{1}{\tau} \ddot{t} - \dot{t} (\ddot{x}^2 - \dot{t}^2) = 0, \quad (44)$$

$$\ddot{x} - \frac{1}{\tau} \ddot{x} - \dot{x} (\ddot{x}^2 - \dot{t}^2) = 0. \quad (45)$$

We can eliminate  $\ddot{t}$  from (45) with use of (40) & (41) to give

$$\ddot{x} - \frac{1}{\tau} \ddot{x} - \frac{\dot{x} \ddot{x}^2}{1 + \dot{x}^2} = 0. \quad (46)$$

Dividing (46) through by  $\ddot{x}$  and integrating with respect to proper time results in

$$\log \ddot{x} - \frac{1}{\tau} \lambda - \frac{1}{2} \log(1 + \dot{x}^2) = C, \quad (47)$$

where  $C$  is a constant of integration. If we choose  $C = \log \tau$ , the above simplifies to

$$\frac{\ddot{x}}{\sqrt{1 + \dot{x}^2}} = \frac{1}{\tau} e^{\lambda/\tau}, \quad (48)$$

which can be integrated again to find the solution

$$\dot{x} = \sinh \left( e^{\lambda/\tau} + C' \right), \quad (49)$$

where  $C'$  is another constant of integration.

Note that as  $\lambda \rightarrow -\infty$  the velocity tends to a constant value  $\dot{x} = \sinh(C')$ , however as  $\lambda$  increases

from  $-\infty$  the velocity steadily increases, despite there being no applied force. This phenomenon is known as a runaway solution.

### Acausal Solutions

Methods exist to eliminate runaway solutions, however they are usually replaced by solutions that exhibit another strange behaviour.

For the sake of simplicity, let us look at the above behaviour of an electron moving slowly compared to the velocity of light<sup>5</sup>. The motion of this electron is then governed by the non-relativistic version[9] of (38);

$$F(\mathbf{x}, t) = m \ddot{\mathbf{x}} - m \tau \dddot{\mathbf{x}}, \quad (50)$$

where  $\mathbf{x} = (x^1, x^2, x^3)$  and  $\dot{\mathbf{x}} = \frac{d\mathbf{x}}{dt}$ .

Additionally, let us constrain this particle to move in only one dimension, along the  $x^1 = x$  axis, and let it be acted upon by a force which is a function only of time  $t$ . Equation (50) then reduces to

$$F(t) = m \ddot{x} - m \tau \dddot{x}. \quad (51)$$

The above is a third order differential equation for  $x$ , but is first order for  $\ddot{x}$ . Setting  $\ddot{x} = a$  and  $\mathfrak{F}(t) = \frac{F(t)}{m}$ , (51) becomes

$$a - \tau \dot{a} = \mathfrak{F}(t), \quad (52)$$

the general solution to which is

$$a(t) = \mathbf{a} e^{\frac{t}{\tau}} + \frac{1}{\tau} \int_t^{\infty} e^{(t-t')/\tau} \mathfrak{F}(t') dt', \quad (53)$$

where  $\mathbf{a}$  is a constant. From inspection of (53), we see that the acceleration blows up as  $t \rightarrow \infty$ ; this is a runaway solution as we discussed above. Note however that you can prevent this by setting  $\mathbf{a} = 0$ . However, now the acceleration at time  $t$  depends on the force at times  $t' > t$ . The future

---

<sup>5</sup>The reader is referred to reference [13] for an examination of runaway solutions in the relativistic regime.

values of the force affect the present behaviour of the electron. This is known as pre-acceleration<sup>6</sup>.

### 1.1.3 The Landau-Lifshitz Equation

As we have seen in Section 1.1.2, the ALD equation admits solutions which appear physically unreasonable. This has led to a plethora of models including the Eliezer-Ford-O'Connell[14][15][16][17], Mo-Papas[18], Bonnor[19] and Sokolov[20] equations<sup>7</sup>. Here we look at the model proposed by Landau and Lifshitz[22]; it is used extensively in the literature and we will obtain a generalisation of this approach in the context of fluid theory in Section 2. Moreover, it has been strongly argued that the solutions to the Landau-Lifshitz equation are *the* correct subset of approximate solutions to the ALD equation, from both physical and mathematical perspectives[23].

We begin with the ALD equation,

$$\ddot{x}^a = -\frac{q}{m}F^{ab}\dot{x}_b + \tau\Delta_b^a\ddot{x}^b, \quad (54)$$

and note that  $\ddot{x}^b$  can be rewritten as  $\frac{d\dot{x}^b}{d\lambda}$ , with  $\dot{x}^b$  appearing on the left-hand side of (54). This allows us to carry out a process of iteration, whereby we can substitute (54) into itself, as follows;

$$\ddot{x}^a = -\frac{q}{m}F^{ab}\dot{x}_b + \tau\Delta_b^a\frac{d}{d\lambda}\left(-\frac{q}{m}F^{bc}\dot{x}_c\right) + \mathcal{O}(\tau^2) \quad (55)$$

$$= -\frac{q}{m}F^{ab}\dot{x}_b - \frac{q}{m}\tau\Delta_b^a\left(\frac{\partial F^{bc}}{\partial x^l}\dot{x}_c\dot{x}^l + F^{bc}\ddot{x}_c\right) + \mathcal{O}(\tau^2) \quad (56)$$

$$= -\frac{q}{m}F^{ab}\dot{x}_b - \frac{q}{m}\tau\Delta_b^a\left(\frac{\partial F^{bc}}{\partial x^l}\dot{x}_c\dot{x}^l - \frac{q}{m}F^{bc}F_{cd}\dot{x}^d\right) + \mathcal{O}(\tau^2), \quad (57)$$

where (57) is obtained by substituting (54) into (56).

If we next assume that the recoil force is small in comparison to the Lorentz force due to the applied field, we can discard terms  $\mathcal{O}(\tau^2)$  in (57) while still keeping a high level of accuracy, thus

---

<sup>6</sup>This effect is sometimes said to be *controlled*, because the exponential  $e^{(t-t')/\tau}$  rapidly decreases for times greater than  $\tau$  into the future.

<sup>7</sup>An interesting review of these approaches can be found in Reference [21].

eliminating the  $\ddot{x}^b$  term from the equation;

$$\ddot{x}^a = -\frac{q}{m} F^{ab} \dot{x}_b - \frac{q}{m} \tau \Delta^a_b \left( \frac{\partial F^{bc}}{\partial x^l} \dot{x}_c \dot{x}^l - \frac{q}{m} F^{bc} F_{cd} \dot{x}^d \right). \quad (58)$$

The above is known as the Landau-Lifshitz equation and is free of the pathologies<sup>8</sup> one finds in the ALD equation. We will now use this equation to model the behaviour of an electron in a plane electromagnetic wave.

### A Solution to Landau Lifshitz

In order to be able to compare the resulting motion to that calculated in Section 1.1.1, let us again choose a wave of the form

$$F = E \cos(v) dv \wedge dx. \quad (59)$$

Substituting (59) into (58) one can obtain the following equations of motion

$$\ddot{u} = \frac{qE}{m} \left\{ 2\dot{x} \cos(v) + \tau \left[ \frac{qE}{m} (1 - \dot{x}^2 - \dot{y}^2) \dot{v} \cos(v)^2 - 2\dot{x} \dot{v} \sin(v) \right] \right\}, \quad (60)$$

$$\ddot{v} = - \left( \frac{qE}{m} \right)^2 \tau \dot{v}^3 \cos(v)^2, \quad (61)$$

$$\ddot{x} = \frac{qE}{m} \left\{ \dot{v} \cos(v) - \tau \left[ \frac{qE}{m} \dot{v}^2 \dot{x} \cos(v)^2 + \dot{v}^2 \sin(v)^2 \right] \right\}, \quad (62)$$

$$\ddot{y} = - \left( \frac{qE}{m} \right)^2 \tau \dot{y} \dot{v}^2 \cos(v)^2, \quad (63)$$

as well as the normalisation condition

$$-\dot{u} \dot{v} + \dot{x}^2 + \dot{y}^2 = -1. \quad (64)$$

As before, in Section 1.1.1, we choose the electron to be initially at rest at the origin of our coordinate system, hence our initial conditions are  $u(0) = v(0) = x(0) = y(0) = \dot{x}(0) = \dot{y}(0) = 0$ .

---

<sup>8</sup>Due to the elimination of the  $\ddot{x}^b$  term.

Additionally, we once again set  $\dot{u}(0) = 1$ , and thus  $\dot{v}(0) = 1$  from (64).

One can obtain analytic solutions to the above system[24][25], however here we will analyse it numerically, and then plot the resulting solutions using Maple. Note however, that in order to compare - with use of a plot - the motion of an electron when radiation reaction is neglected, and when it is taken into account, we must artificially inflate the radiative term<sup>9</sup>. Thus in Figure 2 below, we have set  $\tau = 0.01$  s;<sup>10</sup>

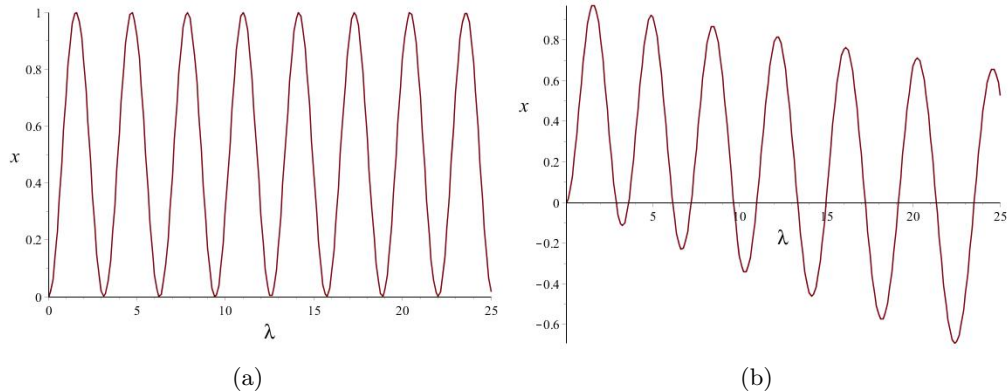


Figure 2: The motion of an electron along  $\hat{x}$  in time. Plot 2(b) includes radiation reaction while plot 2(a) neglects it.

In each case the electron is initially placed at the origin of the coordinate system, which corresponds to the maximum of the wave. Neglecting effects of radiation reaction, placing the electron at a node of the wave guarantees that there will be no net drift of the electron in the plane perpendicular to the direction of propagation of the wave. We see however that this is not so when radiation reaction is taken into account. In Figure 2(a) we see that neglecting radiation reaction the electron simply oscillates along the  $x$ -axis. However, in Figure 2(b) – which takes radiation reaction into account – we see that there is a drift along the  $x$ -axis, in addition to amplitude growth. Surprisingly however it is still possible to eliminate this additional drift by shifting the initial position of the electron slightly to the left of the node of the wave, though the amplitude growth remains.

Another strange phenomena occurs if we examine the behaviour of the electron along the  $z$

<sup>9</sup>Recall from Section 1.1.2 that  $\tau = 10^{-23}$  s, thus the effect of the radiative correction is too small to be able to see in a plot

<sup>10</sup>For simplicity we have set  $q = m = E = 1$

axis. We saw in Section 1.1.1 that if we neglect radiation reaction the electron will drift along the  $z$  axis. From (34) we see that this drift is comprised of a constant term, plus a sinusoidally varying oscillation; hence while the particle has a net velocity along  $\hat{z}$ , it has no net acceleration. However this changes when radiation reaction is taken into account; the electron will now experience a net acceleration along  $\hat{z}$ . This is shown in Figure<sup>11</sup> 3.

While the above behaviour is counterintuitive, an inspection of the results in reference [24] confirms that such behaviour is consistent with analytic solutions to the Landau-Lifshitz equation. However, the aforementioned paper does not emphasise this behaviour. More recent work[25] focusses on the Landau-Lifshitz equation only in the specific case of an electromagnetic pulse, and so – due to the short nature of the pulse – the effect is not seen as clearly as it is here.

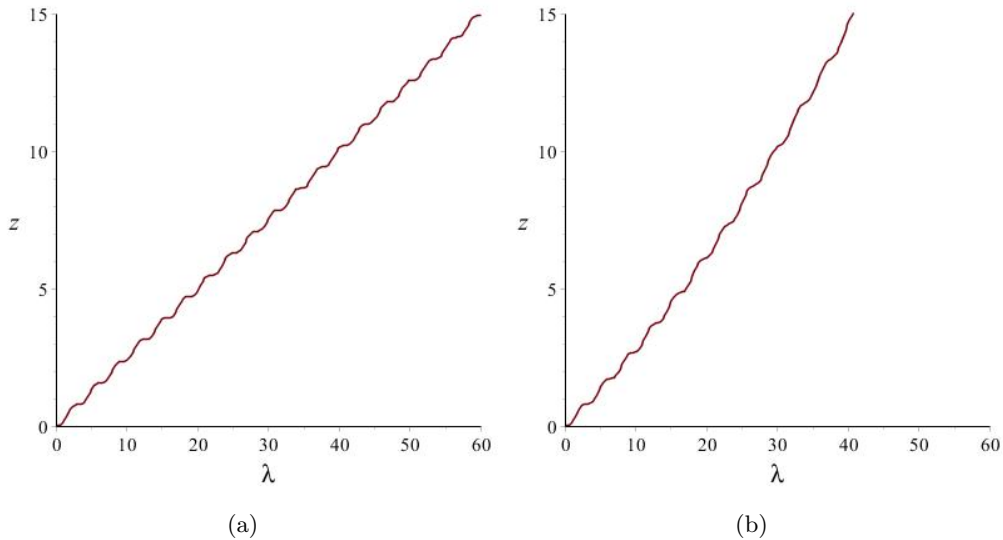


Figure 3: The motion of an electron along  $\hat{z}$  in time. Plot 3(b) includes radiation reaction while plot 3(a) neglects it.

---

<sup>11</sup>Note that we have again amplified the size of the radiative correction in order to better observe its effects

## 1.2 Plasmas

In Section 1.1 we discussed the behaviour of a single particle under the influence of an electromagnetic wave and saw some interesting results. However, direct comparison of such results with experiment is not possible, since modern laser facilities accelerate not single electrons but electron bunches containing  $\sim 10^8$  particles[26]. As such, it is unlikely radiation reaction will be detected for a single particle. A more appropriate focus then, may be on a collection of particles; such a collection can be found in plasmas. In Section 2 we look at methods of modelling such a collection of particles, by use of kinetic and fluid theories. Before we do this though, let us briefly review some properties of plasmas that we will need in order to understand the later sections.

A plasma is a gas in which the atoms have been ionised – resulting in a combination of free electrons and positive ions moving independently – and whose properties are dominated by electric and/or magnetic forces. A plasma is said to be *quasi-neutral*; overall it appears to be charge neutral, but at smaller scales one may see charged regions and electric fields. Plasmas are excellent conductors of electricity owing to the high mobility of their electrons, and hence any regions of charge that develop are quickly neutralised.

Over 99% of the visible universe is in a plasma state[27][28][29], with relativistic plasmas likely to exist in the early universe, active galactic nuclei and blackhole magnetospheres[30]. Whilst most researchers choose to ignore the radiation reaction force when studying relativistic plasmas<sup>12</sup>, this assumption may not be valid in all astrophysical phenomena. For example, acceleration of plasma by radiation pressure is a possible mechanism for the production of relativistic outflows (jets) in active galactic nuclei and galactic black hole candidates[31], and radiation reaction is expected to be significant in such extreme circumstances.

### 1.2.1 Plasma Oscillations

In this thesis, we are concerned primarily with the effect of radiation reaction on electromagnetic waves propagating through warm plasmas, but let us first review such waves when radiation reaction

---

<sup>12</sup>It is assumed small compared to the Lorentz force and so not expected to significantly contribute to the plasma dynamics.

is not taken into account.

Consider a singly ionised<sup>13</sup>, unmagnetised plasma in equilibrium. If an electron within this plasma is displaced slightly, electric fields will be generated that act in such a direction as to return the electron to its initial position, thus restoring the neutrality of the plasma. However, due to its inertia, the electron will overshoot and oscillate around its equilibrium position.

Consider a small amplitude, spatially harmonic perturbation to the equilibrium electron proper number density  $n_e$ , directed along the  $z$  axis;

$$n = n_e + \delta n, \quad (65)$$

with  $\delta n \propto \text{Re} [n_1 e^{(ik \cdot z - i\omega t)}]$  and the complex amplitude  $n_1$  a small correction term.

If one assumes the electrons of the plasma to be isothermal and that the ions are not affected by any induced potentials, one can calculate the Bohm-Gross dispersion<sup>14</sup> relation[32];

$$\omega^2 = \frac{n_e q_e^2}{m_e} + \frac{3}{2} v_{th}^2 k^2, \quad (66)$$

where  $v_{th} = \frac{2k_B T_e}{m_e}$  is the electron thermal speed<sup>15</sup>.

We can see that the group velocity  $v_g = \frac{\partial \omega}{\partial k}$  is non-zero and hence perturbations of the form (65) induce waves which propagate through the plasma. Such waves are known as Langmuir Waves, and we will explore these further in Section 3.

In a cold plasma, defined as one in which the electron's thermal speed  $v_{th} = 0$ , equation (66) reduces to

$$\omega^2 = \omega_p^2, \quad (67)$$

where

$$\omega_p^2 = \frac{n_e q_e^2}{m_e}, \quad (68)$$

is known as the plasma frequency.

---

<sup>13</sup>A plasma whose atoms are each stripped of only one electron.

<sup>14</sup>We will recover the Bohm-Gross dispersion relation later in this thesis.

<sup>15</sup>Note that the derivation of the Bohm-Gross dispersion relation assumes  $v_{th}$  to be non-relativistic.

### 1.2.2 Electromagnetic Waves

Consider an electromagnetic wave of the form

$$F = \text{Re} \left[ (E_x dt \wedge dx + E_y dt \wedge dy + E_z dt \wedge dz - B_z dx \wedge dy - B_y dz \wedge dx - B_x dy \wedge dz) e^{i(kz - \omega t)} \right], \quad (69)$$

where  $\mathbf{E} = (E_x, E_y, E_z)$  and  $\mathbf{B} = (B_x, B_y, B_z)$  are the complex amplitudes of the electric and magnetic fields respectively.

The dispersion relation of such a wave propagating through vacuum takes the form

$$\omega^2 = k^2. \quad (70)$$

Clearly waves of any frequency can propagate through vacuum, however this is not the case for waves travelling through an unmagnetised plasma. Such waves have the modified dispersion relation[32]

$$\omega^2 = \omega_p^2 + k^2. \quad (71)$$

Waves which obey dispersion relations of the form (71) exhibit a phenomenon known as cutoff. Consider a wave with frequency  $\omega$ , propagating through a plasma whose electron number density  $n_e$  gradually increases the farther inside it one travels. From (68) we see that this means that the plasma frequency  $\omega_p$  also increases. At the outer edges of the plasma  $n_e$  and  $\omega_p$  will be relatively small. However as the wave propagates farther into the plasma,  $n_e$  will increase until such time that the frequency of the wave matches the plasma frequency;  $\omega = \omega_p$ . The value of the density at this point is called the critical density  $n_c$ . From (68) and (71) we see that for  $n_e \geq n_c$ ,  $k^2 \leq 0$  and the corresponding frequencies cannot propagate. The value of the frequency at which  $n_e = n_c$  is known as the cutoff frequency  $\omega_{co}$ . Clearly in this case  $\omega_{co} = \omega_p$ , however this is not always the case when considering electromagnetic waves travelling through magnetised plasmas.

When considering a magnetised plasma, an electromagnetic wave of the form (69) has 4 possible modes, determined by the orientation of the wave relative to the plasma's magnetic field  $\mathbf{B}_0$ . Two

of the modes are parallel to the background magnetic field – the R and L modes – and two perpendicular to this field – the O and X modes. The dispersion relations for these types of waves travelling through cold plasmas are given[32] in Table 1 below:

Mode	Properties	Dispersion Relation
R	$\mathbf{k} \parallel \mathbf{B}_0$ (right circ. pol.)	$\frac{k^2}{\omega^2} = 1 - \frac{\omega_p^2/\omega^2}{1-\omega_c/\omega}$
L	$\mathbf{k} \parallel \mathbf{B}_0$ (left circ. pol.)	$\frac{k^2}{\omega^2} = 1 - \frac{\omega_p^2/\omega^2}{1+\omega_c/\omega}$
O	$\mathbf{k} \perp \mathbf{B}_0$ , $\mathbf{E} \parallel \mathbf{B}_0$	$\frac{k^2}{\omega^2} = 1 - \frac{\omega_p^2}{\omega^2}$
X	$\mathbf{k} \perp \mathbf{B}_0$ , $\mathbf{E} \perp \mathbf{B}_0$	$\frac{k^2}{\omega^2} = 1 - \frac{\omega_p^2}{\omega^2} \frac{\omega^2 - \omega_p^2}{\omega^2 - \omega_p^2 - \omega_c^2}$

Table 1: Dispersion relations for the four possible modes of an electromagnetic electron wave travelling through a magnetised plasma.

Note that  $\mathbf{k} = (k_x, k_y, k_z)$  is the wave vector associated with the wave. Additionally  $\omega_c = \frac{q|\mathbf{B}_0|}{m}$  is known as the cyclotron frequency<sup>16</sup>.

### 1.2.3 Laser-Wakefield Accelerators

In addition to the astrophysical phenomena we spoke of earlier, there exist a number of laboratory based relativistic plasmas in which radiation reaction may play a role in the future. One such example is a laser-wakefield accelerator[33].

At present, many particle accelerators use radio frequency cavities to accelerate charged particles to relativistic speeds. For example the Large Hadron Collider at CERN can give each proton an energy of 7 TeV[34]; this corresponds to a speed of merely 3 m/s slower than that of light. However, RF cavities can only sustain  $\sim 100$  MeV per meter of beamline[35]; beyond this the electric fields break down and may generate sufficient heat to melt parts of the accelerator. One solution to this problem is to simply build larger beamlines, but this incurs extra cost. A more cost effective

<sup>16</sup>An electron moving at a constant speed in a static, uniform magnetic field will undergo circular motion described by (1);  $\omega_c$  is the angular frequency of this motion.

solution can be to utilise laser-wakefield technology.

In a laser-wakefield accelerator[36], a single short ( $\leq 1\text{ps}$ ) ultra-high intensity ( $\geq 10^{18}\text{ W/cm}^2$ ) laser is focussed into a gas, ionising the atoms within and creating a plasma. As the laser propagates through underdense regions of the plasma, electrons are expelled from the region of the laser pulse<sup>17</sup>. This generates a plasma wave<sup>18</sup>, or *wakefield*, in the pulse's wake, that has a phase velocity approximately equal to the group velocity of the laser pulse. The component of the electric field parallel to the direction of propagation of such waves can be extremely large, and hence additional electrons can be injected into the wave, causing them to reach relativistic energies over a much shorter distance than conventional accelerators would need[37].

---

<sup>17</sup>This effect is due to the ponderomotive force associated with the laser pulse envelope[36].

<sup>18</sup>A plasma wave consists of electrons, which oscillate with frequency  $\omega \approx \omega_p$  while travelling along with the wave.

## 2 The Fluid Model

In this section we begin by discussing some of the challenges one encounters when attempting to model particle motion within plasmas. We will briefly review how one uses a kinetic approach in such models, thus motivating our need for a fluid description. Finally we will use this new fluid description to obtain information about a magnetised plasma in equilibrium.

### 2.1 A Kinetic Approach

In a plasma the electric and magnetic fields are not prescribed, but rather are determined by the position and motion of the charges themselves. This is known as a self consistent problem – one must find a set of particle trajectories and field lines such that the fields will be generated as the particles move along these trajectories and the fields will cause the particles to move along those exact trajectories. A typical plasma density is  $\sim 10^{12}$  electron-ion pairs per  $\text{cm}^3$ [32]. If one has to solve for the motion of each of these particles in the above manner, predicting the behaviour of all the particles within the plasma would take considerable computational resources. However, the majority of observed plasma behaviour can be described by a simpler model; one that neglects the identity of individual particles and takes only their statistical properties into account.

In order to introduce the methodology used in the generation of such a model, let us first review how such a model can be obtained when the effects of radiation reaction are neglected. We then move on, in Section 2.1.2, to state the form such a model takes when radiation reaction is included.

#### 2.1.1 Derivation of the Vlasov Equation

To proceed, we follow a procedure outlined in [38] and define a relativistic microscopic distribution function  $\mathcal{F}_s$  of the  $s$ th plasma species as

$$\mathcal{F}_s(\mathbf{x}, \mathbf{v}, t) = \sum_{k=1}^{N_0} \delta[\mathbf{x} - \mathbf{x}_k(t)] \delta[\mathbf{v} - \mathbf{v}_k(t)], \quad (72)$$

where  $N_0$  is the number of particles of the  $s$ th species with charge  $q_s$  and mass  $m_s$ ,  $\mathbf{x} = (x^1, x^2, x^3)$  and the relativistically covariant 4-velocity  $v^a = (\gamma, v^1, v^2, v^3) = (\gamma, \mathbf{v})$  with  $v^a v_a = -1$ .

Phase-space conservation requires that

$$\frac{d\mathcal{F}_s}{dt} = 0, \quad (73)$$

expansion of which results in the relativistic Klimontovich equation[39],

$$\frac{\partial \mathcal{F}_s}{\partial t} + \mathbf{u} \cdot \nabla \mathcal{F}_s + \frac{q_s}{m_s} (\mathbf{E}_m + \mathbf{u} \times \mathbf{B}_m) \cdot \nabla_v \mathcal{F}_s = 0, \quad (74)$$

where  $\mathbf{u} = \mathbf{v}/\gamma$  is the 3-velocity,  $\nabla_v$  is the velocity space gradient operator and  $E_m$  and  $B_m$  are the electric and magnetic fields on microscopic scales.

Additionally, the charge and current densities  $\rho$  and  $\mathbf{j}$  can be expressed in terms of the microscopic distribution function  $\mathcal{F}_s$  for each plasma species[40] as

$$\rho = \sum_s q_s \int_{\mathcal{V}} \mathcal{F}_s(\mathbf{x}, \mathbf{v}, t) d^3\mathbf{v}, \quad (75)$$

$$\mathbf{j} = \sum_s q_s \int_{\mathcal{V}} \mathbf{v} \mathcal{F}_s(\mathbf{x}, \mathbf{v}, t) \frac{d^3\mathbf{v}}{\gamma}, \quad (76)$$

where  $\int_{\mathcal{V}} \mathcal{F}_s(\mathbf{x}, \mathbf{v}, t) d^3\mathbf{v}$  is the number density  $n_s(\mathbf{x}, t)$  of plasma species  $s$ , at the point  $\mathbf{x}$  at time  $t$  whose proper velocity  $\mathbf{v}$  is in the region  $\mathcal{V}$  in velocity space.

Combined with Maxwell's equations (10,11) and the definitions of the charge and current densities (75,76), the Klimontovich equation describes the orbits of the particles within the plasma completely; however practical calculations can be troublesome. The distribution function  $\mathcal{F}_s$  is a sum of Dirac delta functions, each following the detailed trajectory of a single particle, and the electric and magnetic fields are complicated on microscopic scales. A more tractable equation can be derived from (74) by using ensemble averaging. The ensemble average distribution function

$$\hat{f}_s = \langle \mathcal{F}_s \rangle_{\text{ensemble}} \quad (77)$$

is smooth, as are the ensemble averaged electric and magnetic fields. However, since  $\mathbf{E}$  and  $\mathbf{B}$

are not statistically independent<sup>19</sup> of  $\mathcal{F}_s$  it can be difficult to extract the ensemble average of the non-linear acceleration term<sup>20</sup> in (74) and severe approximation is often required[41].

It is possible to shift these difficulties into a single operator  $C_s$ , known as the collision operator<sup>21</sup>, allowing us to write the ensemble average of the non-linear acceleration term as

$$\langle \frac{q_s}{m_s} (\mathbf{E}_m + \mathbf{u} \times \mathbf{B}_m) \cdot \nabla_v \mathcal{F}_s \rangle_{\text{ensemble}} = \frac{q_s}{m_s} (\mathbf{E} + \mathbf{u} \times \mathbf{B}) \cdot \nabla_v \hat{f}_s - C_s(\hat{f}_s), \quad (78)$$

where  $\mathbf{E}$  and  $\mathbf{B}$  are the ensemble averages of  $\mathbf{E}_m$  and  $\mathbf{B}_m$  respectively.

Equation (78) allows the ensemble average of the Klimontovich equation to be written in the form

$$\frac{\partial \hat{f}_s}{\partial t} + \mathbf{u} \cdot \nabla \hat{f}_s + \frac{q_s}{m_s} (\mathbf{E} + \mathbf{u} \times \mathbf{B}) \cdot \nabla_v \hat{f}_s = C_s(\hat{f}_s). \quad (79)$$

In general the collision operator is extremely complicated, and is very difficult to obtain and use. A primary aim of kinetic theory is to express the collision operator in terms of just  $\hat{f}_s$  and the average electric and magnetic fields. This can be a considerable undertaking however, and is outside the scope of this thesis.

However, we can eliminate this difficulty by assuming that the plasma we wish to examine – to a first approximation – is collisionless, and so we can set  $C_s = 0$ . This is not an unreasonable assertion because many high temperature plasmas are to a first approximation collisionless; for example in a stars corona the mean free path of the electrons can easily exceed the dimensions of the plasma[42].

In this approximation, (79) reduces to

$$\frac{\partial \hat{f}_s}{\partial t} + \mathbf{u} \cdot \nabla \hat{f}_s + \frac{q_s}{m_s} (\mathbf{E} + \mathbf{u} \times \mathbf{B}) \cdot \nabla_v \hat{f}_s = 0, \quad (80)$$

---

<sup>19</sup>Because they are dependent on the particle trajectories.

<sup>20</sup>The coefficient of  $\nabla_v \mathcal{F}_s$ .

<sup>21</sup>Its name originates from the fact that the most important correlations result from close encounters between particles.

which can be written covariantly as

$$\dot{x}^a \frac{\partial \hat{f}_s}{\partial x^a} + \frac{q_s}{m_s} F^{\mu b} \dot{x}_b \frac{\partial \hat{f}_s}{\partial \dot{x}^\mu} = 0. \quad (81)$$

The above is known as the Vlasov equation, and while amenable in sufficiently simple geometry it is still common to approach it from a fluid perspective when the influence of  $\hat{f}_s$  on  $\mathbf{E}$  and  $\mathbf{B}$  is included. As we shall see, this has the advantage of involving only the 3 spatial degrees of freedom instead of the 6 independent variables in the above. Additionally, many of the quantities that are accessible to experiment correspond to several of the fluid variables - it is most difficult to measure a distribution function accurately. Finally, a kinetic theory will in general contain more information than we require in order to solve for the bulk motion of the particles.

### 2.1.2 A Modified Vlasov Equation Including Radiation Reaction

In the preceding derivation we have used a distribution function of the form  $\hat{f}_s = \hat{f}_s(\mathbf{x}, \mathbf{v}, t)$ , which neglects radiation reaction. In order to take this effect into account we must use a 10 dimensional distribution function  $f_s = f_s(\mathbf{x}, \mathbf{v}, \mathbf{a}, t)$  where  $\mathbf{a} = \frac{d\mathbf{v}}{d\lambda}$ . Note that from this point forward we will represent the ions as a homogeneous background that will be included in the external source 4-current  $[J^a] = (\rho, \mathbf{j})$ . This allows us to model the plasma as a single species (electron) plasma and so we can now drop the species subscript from our distribution function.

Geometric considerations of the Vlasov equation (81) naturally lead to a Vlasov equation that incorporates radiation reaction[43]. It can be shown that

$$Lf + \frac{3}{\tau} f = 0, \quad (82)$$

where

$$\begin{aligned} L &= \dot{x}^a \frac{\partial}{\partial x^a} + a^\mu \frac{\partial}{\partial v^\mu} + \dot{a}^\mu \frac{\partial}{\partial a^\mu} \\ &= \dot{x}^a \frac{\partial}{\partial x^a} + a^\mu \frac{\partial}{\partial v^\mu} + \left[ \ddot{x}^a \ddot{x}_a v^\mu + \frac{1}{\tau} \left( a^\mu + \frac{q}{m} F^\mu_a \dot{x}^a \right) \right] \frac{\partial}{\partial a^\mu}, \end{aligned} \quad (83)$$

is the Liouville operator<sup>22</sup>.

Splitting the 4-current into contributions from the plasma electron fluid  $J_{\text{pef}}^b = qN^b$  and that from the applied fields  $J_{\text{ext}}$ , Maxwell's equations (10) & (11) become

$$\partial_a F^{ab} = qN^b + J_{\text{ext}}^b, \quad (84)$$

$$\partial_a F_{bc} + \partial_b F_{ca} + \partial_c F_{ab} = 0, \quad (85)$$

where  $\partial_a = \partial/\partial x^a$  and  $N^a$  is the number four-current of the plasma-electron fluid;

$$N^a(x) = \int \dot{x}^a f(x, \mathbf{v}, \mathbf{a}) \frac{d^3 v d^3 a}{1 + \mathbf{v}^2}. \quad (86)$$

The factor  $1/(1 + \mathbf{v}^2)$  in (86) and the second term in (82) together ensure that the number 4-current of the plasma-electron fluid is conserved, i.e.  $\partial_a N^a = 0$ .

## 2.2 A Fluid Approach

Kinetic theories, such as the one described in Section 2.1.2, are not always the most convenient tools for an analytical investigation of the collective dynamics of charged matter. Additionally, obtaining solutions to the integro-differential equations found in such systems usually requires extensive computational resources. However, macroscopic fluid theories are typically more amenable to analytical investigation and are less computationally demanding than their kinetic counterparts. Thus, we will now construct a fluid model from the kinetic description outlined in Section 2.1.2.

Let us define the *natural* moments of the 1-particle distribution  $f$  as

$$S^{a_1 \dots a_l : b_1 \dots b_n}(x) = \int \dot{x}^{a_1} \dots \dot{x}^{a_l} \ddot{x}^{b_1} \dots \ddot{x}^{b_n} f(x, \mathbf{v}, \mathbf{a}) \frac{d^3 v d^3 a}{1 + \mathbf{v}^2}. \quad (87)$$

Here we have used the notation first introduced in [43], in which the author defines a tensor  $S$  such that indices associated with four-velocity are located to the left of the colon whilst those associated with four-acceleration are located to the right of the colon – note that the sum  $l + n$  is the rank of

---

<sup>22</sup>Note that  $\dot{x}^\mu$  is obtained by rearranging the ALD equation (38) for  $\ddot{x}^a$ .

the tensor. The symbol  $\emptyset$  is used when no index is present, as follows;

$$S^\emptyset = \int f(x, \mathbf{v}, \mathbf{a}) \frac{d^3 v d^3 a}{1 + \mathbf{v}^2}, \quad (88)$$

$$S^{a_1 \dots a_l : \emptyset}(x) = \int \dot{x}^{a_1} \dots \dot{x}^{a_l} f(x, \mathbf{v}, \mathbf{a}) \frac{d^3 v d^3 a}{1 + \mathbf{v}^2}, \quad (89)$$

$$S^{\emptyset : b_1 \dots b_n}(x) = \int \ddot{x}^{b_1} \dots \ddot{x}^{b_n} f(x, \mathbf{v}, \mathbf{a}) \frac{d^3 v d^3 a}{1 + \mathbf{v}^2}. \quad (90)$$

The above construction acts to encode the 1-particle distribution function  $f$  using a subset of its velocity and acceleration moments, and so by construction a fluid theory will have less information than is contained in the kinetic description upon which it is based. However, in practice  $f$  will usually contain more information than is needed, and as we shall see in the rest of this thesis, we are still able to obtain a large amount of information about the bulk properties of the plasma, as well as the behaviour of electromagnetic waves which propagate through it.

Whilst some of the natural moments may be difficult to interpret from a physical standpoint, a few have an immediate physical interpretation. The number 4-current  $N^a = S^{a:\emptyset}$  and the stress-energy-momentum tensor of the plasma-electron fluid  $T^{ab} = m S^{ab:\emptyset}$ . The energy flux density is  $Q^{abc} = \frac{1}{2} m S^{abc:\emptyset}$ . Additionally the scalar field  $S^\emptyset$  is the relativistic enthalpy.

We may now cast the Vlasov equation as an infinite hierarchy of tensor equations<sup>23</sup>:

$$\partial_a S^{a:\emptyset} = 0, \quad (91)$$

$$\partial_a S^{ab:\emptyset} - S^{\emptyset:b} = 0, \quad (92)$$

$$\partial_a S^{a:b} - S^{b:c} - \frac{1}{\tau} \left( S^{\emptyset:b} + \frac{q}{m} F_c^b S^{c:\emptyset} \right) = 0, \quad (93)$$

$$\partial_a S^{abc:\emptyset} - S^{b:c} - S^{c:b} = 0, \quad (94)$$

$$\partial_a S^{ab:c} - S^{\emptyset:bc} - S^{bc:d} - \frac{1}{\tau} \left( S^{b:c} + \frac{q}{m} F_d^c S^{bd:\emptyset} \right) = 0, \quad (95)$$

---

<sup>23</sup>See Appendix A for a complete derivation of these equations.

$$\partial_a S^{a:bc} - S^{b:cd}{}_d - \frac{1}{\tau} \left( 2 S^{\emptyset:bc} + \frac{q}{m} F_d^b S^{d:c} + \frac{q}{m} F_d^c S^{d:b} \right) = 0, \quad (96)$$

$$\dots\dots\dots \quad (97)$$

The dots represent those equations whose derivative term  $\partial_{a_1} S^{a_1 \dots a_l : b_1 \dots b_n}$  satisfies  $l + n > 3$ . The identities  $\ddot{x}^a \dot{x}_a = 0$  and  $\dot{x}^a \dot{x}_a = -1$  must be satisfied and lead to the following equations, called *constraints*;

$$S^a{}_a{}^{\emptyset} = -S^{\emptyset}, \quad (98)$$

$$S^{a:}{}_a = 0, \quad (99)$$

$$S^{ab}{}_b{}^{\emptyset} = -S^{a:\emptyset}, \quad (100)$$

$$S^a{}_a{}^{:b} = -S^{\emptyset{:b}, \quad (101)$$

$$S^{ab:}{}_a = 0, \quad (102)$$

$$S^{a:}{}_{ab} = 0, \quad (103)$$

$$\dots\dots\dots \quad (104)$$

Again, the dots represent equations containing natural moments with rank greater than 3.

Although exact, an infinite set of equations is impractical for the purposes of extracting solutions, hence a finite set must be chosen from the infinite systems (91) – (97) and (98) – (104). This can be achieved by introduction of the bulk velocity  $U^a$  and bulk acceleration  $A^a$  defined as

$$U^a = \frac{S^{a:\emptyset}}{S^{\emptyset}}, \quad (105)$$

$$A^a = \frac{S^{\emptyset:a}}{S^{\emptyset}}, \quad (106)$$

as well as the *centred* moments

$$\begin{aligned}
R^{a_1 \dots a_l : b_1 \dots b_n} &= \int (\dot{x}^{a_1} - U^{a_1}) \dots (\dot{x}^{a_l} - U^{a_l}) \\
&\quad \times (\ddot{x}^{b_1} - A^{b_1}) \dots (\ddot{x}^{b_n} - A^{b_n}) \times f \Omega,
\end{aligned} \tag{107}$$

where  $\Omega = \frac{d^3 v d^3 a}{1+v^2}$ .

We then make the assumption that all centred moments of a particular rank or greater are negligible. Choosing which rank to assume to be negligible follows from the physical requirements of the distribution  $f$ . However, the first order centred moments automatically vanish. From (105) - (107) we see that

$$\begin{aligned}
R^{a:\emptyset} &= \int (\dot{x}^a - U^a) f \Omega \\
&= \int \dot{x}^a f \Omega - U^a \int f \Omega \\
&= S^{a:\emptyset} - U^a S^\emptyset \\
&= 0,
\end{aligned} \tag{108}$$

and similarly

$$\begin{aligned}
R^{\emptyset:a} &= \int (\ddot{x}^a - A^a) f \Omega \\
&= \int \ddot{x}^a f \Omega - A^a \int f \Omega \\
&= S^{\emptyset:a} - A^a S^\emptyset \\
&= 0,
\end{aligned} \tag{109}$$

by definition<sup>24</sup>.

---

<sup>24</sup>All centred moments can be written in terms of  $U$ ,  $A$ ,  $S^\emptyset$  and higher rank natural moments. For a complete list of such expansions see Appendix B.

### 2.2.1 Cold Fluid

If we choose to set all centred moments of second rank or greater to zero, the constraints (98) and (99) reduce to

$$U^a U_a = -1, \quad (110)$$

and

$$U^a A_a = 0, \quad (111)$$

with the rest being identically satisfied. The moment equations (91) - (93) become

$$\partial_a (U^a S^\theta) = 0, \quad (112)$$

$$\partial_a (U^a U^b S^\theta) - S^\theta A^b = 0, \quad (113)$$

$$\partial_a (U^a A^b S^\theta) - U^b A^c A_c S^\theta - \frac{1}{\tau} \left( A^b S^\theta + \frac{q}{m} F^b_c U^c S^\theta \right) = 0, \quad (114)$$

respectively, and the rest are satisfied identically.

Equation (113) allows us to rewrite the bulk acceleration  $A^a$  in terms of the bulk velocity  $U^a$  as follows,

$$\begin{aligned} \partial_a (U^a U^b S^\theta) - S^\theta A^b &= \underbrace{U^b \partial_a (U^a S^\theta)}_{=0 \text{ from (112)}} + S^\theta U^a \partial_a U^b - S^\theta A^b = 0, \\ \Rightarrow A^b &= -U^a \partial_a U^b. \end{aligned} \quad (115)$$

This allows (114) to be written as

$$U^a \partial_a U^b = -\frac{q}{m} F^b_c U^c + \tau \left( U^a \partial_a (U^f \partial_f U^b) - U^b U^f \partial_f U^c U^e \partial_e U_c \right). \quad (116)$$

Now,

$$U^b U^f \partial_f U^c U^e \partial_e U_c = U^b U^a \partial_a \left( \underbrace{U^c U^f \partial_f U_c}_{=0 \text{ from (111)}} \right) - U^b U^c U^a \partial_a (U^f \partial_f U_c), \quad (117)$$

hence (116) can be written

$$U^a \partial_a U^b = -\frac{q}{m} F^b{}_c U^c + \tau \left( U^a \partial_a \left( U^f \partial_f U^b \right) + U^b U^c U^a \partial_a \left( U^f \partial_f U_c \right) \right). \quad (118)$$

Recalling equations (2) and (38) from Section 1, and comparing with the above, one realises that equation (118) is simply the ALD equation for  $U^b$ , and (110) the corresponding normalisation condition<sup>25</sup>. This is to be expected, since choosing to set all centred moments to zero imposes the condition that the electron distribution has zero spread in velocity and acceleration, and hence the plasma is said to be “cold”.

This is not the type of plasma we wish to examine in this thesis, yet neither do we wish to choose a closure system that results in a system of moment equations that is too large and impractical to solve with readily available computer hardware.

### 2.2.2 Warm Fluid

With this in mind, it can be helpful to follow, and extend, an approach analogous to that introduced by Amendt[44]. We begin by introducing a scalar field  $\epsilon = \sqrt{1 + U^a U_a}$  and hypothesize that  $R^{a_1 \dots a_l; b_1 \dots b_n} = \mathcal{O}(\epsilon^{l+n})$  with  $S^\emptyset = \mathcal{O}(\epsilon^0)$  and  $U^a = \mathcal{O}(\epsilon^0)$  and  $A^a = \mathcal{O}(\epsilon^0)$ . We then choose to set all terms  $\mathcal{O}(\epsilon^3)$  to zero.

Such an approximation corresponds to a collection of electrons whose distribution has a small but non-negligible spread about the bulk velocity and bulk acceleration, a situation known as a *warm* fluid. The total number of independent components of (91) – (96) and (98) – (103) is equal to the number of independent components of the variables  $S^\emptyset$ ,  $U^a$ ,  $A^a$ ,  $R^{ab;\emptyset}$ ,  $R^{a;b}$  and  $R^{\emptyset;ab}$ , indicating that the field equations arising from such an approximation could be solvable.

It is important to note however that it is not always possible to find solutions to the resulting field equations that also satisfy the constraints (98) – (103) with all  $\mathcal{O}(\epsilon^3)$  terms set to zero in those constraints. Instead we impose only the weaker condition[45] that (98) – (103) need only be satisfied to  $\mathcal{O}(\epsilon^3)$ , which leads to

---

<sup>25</sup>The remaining constraint (111) is trivially satisfied, by differentiating (110).

$$R^a{}_{:a}{}^{\cdot\emptyset} + S^{\emptyset} (1 + U^a U_a) = \mathcal{O}(\epsilon^3), \quad (119)$$

$$R^{a:}{}_{:a} + S^{\emptyset} U^a A_a = \mathcal{O}(\epsilon^3), \quad (120)$$

$$U^b R^a{}_{:b}{}^{\cdot\emptyset} = \mathcal{O}(\epsilon^3), \quad (121)$$

$$U^a R_a{}^{\cdot b} = \mathcal{O}(\epsilon^3), \quad (122)$$

$$U^a R^{b:}{}_{:a} + A_a R^{ab:}{}^{\cdot\emptyset} = \mathcal{O}(\epsilon^3), \quad (123)$$

$$U^a R^{\emptyset:}{}_{:ab} + A_a R^{a:}{}_{:b} = \mathcal{O}(\epsilon^3). \quad (124)$$

A warm fluid model including the radiative self force is then obtained by setting to zero all terms that are  $\mathcal{O}(\epsilon^3)$  in (91) – (96), and solutions to the resulting PDEs are sought which satisfy (119) – (124).

### 2.3 An Examination of a Magnetised Plasma in Equilibrium

In Section 1.2 we discussed some properties of unmagnetised plasmas. A magnetised plasma is one in which the ambient magnetic field  $\mathbf{B}_0$  is strong enough to significantly alter particle trajectories. Unlike unmagnetised plasmas, magnetised plasmas are anisotropic; their properties in the direction perpendicular to the field are different from those in the direction parallel to it.

In order to obtain analytic solutions to (91 - 96) we use a perturbative approach, whereby we perturb the system about its equilibrium state. Thus, it is first necessary to solve (91 - 96) for a magnetised plasma in equilibrium.

If a plasma is in equilibrium we do not expect any of its properties to vary with time, hence to model a plasma in equilibrium, set all derivatives to zero in (91-96). Then, rewriting the natural moments in terms of centred moments we find,

$$A^a S^\theta = 0, \quad (125)$$

$$U^b R^{\theta:c} + \frac{1}{\tau} \frac{q}{m} F_c^b U^c S^\theta = 0, \quad (126)$$

$$R^{a:b} = -R^{b:a}, \quad (127)$$

$$-R^{\theta:bc} - 3U^b U^c R^{\theta:d} - \frac{1}{\tau} \left[ R^{b:c} + \frac{q}{m} F_d^c \left( R^{bd:\theta} + U^b U^d S^\theta \right) \right] = 0, \quad (128)$$

$$2R^{\theta:bc} + \frac{q}{m} \left( F_d^b R^{d:c} + F_d^c R^{d:b} \right) = 0. \quad (129)$$

The relativistic enthalpy  $S^\theta$  cannot be zero, since  $f \geq 0$  and  $f > 0$  somewhere<sup>26</sup>. Hence (125) tells us that the bulk acceleration vanishes;

$$A^a = 0, \quad (130)$$

as expected in an equilibrium state.

Contracting (126) with  $U^b$  yields

$$U_b U^b R^{\theta:c} + \frac{1}{\tau} \frac{q}{m} U_b F_c^b U^c S^\theta = 0, \quad (131)$$

---

<sup>26</sup>See (88).

and noting that  $U_b F^b_c U^c = 0$  due to symmetry we find

$$R^{\emptyset:c} = 0. \quad (132)$$

Substitution of the above result into (126) yields

$$F^b_c U^c = 0. \quad (133)$$

Equation (133) tells us that in the fluid frame the electric field vanishes, which is certainly expected for a system in equilibrium since any electric fields would cause the electrons to accelerate<sup>27</sup>. Making use of the results (130), (132) and (133), the system of equations (125-129) can be reduced to the equations

$$R^{\emptyset:bc} + \frac{1}{\tau} \left( R^{b:c} + \frac{q}{m} F^c_d R^{bd:\emptyset} \right) = 0, \quad (134)$$

$$R^{b:c} + \frac{q}{2m} \left( F^c_d R^{bd:\emptyset} - F^b_d R^{cd:\emptyset} \right) = 0, \quad (135)$$

$$R^{\emptyset:bc} + \frac{q}{2m} \left( R^{d:b} F^c_d + R^{d:c} F^b_d \right) = 0. \quad (136)$$

Rearranging (135) and (136) into an expression for  $R^{b:c}$  and  $R^{\emptyset:bc}$  respectively, subsequent substitution into (134), with appropriate rearrangement of indices, results in

$$\frac{q}{2m} \left( -F^b_d R^d_e{}^{\emptyset} F^e_c - F^b_d F^d_e R^e_c{}^{\emptyset} - F^b_e R^d_e{}^{\emptyset} F^d_c - R^b_e{}^{\emptyset} F^e_d F^d_c \right) = \frac{1}{\tau} \left( F^b_d R^d_c{}^{\emptyset} - R^b_d{}^{\emptyset} F^d_c \right). \quad (137)$$

Defining the matrices

$$\mathcal{R} = \left[ R^a_b{}^{\emptyset} \right], \quad (138)$$

and

$$\mathcal{F} = \left[ F^a_b \right], \quad (139)$$

---

<sup>27</sup>Note however that (133) provides no information about the magnetic field

allows (137) to be written in the simpler form

$$\frac{q}{2m} \{\mathcal{F}, \{\mathcal{F}, \mathcal{R}\}\} - \frac{1}{\tau} [\mathcal{F}, \mathcal{R}] = 0, \quad (140)$$

where  $\{\mathcal{A}, \mathcal{B}\} = \mathcal{A}\mathcal{B} + \mathcal{B}\mathcal{A}$  denotes the anti-commutator and  $[\mathcal{A}, \mathcal{B}] = \mathcal{A}\mathcal{B} - \mathcal{B}\mathcal{A}$  denotes the commutator of the matrices  $\mathcal{A}, \mathcal{B}$ . Additionally  $\mathcal{A}\mathcal{B} = [A^a_b] [B^b_c]$  is the matrix product.

### Obtaining a Solution

We wish to solve (140) to obtain an expression for  $\mathcal{R}$  in terms of  $\mathcal{F}$ . Direct rearrangement of the equation is not possible however, so instead, let us choose a reasonable ansatz for  $\mathcal{R}$  which satisfies (140).

From inspection of (140) it would seem clear that  $\mathcal{R}$  is some function of  $\mathcal{F}$ , the identity matrix  $I$  and possibly  $\star\mathcal{F} = [\frac{1}{2}\varepsilon^a_{bc} F^c_d]$ . Additionally we know that  $R^{ab;\emptyset}$  is symmetric by definition. This implies that  $R^{ab;\emptyset}$  must be composed only of even powers of the (anti-symmetric) electromagnetic field tensor  $F^{ab}$ . Hence a viable solution to (140) could be an infinite series in  $F^{ab}$ , however such a solution is not ideal. Fortunately, it is possible to truncate such a series with the help of the Cayley-Hamilton Theorem[46], which implies that every square matrix over the real or complex numbers satisfies its own characteristic equation. To proceed then, we must determine the characteristic equation for  $\mathcal{F}$ , given by

$$\det(\mathcal{F} - \phi I) = 0, \quad (141)$$

where  $\det$  is the determinant,  $I$  is the identity matrix and  $\phi$  is an eigenvalue of the matrix  $\mathcal{F}$ .

In a Cartesian coordinate system, (141) takes the form

$$\begin{aligned}
\det(\mathcal{F} - \phi I) &= \det \left( \begin{bmatrix} -\phi & -E_x & -E_y & -E_z \\ -E_x & -\phi & -B_z & B_y \\ -E_y & B_z & -\phi & -B_x \\ -E_z & -B_y & B_x & -\phi \end{bmatrix} \right) \\
&= \phi^4 + \phi^2 (B_x^2 + B_y^2 + B_z^2 - E_x^2 - E_y^2 - E_z^2) \\
&\quad + E_x^2 B_x^2 + E_y^2 B_y^2 + E_z^2 B_z^2 + 2(E_x E_z B_x B_z + E_x E_y B_x B_y + E_y E_z B_y B_z) \\
&= \phi^4 - \phi^2 \frac{1}{2} \text{Tr}(\mathcal{F}^2) - \det(\mathcal{F}) = 0.
\end{aligned} \tag{142}$$

If we now apply the Cayley-Hamilton theorem to (142), we are able to write any term of an even power in  $\mathcal{F}$  and  $\mathcal{O}(\mathcal{F}^4)$  or higher, in terms of  $\mathcal{F}$  and  $\mathcal{F}^2$ . For example,

$$\mathcal{F}^4 = \frac{1}{2} \text{Tr}(\mathcal{F}^2) \mathcal{F}^2 + \det(\mathcal{F}), \tag{143}$$

$$\begin{aligned}
\mathcal{F}^6 &= \mathcal{F}^4 \mathcal{F}^2 \\
&= \frac{1}{2} \mathcal{F}^4 \text{Tr}(\mathcal{F}^2) - \mathcal{F}^2 \det(\mathcal{F}) \\
&= \frac{1}{2} \left( \frac{1}{2} \text{Tr}(\mathcal{F}^2) \mathcal{F}^2 - \det(\mathcal{F}) \right) \text{Tr}(\mathcal{F}^2) - \mathcal{F}^2 \det(\mathcal{F}) \\
&= \left( \frac{1}{4} \text{Tr}(\mathcal{F}^2) - \det(\mathcal{F}) \right) \mathcal{F}^2 - \frac{1}{2} \det(\mathcal{F}) \text{Tr}(\mathcal{F}^2),
\end{aligned} \tag{144}$$

and similarly for  $\star\mathcal{F}$ .

The situation is simplified further by realising that the determinant of  $\mathcal{F}$  is an electromagnetic invariant;

$$\det(\mathcal{F}) = -\frac{1}{4} \left( \star F_{ab} F^{ab} \right)^2 = (\mathbf{B} \cdot \mathbf{E})^2. \tag{145}$$

Recall from (133) that the electric field vanishes in the fluid frame and hence from (145) we see that  $\det(\mathcal{F}) = 0$  in this frame. Furthermore, since (145) is a Lorentz-invariant quantity, the result

$\det(\mathcal{F}) = 0$  holds in any frame. Generalising (143) to any order in  $\mathcal{F}$  we find,

$$\mathcal{F}^n = \left( \frac{1}{2} \text{Tr}(\mathcal{F}^2) \right)^{\frac{n}{2}-1} \mathcal{F}^2, \quad (146)$$

and

$$\star \mathcal{F}^n = \left( -\frac{1}{2} \text{Tr}(\mathcal{F}^2) \right)^{\frac{n}{2}-1} \star \mathcal{F}^2, \quad (147)$$

where  $n$  is any positive, even integer. Note the minus sign in (147) arises due to the identity  $\text{Tr}(\mathcal{F}^2) = -\text{Tr}(\star \mathcal{F}^2)$ .

Additionally, one can show the following two identities:

$$\mathcal{F}^2 + \star \mathcal{F}^2 = \frac{1}{2} \text{Tr}(\mathcal{F}^2) I, \quad (148)$$

$$\mathcal{F} \star \mathcal{F} = \star \mathcal{F} \mathcal{F} = 0. \quad (149)$$

All of the above suggest that we can write  $\mathcal{R}$  as a linear superposition of the matrices

$$\mathcal{P} = \frac{2\mathcal{F}^2}{\text{Tr}(\mathcal{F}^2)}, \quad (150)$$

and

$$\check{\mathcal{P}} = \frac{2\star \mathcal{F}^2}{\text{Tr}(\star \mathcal{F}^2)}. \quad (151)$$

From (146) - (149) it is clear that  $\mathcal{P}$  and  $\check{\mathcal{P}}$  are idempotent matrices:

$$\mathcal{P}\mathcal{P} = \mathcal{P}, \quad (152)$$

$$\check{\mathcal{P}}\check{\mathcal{P}} = \check{\mathcal{P}}, \quad (153)$$

and that they are orthogonal:

$$\mathcal{P}\check{\mathcal{P}} = \check{\mathcal{P}}\mathcal{P} = 0, \quad (154)$$

$$\mathcal{P} + \check{\mathcal{P}} = \mathcal{I}. \quad (155)$$

Finally we must ensure that any expression for  $\mathcal{R}$  satisfies the constraints (119 - 124). Equation (121) tells us that  $\mathcal{R}$  must be orthogonal to the bulk velocity  $[U^a]$  to  $\mathcal{O}(\epsilon^3)$ . While this is certainly true of  $\mathcal{P}$  - due to (133) - the same is not necessarily true of  $\check{\mathcal{P}}$ .

This suggests the introduction of the idempotent

$$\Pi = \left[ \delta_b^a + \frac{U^a U_b}{|U|^2} \right], \quad (156)$$

where  $|U| = \sqrt{-U^a U_a}$ , which acts to project vectors into the space orthogonal to  $U^a$ . It can be seen  $\Pi \mathcal{F} = \mathcal{F} \Pi = \mathcal{F}$  since the electric field vanishes in the fluid frame. Hence natural idempotents for constructing the solution to (140) are  $\Pi \mathcal{P} \Pi$  and  $\Pi \check{\mathcal{P}} \Pi$ .

Thus, a suitable ansatz for  $\mathcal{R}$  is

$$\mathcal{R} = \frac{p_\perp}{m} \Pi \mathcal{P} \Pi + \frac{p_\parallel}{m} \Pi \check{\mathcal{P}} \Pi, \quad (157)$$

where  $p_\perp$  and  $p_\parallel$  are the pressures perpendicular and parallel to the magnetic field respectively.

Substituting this solution into the matrix equation (140) and using the identities (152) - (155), the commutator term vanishes resulting in

$$\frac{p_\perp q}{m^2} \mathcal{F}^2 = 0. \quad (158)$$

Clearly, for the above to be satisfied - and still generate interesting results - we must set the pressure term perpendicular to the field to zero, or demand that the magnetic field vanishes. Hence, if the magnetic field is non-zero a suitable form for  $\mathcal{R}$  isotropic around the magnetic field lines is

$$\mathcal{R} = \frac{p}{m} \Pi \check{\mathcal{P}} \Pi, \quad (159)$$

where  $p = p_\parallel$  is the only component of the pressure.

The above result has a straightforward physical interpretation. In principle, an electron can have a component of velocity parallel to, and a component perpendicular to, the background magnetic

field. Motion perpendicular to the field will cause the electron to spiral around the magnetic field lines and emit cyclotron radiation, whereas there is no such emission from the component of velocity along the magnetic field lines. Recall that at the beginning of this section, we chose to perturb around a set of equilibrium solutions; (159) informs us that in this equilibrium state, motion perpendicular to the field is not permitted and thus the electron's velocity is directed parallel to the magnetic field lines.

Armed with (157) we can now obtain an expression for the bulk velocity  $U^a$ . Recall from (105) that

$$U^a = \frac{S^{a:\emptyset}}{S^\emptyset} = \frac{N^a}{S^\emptyset}, \quad (160)$$

where  $N^a$  is the number 4-current.

For a plasma in equilibrium the number 4-current is equal to that of the background ion's number 4-current;  $N^a = N_{\text{ion}}^a = n_{\text{ion}} \delta_0^a$  where  $n_{\text{ion}}$  is the proper number density of the ions, hence

$$U^a = \frac{n_{\text{ion}}}{S^\emptyset} \delta_0^a. \quad (161)$$

$S^\emptyset$  can be found from the constraint (119) yielding

$$\begin{aligned} S^\emptyset &= -\frac{R^a_a{}^{:\emptyset}}{1 + U^b U_b} \\ &= \frac{p}{m(1 + U^b U_b)} \Pi^a_c \tilde{\mathcal{P}}^c_d \Pi^d_a, \end{aligned} \quad (162)$$

where  $S^\emptyset = \mathcal{O}(\epsilon^0)$ ,  $p = \mathcal{O}(\epsilon^2)$  and  $1 + U^a U_a = \mathcal{O}(\epsilon^2)$ .

### 3 An Examination of Electric Waves

In this section we will use the fluid model that we built in Section 2 to investigate the properties of an electric wave as it propagates through a plasma, as well as the effect such a wave has on the bulk properties of the plasma. We will begin with the simpler case of an unmagnetised plasma, before moving on to examine what effect an ambient magnetic field has on the system.

#### 3.1 In an Unmagnetised Plasma

In the absence of a background magnetic field  $\mathcal{R}$  must be isotropic and hence takes the form

$$\begin{aligned} \mathcal{R} &= \frac{p}{m} \Pi \\ &= \begin{bmatrix} 0 & 0 & 0 & 0 \\ 0 & \frac{p}{m} & 0 & 0 \\ 0 & 0 & \frac{p}{m} & 0 \\ 0 & 0 & 0 & \frac{p}{m} \end{bmatrix}, \end{aligned} \tag{163}$$

instead of (159).

As we discussed in Section 1.2, a small amplitude, spatially harmonic, perturbation to the equilibrium proper number density induces an electric wave that will propagate through the plasma. We choose our coordinate system such that this electric wave propagates along the  $z = x^3$  axis in the rest frame of the ions. We denote  $t = x^0$  and write the enthalpy as

$$S^\emptyset = S_{(0)}^\emptyset + \text{Re} \left[ S_{(1)}^\emptyset e^{(ikz - i\omega t)} \right], \tag{164}$$

where  $S_{(0)}^\emptyset$  is the enthalpy in equilibrium and  $S_{(1)}^\emptyset$  is the complex amplitude of a small perturbation to  $S_{(0)}^\emptyset$ . We introduce similar expressions for the other fields.

As there is no background magnetic field, and the applied field is purely electric, the electro-

magnetic field tensor takes the form

$$F = \text{Re} \left[ E_{z(1)} e^{(ikz - i\omega t)} dt \wedge dz \right], \quad (165)$$

where  $E_{z(1)}$  is the complex amplitude of the perturbation. Note that there is no  $\mathbf{E}_{(0)}$  term since in the equilibrium state any electric fields - in the rest frame of the plasma - vanish.

A linearisation of (91 - 96), with respect to the perturbation then yields

$$S_{(1)}^\emptyset = -\frac{1}{k_a U_{(0)}^a} S_{(0)}^\emptyset k_b U_{(1)}^b, \quad (166)$$

$$A_{(1)}^b = ik_a \left( \frac{1}{S_{(0)}^\emptyset} R_{(1)}^{ab:\emptyset} + U_{(0)}^a U_{(1)}^b \right), \quad (167)$$

$$ik_a \left( R_{(1)}^{a:b} + S_{(0)}^\emptyset U_{(0)}^a A_{(1)}^b \right) - U_{(0)}^b R_{(1)}^{\emptyset:c} - 2A_{(1)}^c R_{(0)}^{b:c} - \frac{1}{\tau} \left[ S_{(0)}^\emptyset A_{(1)}^b + \frac{q}{m} F_{\{(0) c} U_{(1)}^c \right], \quad (168)$$

$$R_{(1)}^{b:c} + R_{(1)}^{c:b} = ik_a \left( R_{\{(0) c}^{bc:\emptyset} U_{(1)}^a + R_{(0)}^{ac:\emptyset} U_{(1)}^b + R_{(0)}^{ab:\emptyset} U_{(1)}^c \right), \quad (169)$$

$$\begin{aligned} R_{(1)}^{\emptyset:bc} &= ik_a \left( R_{\{(0) c}^{b:c} U_{(1)}^a + R_{(0)}^{a:c} U_{(1)}^b + R_{(0)}^{ab:\emptyset} A_{(1)}^c \right) - 2U_{(0)}^c A_{(1)}^d R_{(0)}^{b:d} \\ &\quad - \frac{1}{\tau} \left( R_{(1)}^{b:c} + \frac{q}{m} F_{\{(0) d}^c R_{(1)}^{bd:\emptyset} \right), \end{aligned} \quad (170)$$

$$\begin{aligned} 0 &= ik_a \left( R_{\{(0) c}^{\emptyset:bc} U_{(1)}^a + R_{(0)}^{a:c} A_{(1)}^b + R_{(0)}^{a:b} A_{(1)}^c \right) - 2U_{(0)}^b A_{(1)}^d R_{(0)}^{\emptyset:c} \\ &\quad - 2U_{(0)}^c A_{(1)}^d R_{(0)}^{\emptyset:b} - \frac{1}{\tau} \left[ 2R_{(1)}^{\emptyset:bc} + \frac{q}{m} \left( F_{\{(0) d}^b R_{(1)}^{d:c} + F_{\{(0) d}^c R_{(1)}^{d:b} \right) \right], \end{aligned} \quad (171)$$

where  $k^a = (\omega, \mathbf{k})$  is the wave's 4-vector.

Terms with a subscript (0) represent solutions to the equilibrium state found in Section 2.3, while those with a subscript (1) represent the first order corrections resulting from the perturbation.

Additionally, the notation

$$A_{\{(0) B_{(1)\}} = A_{(0)} B_{(1)} + A_{(1)} B_{(0)}, \quad (172)$$

has been used.

Substitution of our equilibrium solutions from Section 2.3 into (166 - 171), and combined with Maxwell's equations<sup>28</sup> (85,84), results in a system of 22 equations for 22 unknowns. We can rewrite this system as a single matrix equation of the form

$$\begin{bmatrix} \text{Matrix} \\ \text{of} \\ \text{Coefficients} \end{bmatrix} \begin{bmatrix} \mathbf{V} \end{bmatrix} = \begin{bmatrix} \mathbf{0} \end{bmatrix}, \quad (173)$$

where the column vector  $\mathbf{V}$  contains all of the field variables and the right-hand side is simply the zero column vector.

Rather than solving directly for the fields, we can instead obtain a relation between the coefficients of the field variables. We do this by taking the determinant of the matrix on the left-hand side, and demanding that this be zero. The result is a dispersion relation of the form

$$\begin{aligned} 0 = & 4\omega^2 (\omega^2 - \omega_p^2) + \theta (10\omega_p^2\omega^2 + 4\omega_p^2k^2 - 16\omega^2k^2) + i\tau (42\omega^5 - 38\omega^3\omega_p^2) \\ & + i\tau\theta (38\omega^3\omega_p^2 - 168\omega^3k^2 + 63\omega^5 + 30\omega\omega_p^2k^2) + \mathcal{O}(\tau^2, \theta^2), \end{aligned} \quad (174)$$

where the normalised equilibrium temperature  $\theta$  is given by<sup>29</sup>

$$\theta = \frac{p}{n_{\text{ion}}m} \quad (175)$$

and  $\omega_p$  is the plasma frequency.

We seek a solution of (174) such that in the limit  $\tau \rightarrow 0$ ,  $\theta \rightarrow 0$  the solution collapses to that of the cold non-radiating<sup>30</sup> fluid  $\omega = \omega_p$ , discussed in Section 1.2.1. Thus we choose the angular frequency to be of the form

$$\omega(k) = \omega_p + \alpha(k)\theta + i\tau\beta(k) + i\tau\theta\zeta(k) + \mathcal{O}(\tau^2, \theta^2), \quad (176)$$

---

<sup>28</sup>Note these must also be linearised with respect to the perturbation.

<sup>29</sup>Note that since  $p$  is  $\mathcal{O}(\epsilon^2)$ ,  $\theta$  is  $\mathcal{O}(\epsilon^2)$  also.

<sup>30</sup>By a non-radiating fluid we mean a fluid in which the effects of radiation reaction are not considered.

where  $\alpha(k)$ ,  $\beta(k)$ ,  $\zeta(k)$  are as yet undetermined functions.

Substituting (176) into (174) and equating the resulting coefficients of  $\theta$ ,  $\tau$  and  $\tau\theta$  to zero, one can solve for the unknown functions  $\alpha(k)$ ,  $\beta(k)$ ,  $\zeta(k)$ . Substitution of these solutions into the ansatz (176) then yields

$$\omega = \omega_p + \left( \frac{3}{2} \frac{k^2}{\omega_p} - \frac{5}{4} \omega_p \right) \theta - \frac{i\tau}{2} [\omega_p^2 - (2k^2 + \omega_p^2) \theta] + \mathcal{O}(\tau^2, \theta^2). \quad (177)$$

In the limit  $\tau \rightarrow 0$ , (177) reduces to Clemmow and Wilson's relativistic generalisation of the Bohm-Gross dispersion relation[47].

Due to the nature of the perturbation  $e^{i(kx - \omega t)}$ , the real part of the perturbation to  $\omega_p$  will act only to shift the frequency of the wave, whilst the imaginary part of  $\omega$  will be the cause of the damping. We can see that for non-radiating plasmas, where  $\tau = 0$ , the imaginary part vanishes and  $\omega$  is real, hence, as expected, damping only occurs when radiation reaction is taken into account. The first damping term,  $-\frac{i}{2} \tau \omega_p^2$ , is a long standing result[48] that frequently appears in kinetic theories that include radiation reaction. The second damping term,  $\frac{i}{2} \tau \theta (2k^2 + \omega_p^2)$ , is dependent on temperature and can be shown to agree[1] with recent results presented elsewhere[26].

Note that the damping term is larger as  $k$  increases, hence the higher frequency modes will experience a greater amount of damping than the low frequency modes.

Armed with (177) and the equilibrium solutions we can solve (166 - 171) for all of the fields in terms of the complex amplitude  $S_{(1)}^\theta$  of the perturbation to the enthalpy.

Up to this point, we have not discarded any terms in our equations. However recall from Section 2.2 that in order to generate a finite set of equations, we applied the warm fluid approximation, discarding terms of  $\mathcal{O}(\epsilon^3)$ . Since  $\theta = \frac{p}{n_{\text{ion}} m}$  from (175), and  $p$  is  $\mathcal{O}(\epsilon^2)$  we see that to remain within this approximation, terms  $\mathcal{O}(\theta^2)$  must be discarded. Additionally, we saw in Section 1.1.3 that the ALD equation – upon which this model is based – contains undesirable solutions, and we went on to review an approximation scheme derived by Landau and Lifshitz. This approximation scheme eliminates these unwanted solutions by performing a series expansion in  $\tau$ , and then truncating the series by discarding all terms above a certain order in  $\tau$ . We must also do the same here, and we

choose to discard terms  $\mathcal{O}(\tau^2)$ , since they will be negligible in comparison to the terms  $\mathcal{O}(\theta^2)$ .

Discarding any terms of  $\mathcal{O}(\tau^2, \theta^2)$  in the above solutions, we find

$$U_{(1)}^0 = \frac{q^2}{m \omega_p^2} S_{(1)}^\theta \theta (1 + i \tau \omega_p), \quad (178)$$

$$U_{(1)}^3 = \frac{q^2}{4 m \omega_p^3 k} S_{(1)}^\theta \{4 \omega_p^2 + \theta (11 \omega_p^2 + 6 k^2) - i \tau [2 \omega_p^3 + \theta (2 \omega_p^3 - 4 k^2 \omega_p)]\}, \quad (179)$$

$$A_{(1)}^0 = \frac{q^2}{m} \tau \theta S_{(1)}^\theta, \quad (180)$$

$$A_{(1)}^3 = -\frac{q^2}{4 k m \omega_p} S_{(1)}^\theta \{4 i \omega_p + 16 i \omega_p \theta + \tau [4 \omega_p^2 + \theta (13 \omega_p^2 + 6 k^2)]\}, \quad (181)$$

$$R_{(1)}^{33:\theta} = (3 + 2 i \tau \omega_p) \theta S_{(1)}^\theta, \quad (182)$$

$$R_{(1)}^{30:\theta} = -\frac{\omega_p}{k} \theta S_{(1)}^\theta (-2 + i \tau \omega_p), \quad (183)$$

$$R_{(1)}^{11:\theta} = \theta S_{(1)}^\theta, \quad (184)$$

$$R_{(1)}^{22:\theta} = \theta S_{(1)}^\theta, \quad (185)$$

$$R_{(1)}^{3:0} = -\frac{\omega_p^2}{k} \theta S_{(1)}^\theta (i + \tau \omega_p), \quad (186)$$

$$R_{(1)}^{3:3} = \tau \theta S_{(1)}^\theta \omega_p^2, \quad (187)$$

$$E_{z(1)} = -\frac{q}{2 k} S_{(1)}^\theta (2 i + 5 i \theta - 2 \tau \theta \omega_p). \quad (188)$$

All other field variables vanish. Additionally, one can show that the set of solutions (178-188) satisfy the constraints (119-124).

At this point, one might wonder why we chose to take moments of a kinetic theory based upon the ALD equation, when, in order to obtain solutions, we still need to apply the approximation procedure used to obtain the Landau-Lifshitz (LL) equation. We could have chosen a kinetic description based upon the LL equation, and taken moments of this description to derive a set of fluid equations; thus removing the need to eliminate terms  $\mathcal{O}(\tau^2)$  in our resulting expressions.

While in principle such a model would be equivalent, the fluid equations (91 - 96) would not

take on as compact a form as they do here, and the complexity of the analysis would be greatly increased from the outset. From this perspective, it is perhaps not surprising that the dispersion relations obtained later in this thesis are new results.

### 3.2 In a Magnetised Plasma

We next consider the case of a plasma with a background magnetic field running through it. If we choose the  $z = x^3$  axis to lie parallel to the magnetic field lines in the rest frame of the ions, and perturb the equilibrium proper number density as we did in the previous section, we again generate an electric wave, this time travelling along the magnetic field lines of the plasma. Such a wave is of the form

$$F = -B_0 dx \wedge dy + \text{Re} \left[ E_{z(1)} e^{(ikz - i\omega t)} dt \wedge dz \right], \quad (189)$$

where  $B_0$  is the amplitude of the background magnetic field and  $E_{z(1)}$  is the complex amplitude of the perturbation.

Due to the addition of a background magnetic field,  $\mathcal{R}$  is no longer isotropic. In Section 2.3 we found that in such a field any pressure terms perpendicular to the background field must vanish and hence  $\mathcal{R}$  now takes the form

$$\begin{aligned} \mathcal{R} &= \frac{p}{m} \Pi \check{\mathcal{P}} \Pi \\ &= \begin{bmatrix} 0 & 0 & 0 & 0 \\ 0 & 0 & 0 & 0 \\ 0 & 0 & 0 & 0 \\ 0 & 0 & 0 & \frac{p}{m} \end{bmatrix}. \end{aligned} \quad (190)$$

The linearised system is once more composed of (166) - (171); if we again substitute the above and the other equilibrium solutions into our system of equations, and combine with Maxwell's equations, we can obtain the dispersion relation

$$\begin{aligned} 0 &= 4\omega^2 (\omega^2 - \omega_p^2) + (4\omega^4 + 4k^2 \omega_p^2 - 16\omega^2 k^2 + 2\omega^2 \omega_p^2) \theta + i(30\omega^5 - 26\omega^3 \omega_p^2) \tau \\ &\quad + i\tau \theta (18\omega \omega_p^2 k^2 - 120k^2 \omega^3 + 45\omega^5) + \mathcal{O}(\tau^2, \theta^2). \end{aligned} \quad (191)$$

Again seeking a solution to the above of the form  $\omega(k) = \omega_p + \alpha(k)\theta + i\tau\beta(k) + i\tau\theta\zeta(k) +$

$\mathcal{O}(\tau^2, \theta^2)$ , we find

$$\omega = \omega_p + \left( \frac{3k^2}{2\omega_p} - \frac{3}{4}\omega_p \right) \theta - \frac{i\tau}{2} [\omega_p^2 - (2k^2 + \omega_p^2) \theta] + \mathcal{O}(\tau^2, \theta^2). \quad (192)$$

Note that in the limit  $\tau \rightarrow 0$ , the above does not reduce to (177), the dispersion relation in the unmagnetised plasma, taken to the same limit. The difference is the numerical factor  $\frac{3}{4}$  in the relativistic correction to the frequency shift; this is due to the anisotropy of  $R^{ab;\theta}$  in equilibrium. The coefficient of  $\tau$  however is the same in both the magnetised and non-magnetised cases. Hence the presence of a background magnetic field in the plasma simply acts to further shift the frequency of the electric waves, but has no effect on the radiative damping.

Once again, using (192) and the equilibrium solutions found in Section 2.3, one can calculate the field variables to be

$$U_{(1)}^3 = \frac{q^2 S_{(1)}^\theta}{4m\omega_p^3 k} \{4\omega_p^2 + \theta(5\omega_p^2 + 6k^2) - i\tau[2\omega_p^3 - \theta(\omega_p^3 + 2k^2\omega_p)]\}, \quad (193)$$

$$A_{(1)}^3 = -\frac{q^2}{4km\omega_p} S_{(1)}^\theta \{4i\omega_p + 8i\omega_p\theta + \tau[4\omega_p^2 + \theta(3\omega_p^2 + 6k^2)]\}, \quad (194)$$

$$E_{z(1)} = -\frac{q}{2k} S_{(1)}^\theta (2i + 3i\theta - 2\tau\theta\omega_p), \quad (195)$$

with all other field variables being equal to those found in the previous section. Note that in the above solutions we have highlighted in red the terms which are changed by the introduction of a background magnetic field.

Once again, it can be shown that all of the above solutions satisfy the constraints (119-124).

## 4 An Examination of Electromagnetic Waves

We now turn our attention to a small amplitude electromagnetic wave propagating along the magnetic field lines of a plasma. Such a wave can be written as

$$F = -B_0 dx \wedge dy - \operatorname{Re} [(B_x dy \wedge dz + E_x dx \wedge dt + B_y dx \wedge dz + E_y dy \wedge dt + B_z dx \wedge dy + E_z dz \wedge dt) e^{i(kz - \omega t)}], \quad (196)$$

where  $B_0$  is the strength of the background field of the plasma, directed along  $\hat{z}$ , and  $\mathbf{E} = (E_x, E_y, E_z)$  and  $\mathbf{B} = (B_x, B_y, B_z)$  are the complex amplitudes of the electric and magnetic fields of the wave respectively.

Using the method of Section 3.2 we once again rewrite the system as a matrix equation, generate a matrix of coefficients, and demand that its determinant is zero. However, this expression is much more complicated than that generated by the electric wave of the previous section; we are now dealing with a 47th order polynomial in  $\omega$  and 20th order polynomial<sup>31</sup> in  $k$ . Solving the equation directly for  $\omega$  generates 47 possible roots, but determining which roots represent real waves is problematic. The unphysical roots do not exist in the limit  $\tau, \theta, B_0 \rightarrow 0$ . Thus, we factor the determinant into products of terms, examine these terms in the limit  $\tau, \theta, B_0 \rightarrow 0$  and solve each of them for  $k(\omega)$ . We then seek out the ones which collapse to (71);

$$\omega^2 = \omega_p^2 + k^2. \quad (197)$$

There are two terms that collapse to the above; these correspond to the L and R modes of the electromagnetic wave<sup>32</sup>.

Armed with the knowledge of which terms provide the solutions we are interested in, we now simply isolate both of these terms in turn and set them to zero. The resulting expressions, which can be found in Sections 4.1 & 4.2, are used as the starting points in our analysis of the L & R

---

<sup>31</sup>Note that (191) was merely 5th order in  $\omega$  and quadratic in  $k$ .

<sup>32</sup>In order to determine which term corresponds to the R mode, and which to the L mode, it is useful to set  $\tau = \theta = 0$ , solve for  $k^2$  and then compare with Table 1.

modes of the wave.

An electromagnetic field tensor of the form (196) does not generate O and X modes. As we can see from Table 1 in Section 1.2, these modes arise only when the wave is propagating along an axis perpendicular to the direction of the background magnetic field. Hence, to explore the properties of these modes one must begin with an electromagnetic field of the form

$$F = B_0 dx \wedge dz - \operatorname{Re} [(B_x dy \wedge dz + E_x dx \wedge dt + B_y dx \wedge dz + E_y dy \wedge dt + B_z dx \wedge dy + E_z dz \wedge dt) e^{i(kz - \omega t)}]. \quad (198)$$

One then follows a procedure identical to that detailed above, but now the two solutions which collapse to (197) in the limit  $\tau, \theta, B_0 \rightarrow 0$  correspond to the O and X modes of the wave. These solutions can be found in Sections 4.3 & 4.4.

Table 1 is referred to often in this section, and hence for the convenience of the reader, we replicate it below.

Mode	Properties	Dispersion Relation
R	$\mathbf{k} \parallel \mathbf{B}_0$ (right circ. pol.)	$\frac{k^2}{\omega^2} = 1 - \frac{\omega_p^2/\omega^2}{1 - \omega_c/\omega}$
L	$\mathbf{k} \parallel \mathbf{B}_0$ (left circ. pol.)	$\frac{k^2}{\omega^2} = 1 - \frac{\omega_p^2/\omega^2}{1 + \omega_c/\omega}$
O	$\mathbf{k} \perp \mathbf{B}_0$ , $\mathbf{E} \parallel \mathbf{B}_0$	$\frac{k^2}{\omega^2} = 1 - \frac{\omega_p^2}{\omega^2}$
X	$\mathbf{k} \perp \mathbf{B}_0$ , $\mathbf{E} \perp \mathbf{B}_0$	$\frac{k^2}{\omega^2} = 1 - \frac{\omega_p^2}{\omega^2} \frac{\omega^2 - \omega_p^2}{\omega^2 - \omega_p^2 - \omega_c^2}$

Table 2: Dispersion relations for the four possible modes of an electromagnetic electron wave travelling through a magnetised plasma.

## 4.1 R Mode

The R Mode is right hand circularly polarised, its dispersion relation is of the form

$$\begin{aligned}
0 = & -(\omega - \omega_c) (\omega_c k^2 - \omega_c \omega^2 + \omega^3 - k^2 \omega - \omega_p^2 \omega) \\
& + \theta \left( \omega^2 \omega_c^2 - \frac{1}{2} \omega_p^2 \omega^2 - k^2 \omega_c^2 + k^2 \omega^2 + \omega \omega_c k^2 - k^4 - \omega_p^2 k^2 + \omega \omega_p^2 \omega_c - \omega^3 \omega_c \right) \\
& - i\tau \left[ (2\omega_c k^2 - 2\omega_c \omega^2 + 2\omega^3 - 2k^2 \omega - \omega_p^2 \omega) \omega^2 - \theta (-2\omega_c k^2 \omega^2 + \omega^5 + \omega_p^2 k^2 \omega \right. \\
& \left. - 3k^2 \omega^3 + 2k^4 \omega + 2\omega_c k^4) \right] + \mathcal{O}(\theta^2, \tau^2). \tag{199}
\end{aligned}$$

Note that in order to obtain the above, we have used the substitution  $B_0 = \frac{m\omega_c}{q}$  where  $\omega_c$  is the cyclotron frequency, and  $\theta = \frac{p}{n_{\text{ion}} m}$ .

In Section 3 we sought a solution of the form (176);

$$\omega(k) = \omega_p + \alpha(k) \theta + i\tau \beta(k) + i\tau \theta \zeta(k) + \mathcal{O}(\tau^2, \theta^2). \tag{200}$$

Finding  $\omega(k)$  is much more difficult when modelling electromagnetic waves; as we can see from Table 2, the unperturbed dispersion relations (i.e. for  $\tau, \theta \rightarrow 0$ ) are considerably less complicated when written as  $k(\omega)$  rather than  $\omega(k)$ . The difficulty arises from the fact that the results in Table 2 have more than one root for  $\omega$  and one must take care to choose the correct root. This becomes even more difficult when working in the warm plasma approximation and taking radiation reaction into account<sup>33</sup>.

Thus, a more successful approach is to seek a solution to (199) of the form

$$k(\omega) = k_0(\omega) + \mathfrak{f}(\omega) \theta + i\tau \mathfrak{g}(\omega) + i\tau \theta \mathfrak{h}(\omega) + \mathcal{O}(\theta^2, \tau^2), \tag{201}$$

where  $k_0(\omega)$  is the wave number in the limit  $\tau, \theta \rightarrow 0$  and  $\mathfrak{f}(\omega)$ ,  $\mathfrak{g}(\omega)$  and  $\mathfrak{h}(\omega)$  are as yet undetermined functions. Substituting (201) into (199) and equating coefficients of  $\theta$ ,  $\tau$ ,  $\tau\theta$  etc to zero, one can

---

<sup>33</sup>In this case, conventional root finding techniques employed in computer software such as Maple are unable to generate possible roots, probably a result of the polynomial in  $\omega$  being of too high an order for such techniques to be employed.

solve for  $f(\omega)$ ,  $g(\omega)$ , and  $h(\omega)$ . Subsequent substitution of these solutions back into (201) yields the dispersion relation

$$\begin{aligned} \frac{k^2}{\omega^2} = & \frac{\omega \omega_c - \omega^2 + \omega_p^2}{\omega(\omega_c - \omega)} + \frac{\theta}{2} \left( \frac{(\omega^3 + 3\omega \omega_c^2 - 4\omega^2 \omega_c + 2\omega_c \omega_p^2) \omega_p^2}{\omega(\omega_c - \omega)^4} \right) \\ & + i\tau \left[ \frac{\omega \omega_p^2}{\omega^2 - 2\omega \omega_c + \omega_c^2} + \frac{\omega_c \omega_p^2 \theta (4\omega \omega_c^2 + \omega^3 + \omega \omega_p^2 - 5\omega^2 \omega_c + 3\omega_c \omega_p^2)}{(\omega_c - \omega)^5} \right] \\ & + \mathcal{O}(\theta^2, \tau^2). \end{aligned} \quad (202)$$

In order to plot the above dispersion relation we must define some range of  $\omega$ . Note however that the right-hand side of the above expression appears complex, yet we know that  $k$  must be real, hence  $\omega$  must be complex; this makes determining the domain of  $\omega$  difficult. In order to carry out such an analysis it is fruitful to rewrite both  $k$  and  $\omega$  parametrically as functions of  $\omega_0$ , the angular frequency in the case of a magnetised, cold, non-radiating plasma. The advantage of this approach is that we only consider values of  $\omega_0$  that are real<sup>34</sup>.

For the sake of clarity, let us introduce some new notation before proceeding. Let us assume that both  $\theta$  and  $\tau$  are order  $\chi$  where  $\chi$  is some small parameter. Thus  $\tau\theta$ ,  $\tau^2$  and  $\theta^2$  are order  $\chi^2$ . One can then write  $k$  as a power series<sup>35</sup> in  $\chi$

$$k^2 = f(\omega) + h(\omega) + g(\omega) + \mathcal{O}(\chi^3), \quad (203)$$

with  $f(\omega) = \mathcal{O}(\chi^0)$ ,  $h(\omega) = \mathcal{O}(\chi^1)$ ,  $g(\omega) = \mathcal{O}(\chi^2)$  and where

$$f(\omega) = \frac{\omega(\omega \omega_c - \omega^2 + \omega_p^2)}{\omega_c - \omega}, \quad (204)$$

$$h(\omega) = \frac{\theta}{2} \frac{(\omega^3 + 3\omega \omega_c^2 - 4\omega^2 \omega_c + 2\omega_c \omega_p^2) \omega \omega_p^2}{(\omega_c - \omega)^4} + i\tau \frac{\omega^3 \omega_p^2}{\omega^2 - 2\omega \omega_c + \omega_c^2}, \quad (205)$$

---

<sup>34</sup>Note that values of  $\omega_0$  below the cutoff frequency are imaginary, but since we are only interested in the frequencies of physical waves, we can neglect these frequencies when choosing which range to take  $\omega_0$  over.

<sup>35</sup>Note that  $f(\omega)$  below has no relation to the 1-particle distribution function  $f$  used in previous sections.

and

$$g(\omega) = \frac{\omega^2 \omega_c \omega_p^2 \theta \tau (4 \omega \omega_c^2 + \omega^3 + \omega \omega_p^2 - 5 \omega^2 \omega_c + 3 \omega_c \omega_p^2)}{(\omega_c - \omega)^5}, \quad (206)$$

can be seen from inspection of (202).

With use of Table 2, we can recast  $k$  in terms of  $\omega_0$  to give

$$k^2 = \frac{\omega_0 (\omega_0 \omega_c - \omega_0^2 + \omega_p^2)}{\omega_c - \omega_0}. \quad (207)$$

Combining (207) and (203) we see that

$$f(\omega_0) = f(\omega) + h(\omega) + g(\omega) + \mathcal{O}(\chi^2). \quad (208)$$

Next, assume that  $\omega$  is of the form

$$\omega = \omega_0 + \alpha(\omega_0) + \beta(\omega_0) + \mathcal{O}(\chi^3), \quad (209)$$

with  $\alpha(\omega_0) = \mathcal{O}(\chi^1)$  and  $\beta(\omega_0) = \mathcal{O}(\chi^2)$ .

Substituting (209) into (208), expanding the result as a power series in  $\chi$ , collecting together coefficients of like orders of  $\chi$ , and setting each of these terms to zero in turn, leads to equations for the functions  $\alpha$  and  $\beta$  in terms of the functions  $f$ ,  $h$  and  $g$ . This allows (209) to be rewritten as

$$\omega(\omega_0) = \omega_0 - \frac{h(\omega_0)}{f'(\omega_0)} - \frac{1}{2} \frac{1}{f'(\omega_0)} \left( \frac{f''(\omega_0) h(\omega_0)^2}{f'(\omega_0)^2} + 2g(\omega_0) - \frac{2h'(\omega_0) h(\omega_0)}{f'(\omega_0)} \right) + \mathcal{O}(\chi^3), \quad (210)$$

where  $f' = \frac{df}{d\omega_0}$ .

The dispersion relation can then be obtained by substitution of (204 - 206) into the above. Note however that in order to remain within the warm fluid approximation, we must discard any terms of order  $\mathcal{O}(\theta^2)$ . Additionally, terms of  $\mathcal{O}(\tau^2)$  should also be discarded, since in practice they will be negligible in comparison to the  $\mathcal{O}(\theta^2)$  terms. The dispersion relation for the R mode is long, hence we do not include it here. In the following section we examine each part of it in turn, but for reference it can be seen in its complete form in Appendix C, as can the dispersion relations for

the L, O and X modes.

#### 4.1.1 Analysis of the Dispersion Relation

##### Frequency Shift

Note that once again due to the nature of the perturbation,  $e^{i(kz-\omega t)}$ , the real part of  $\omega$  will act only to shift the frequency of the wave, whilst the imaginary part of  $\omega$  is expected to cause damping. We can see from inspection of the expression for  $\omega(\omega_0)$  that this shift is composed of two parts; the shift that would be seen in a cold non-radiating plasma, plus a correction term due to the warm fluid approximation. The parameter  $\tau$  is absent from the real part of  $\omega(\omega_0)$  and hence inclusion of radiation reaction has no effect on the frequency shift. This holds true for all modes, as we will see in the following sections.

The correction to the frequency shift of the R mode predicted by the warm fluid model is

$$-\frac{\theta}{2} \frac{(3\omega_c^2\omega_0 + 2\omega_c\omega_p^2 - 4\omega_c\omega_0^2 + \omega_0^3)\omega_p^2\omega_0}{(\omega_c - \omega_0)^2(2\omega_c^2\omega_0 + \omega_c\omega_p^2 - 4\omega_c\omega_0^2 + 2\omega_0^3)}. \quad (211)$$

##### Dominant Damping

Note that the imaginary part of (210) is of the form

$$\text{Im}[\omega] = \zeta_r\tau + \sigma_r\tau\theta, \quad (212)$$

to first order in  $\tau$  and  $\theta$ . Since this work is valid only in the warm fluid approximation,  $\theta \ll 1$  and the strength of the damping will be primarily due to  $\zeta_r$ , hence we refer to  $\zeta_r$  as the dominant term, and to  $\sigma_r$  as the subdominant term<sup>36</sup>.

The dominant damping term for the R mode is of the form

$$\zeta_r = -\frac{\omega_p^2\omega_0^3}{2\omega_0\omega_c^2 - 4\omega_0^2\omega_c + \omega_c\omega_p^2 + 2\omega_0^3}. \quad (213)$$

---

<sup>36</sup>The imaginary part of  $\omega(\omega_0)$  is of this form for all modes, hence we will use this form throughout the following sections with  $\zeta_l$ ,  $\zeta_o$ ,  $\zeta_x$  and  $\sigma_l$ ,  $\sigma_o$ ,  $\sigma_x$  representing the dominant and subdominant terms for the L, O and X modes respectively.

Insight can be gained from looking at (213) when  $\omega_0$  is close to, and far from, the cutoff frequency  $\omega_{\text{co}}$ . Recall from Section 1.2.2 our discussion of the cutoff frequency; for the R mode,  $\omega_{\text{co}} \leq \omega_0 \leq \infty$  where<sup>37</sup>

$$\omega_{\text{co}} = \frac{1}{2} \left( \sqrt{\omega_c^2 + 4\omega_p^2} + \omega_c \right). \quad (214)$$

When  $\omega_0 \gg \omega_{\text{co}}$ ,  $\zeta_r$  takes the form

$$\zeta_r \approx -\frac{\omega_p^2}{2}, \quad (215)$$

and is independent of  $\omega_c$ . Hence irrespective of the strength of the background field, all frequencies much larger than the cutoff frequency will experience an equal amount of damping due to this term.

This is not the case for frequencies near the cutoff. In this regime, (213) takes the form

$$\zeta_r \approx \frac{1}{2} \frac{\left( \omega_c + \sqrt{\omega_c^2 + 4\omega_p^2} \right)^2 \omega_p^2}{\left( \omega_c - \sqrt{\omega_c^2 + 4\omega_p^2} \right) \sqrt{\omega_c^2 + 4\omega_p^2}}. \quad (216)$$

When the background field is sufficiently low, such that  $\omega_c \ll \omega_p$ , (216) reduces to (215). However if the field is sufficiently strong such that  $\omega_c \gg \omega_p$ ,

$$\zeta_r \approx -\omega_c^2. \quad (217)$$

Hence the strength of the magnetic field has a strong influence on those waves whose frequency is close to cutoff.

This behaviour can be seen more clearly in Figure 4, which parametrically plots  $k(\omega_0)$  vs  $\zeta_r(\omega_0)$  for varying values of the cyclotron frequency (and hence magnetic field strength). As can be seen, as the magnitude of the cyclotron frequency becomes large compared to that of the plasma frequency,  $\zeta_r$  takes on a form similar to that of a step function, strongly damping those frequencies that are close to cutoff, while having relatively little effect on higher frequencies.

---

<sup>37</sup>Note that we will suppress the mode label on the cutoff frequency for convenience, though it is important to keep in mind that each mode has a different cutoff frequency.

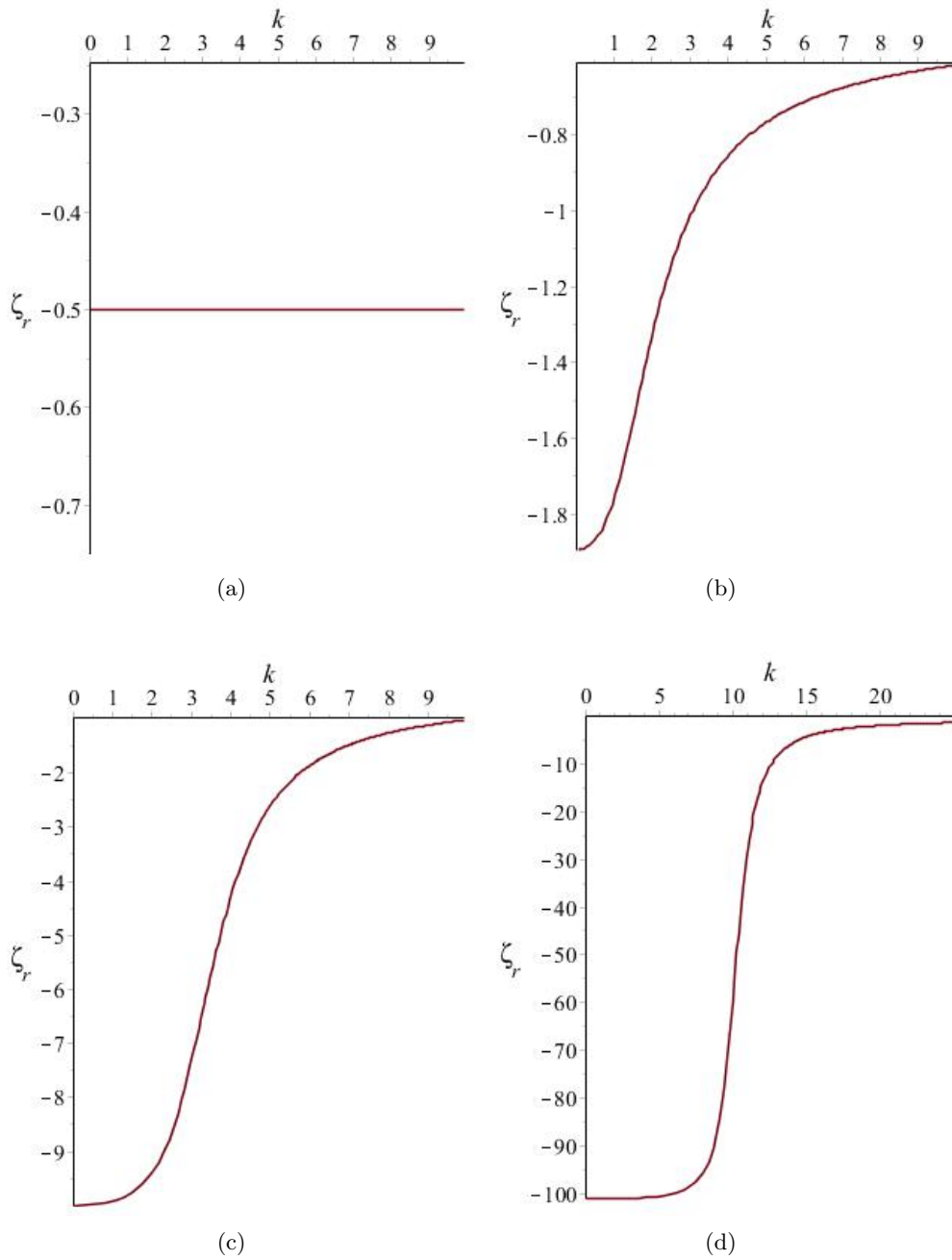


Figure 4: Plots of the dominant damping term  $\zeta_r(\omega_0)$  vs  $k(\omega_0)$  for a)  $\frac{\omega_c}{\omega_p} = 0$ , b)  $\frac{\omega_c}{\omega_p} = 1$ , c)  $\frac{\omega_c}{\omega_p} = 3$  and d)  $\frac{\omega_c}{\omega_p} = 10$ .

### **Subdominant Damping**

The remaining term,  $\sigma_r \tau \theta$ , contains a product of  $\tau$  and  $\theta$ ; thus while having an effect on the amplitude of the wave it will not be as strong an effect as seen above. In the absence of a background field the term vanishes, but has an interesting behaviour as  $\omega_c$  approaches and exceeds  $\omega_p$ . This is shown in Figure 5 below.

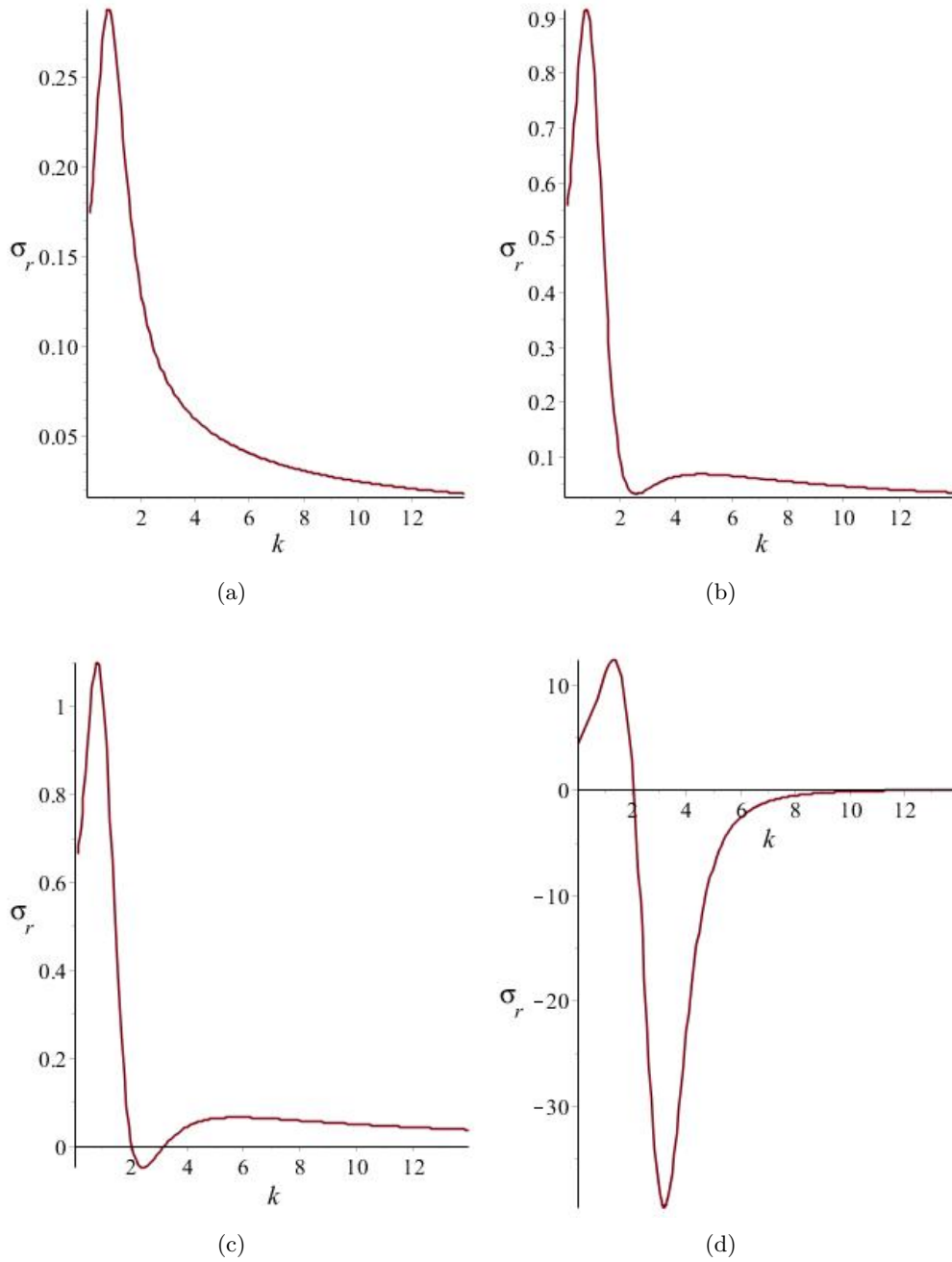


Figure 5: Plots of the subdominant damping term  $\sigma_r(\omega_0)$  vs  $k(\omega_0)$  for a)  $\frac{\omega_c}{\omega_p} = \frac{1}{2}$ , b)  $\frac{\omega_c}{\omega_p} = 1$ , c)  $\frac{\omega_c}{\omega_p} = 1.1$  and d)  $\frac{\omega_c}{\omega_p} = 3$ .

For background magnetic field strengths sufficiently low such that  $0 < \frac{\omega_c}{\omega_p} \lesssim 1$ , inspection of Figures 5(a) and 5(b) reveal the subdominant damping term to be positive for all frequencies, and

hence  $\sigma_r$  will act to counter the damping from the dominant term. The greatest effect will be felt by the lowest frequency waves. Additionally, note that unlike  $\zeta_r$ ,  $\sigma_r$  contains a turning point. This maximum increases as the background field is increased.

Interesting behaviour occurs just after  $\omega_c$  exceeds  $\omega_p$ , as seen in Figure 5(c). Past this point,  $\sigma_r$  develops a second turning point, and additionally becomes negative for certain frequencies, enhancing the damping due to  $\zeta_r$ . We can see from Figure 5(d) that the range of frequencies over which this enhancement occurs grows larger, the stronger the background field becomes.

### Examination of the turning points

While obtaining the exact values of  $\omega_0$  that correspond to the turning points of  $\sigma_r$  would be ideal,  $\frac{d\sigma_r}{d\omega_0}$  is a twelfth order polynomial in  $\omega_0$ ,

$$\begin{aligned}
\frac{d\sigma_r}{d\omega_0} = & 136 \omega_c^7 \omega_p^2 \omega_0^3 - 344 \omega_c^7 \omega_0^5 + 112 \omega_c^6 \omega_p^4 \omega_0^2 - 496 \omega_c^6 \omega_p^2 \omega_0^4 + 712 \omega_c^6 \omega_0^6 + 42 \omega_c^5 \omega_p^6 \omega_0 \\
& - 245 \omega_c^5 \omega_p^4 \omega_0^3 + 452 \omega_c^5 \omega_p^2 \omega_0^5 - 632 \omega_c^5 \omega_0^7 + 6 \omega_c^4 \omega_p^8 - 40 \omega_c^4 \omega_p^6 \omega_0^2 - 45 \omega_c^4 \omega_p^4 \omega_0^4 \\
& + 420 \omega_c^4 \omega_p^2 \omega_0^6 + 40 \omega_c^4 \omega_0^8 - 59 \omega_c^3 \omega_p^6 \omega_0^3 + 440 \omega_c^3 \omega_p^4 \omega_0^5 - 1040 \omega_c^3 \omega_p^2 \omega_0^7 + 376 \omega_c^3 \omega_0^9 \\
& + 75 \omega_c^2 \omega_p^6 \omega_0^4 - 280 \omega_c^2 \omega_p^4 \omega_0^6 + 664 \omega_c^2 \omega_p^2 \omega_0^8 - 296 \omega_c^2 \omega_0^{10} - 18 \omega_c \omega_p^6 \omega_0^5 - 27 \omega_c \omega_p^4 \omega_0^7 \\
& - 124 \omega_c \omega_p^2 \omega_0^9 + 88 \omega_c \omega_0^{11} + 45 \omega_p^4 \omega_0^8 - 12 \omega_p^2 \omega_0^{10} - 8 \omega_0^{12} + 64 \omega_c^8 \omega_0^4. \tag{218}
\end{aligned}$$

Obtaining analytical information about the roots of such a polynomial is difficult. However, we can still obtain some information by examining  $\sigma_r$  in the limit  $\omega_c \ll \omega_p$ . In Figure 5 we parametrically plotted  $\sigma_r(\omega_0)$  vs  $k(\omega_0)$ ; however for the purposes of examining the turning point it is convenient to plot  $\sigma(\omega_0)$  vs  $\omega_0$ . Figure 6 below, is such a plot, taken over a small range of  $\omega_0$  about the turning point, for  $\omega_c = 0.01$  and  $\omega_p = 1$ .

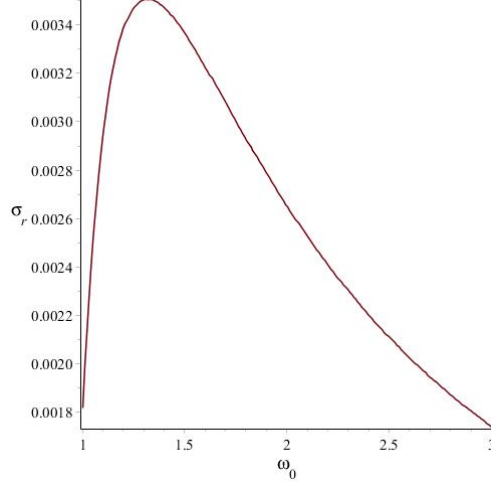


Figure 6: A closer examination of the first turning point of  $\sigma_r(\omega_0)$ , with  $\frac{\omega_c}{\omega_p} = 0.01$ .

From inspection of this plot, we can see that the turning point occurs close to the point at which  $\omega_0 \approx \omega_p$ . This suggests the introduction of

$$\chi_r = \frac{\omega_0}{\omega_p}, \quad (219)$$

and

$$\psi_r = \frac{\omega_c}{\omega_p}. \quad (220)$$

Recasting  $\frac{d\sigma_r}{d\omega_0}$  in terms of  $\chi_r$  and  $\psi_r$  and discarding terms  $\mathcal{O}(\psi_r)$  and higher, one obtains the quartic equation

$$8\chi_r^4 + 12\chi_r^2 - 45 = 0. \quad (221)$$

This can then be solved, informing us that the turning point occurs at

$$\omega_0 = 1.32\omega_p. \quad (222)$$

The second turning point does not exist when  $\omega_c \ll \omega_p$ ; however from inspection of Figure 5, one might conclude that the second turning point remains in the limit  $\omega_c \gg \omega_p$ , and hence an analysis in this limit is called for.

However, note that  $\sigma_r$  contains a factor of  $\frac{1}{\omega_c - \omega_0}$ . Hence we encounter a singularity when  $\omega_0$  is equal to the cyclotron frequency. An inspection of (214) reveals that this can occur in the limit  $\omega_c \gg \omega_p$ , in fact it occurs precisely at the cutoff frequency. Hence it is inadvisable to work in such a limit.

Note that this is not an effect of radiation reaction, or a result of working in the warm fluid model, but rather a known feature of the R mode. This can clearly be seen by inspection of Table 2.

## 4.2 L Mode

The L mode is left hand circularly polarised. Using the same method as Section 4.1 one can show the L mode satisfies a dispersion relation of the form

$$\frac{k^2}{\omega^2} = \frac{\omega \omega_c + \omega^2 - \omega_p^2}{\omega(\omega + \omega_c)} + \frac{\theta}{2} \left( \frac{(\omega^3 + 3\omega \omega_c^2 + 4\omega^2 \omega_c - 2\omega_c \omega_p^2) \omega_p^2}{\omega (\omega_c + \omega)^4} \right) + i\tau \left[ \frac{\omega \omega_p^2}{(\omega + \omega_c)^2} + \frac{\omega_c \omega_p^2 \theta (4\omega \omega_c^2 + \omega^3 + \omega \omega_p^2 + 5\omega^2 \omega_c - 3\omega_c \omega_p^2)}{(\omega_c + \omega)^5} \right].$$

We again express  $k$  in terms of  $\omega_0$ , but this time with

$$k^2 = \frac{\omega_0 (\omega_0 \omega_c + \omega_0^2 - \omega_p^2)}{\omega_c + \omega_0}. \quad (223)$$

Continuing the procedure of the previous section, one can obtain an expression for  $\omega$ , which can be found in Appendix C, and is examined below.

### 4.2.1 Analysis of the Dispersion Relation

#### Frequency Shift

As with the R mode, the real part of  $\omega$  acts only to shift the frequency of the wave, and once again this shift has no dependence on  $\tau$ . The warm fluid correction to the frequency shift of the L mode is

$$-\frac{\theta}{2} \frac{(3\omega_c^2 \omega_0 - 2\omega_c \omega_p^2 + 4\omega_c \omega_0^2 + \omega_0^3) \omega_p^2 \omega_0}{(\omega_c + \omega_0)^2 (2\omega_c^2 \omega_0 - \omega_c \omega_p^2 + 4\omega_c \omega_0^2 + 2\omega_0^3)}. \quad (224)$$

#### Dominant Damping

The imaginary part of  $\omega$  is again of the form  $\zeta_l \tau + \sigma_l \tau \theta$ , and so again the damping effect will be dominated by the  $\zeta_l$  term. In the case of the L mode,

$$\zeta_l = -\frac{\omega_p^2 \omega_0^3}{2\omega_0 \omega_c^2 + 4\omega_0^2 \omega_c - \omega_c \omega_p^2 + 2\omega_0^3}. \quad (225)$$

The L mode has a cutoff frequency

$$\omega_{\text{co}} = \frac{1}{2} \left( \sqrt{\omega_c^2 + 4\omega_p^2} - \omega_c \right). \quad (226)$$

As was the case with the R mode, for  $\omega_0$  much larger than the cutoff frequency

$$\zeta_l \approx -\frac{1}{2} \omega_p^2, \quad (227)$$

and so all frequencies in this region will experience the same amount of damping. Additionally the strength of this damping will have no dependence on the strength of the background field.

However, for frequencies close to  $\omega_{\text{co}}$ ,  $\zeta_l$  takes the form

$$\zeta_l \approx -\frac{1}{2} \frac{\left( \omega_c - \sqrt{\omega_c^2 + 4\omega_p^2} \right)^2 \omega_p^2}{\left( \omega_c + \sqrt{\omega_c^2 + 4\omega_p^2} \right) \sqrt{\omega_c^2 + 4\omega_p^2}}. \quad (228)$$

If the background field is sufficiently strong such that  $\omega_c \gg \omega_p$ , then

$$\zeta_l \approx 0. \quad (229)$$

Hence, in a strongly magnetised plasma, frequencies close to  $\omega_{\text{co}}$  will experience negligible damping.

If, on the other hand,  $\omega_c \ll \omega_p$ ,

$$\zeta_l \approx -\frac{1}{2} \omega_p^2. \quad (230)$$

Thus, just as was the case with the R mode, the strength of the background field will affect those waves with frequency close to cutoff.

This can be seen more clearly from an examination of Figure 7 below.

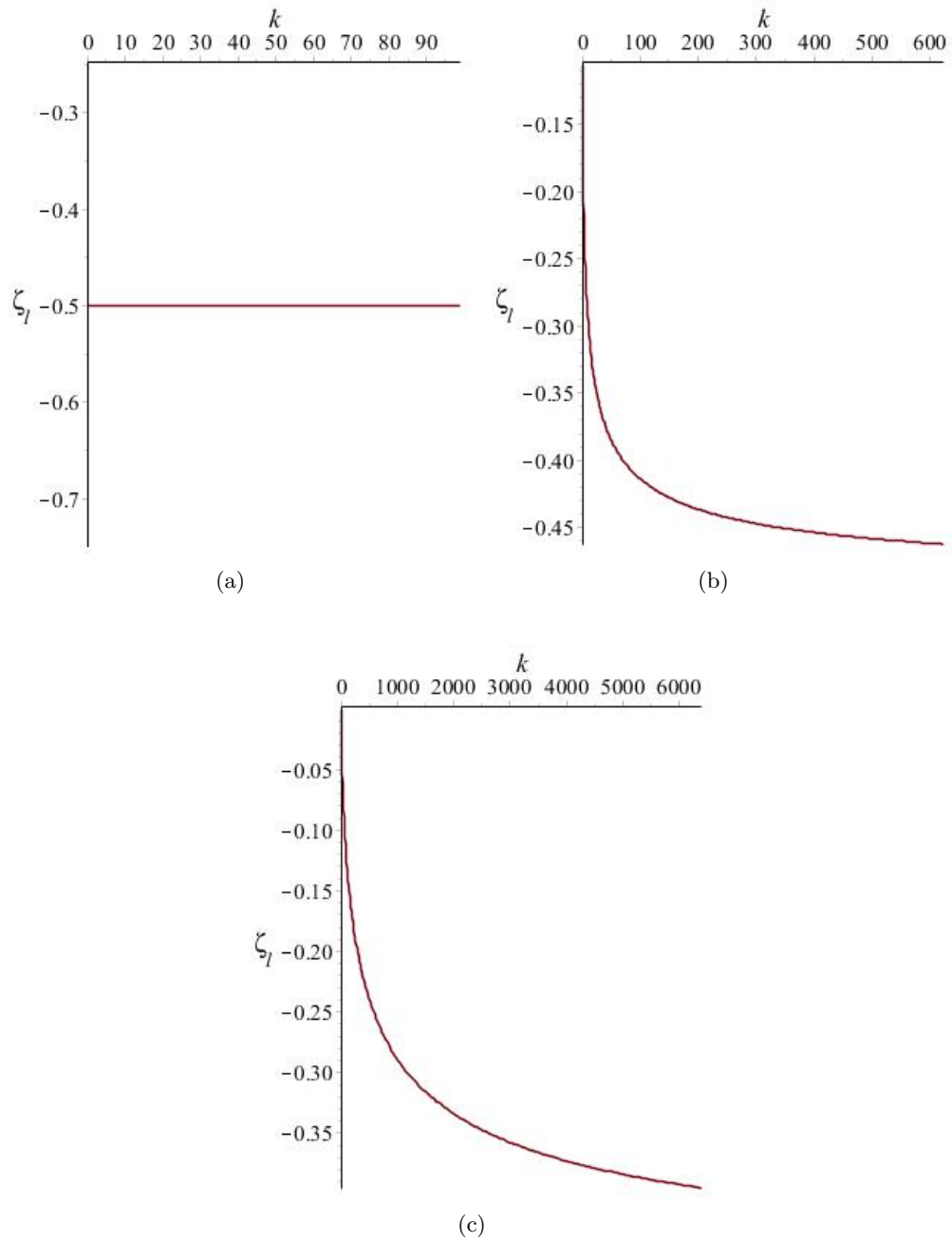


Figure 7: Plots of the dominant damping term  $\zeta_l(\omega_0)$  vs  $k(\omega_0)$  for a)  $\frac{\omega_c}{\omega_p} = 0$ , b)  $\frac{\omega_c}{\omega_p} = 1$  and c)  $\frac{\omega_c}{\omega_p} = 10$ . Note that the horizontal scale differs from that of Figure 4.

### **Subdominant Damping**

The subdominant damping term close to, and far from, cutoff has a simple behaviour. Repeating the procedure we performed when studying  $\sigma_r$  reveals that  $\sigma_l$  vanishes for frequencies close to, and far from, cutoff, irrespective of the strength of the background field.

However, we once again see interesting behaviour between these limits, as shown in Figure 8:

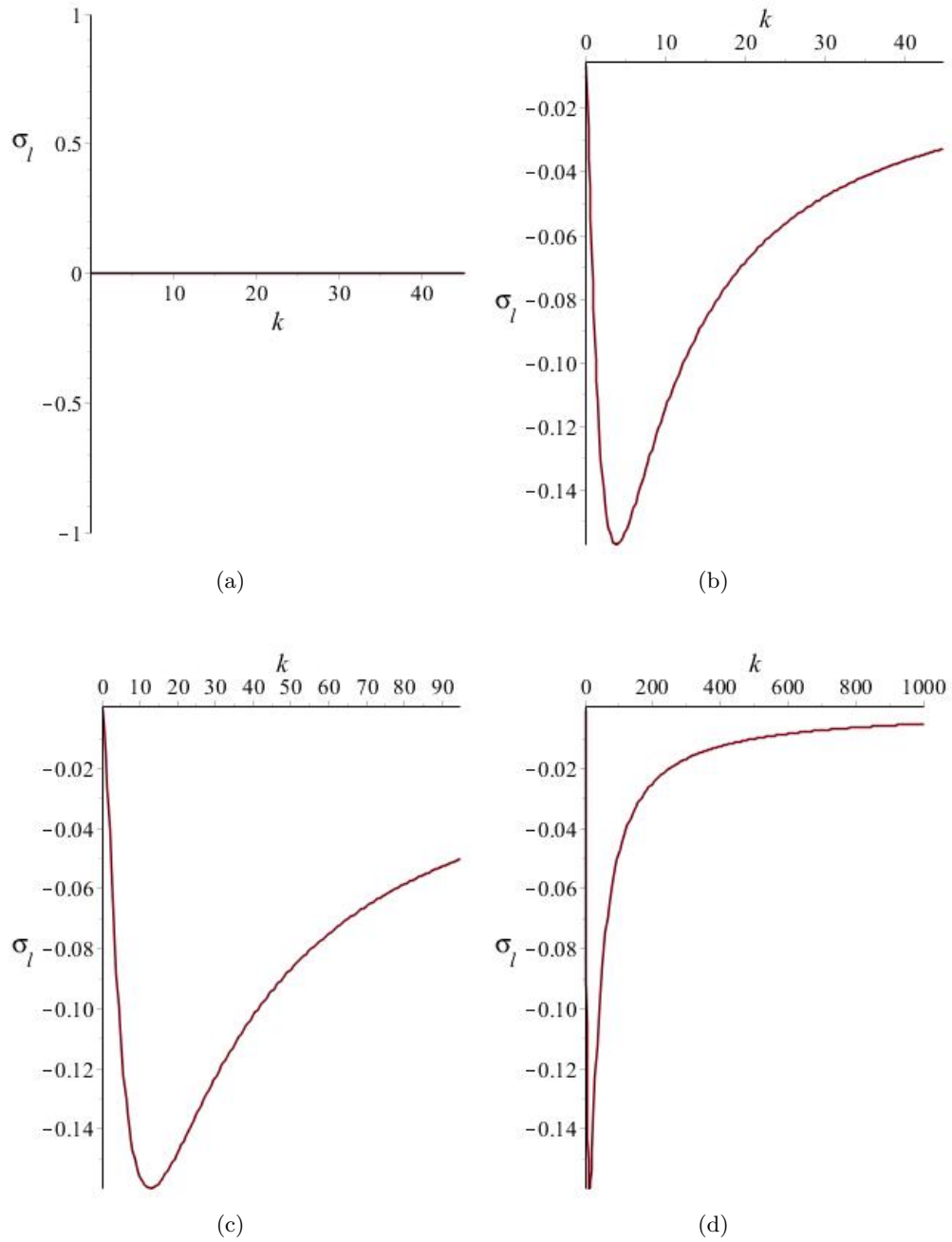


Figure 8: Plots of the subdominant damping term  $\sigma_l(\omega_0)$  vs  $k(\omega_0)$  for a)  $\frac{\omega_c}{\omega_p} = 0$ , b)  $\frac{\omega_c}{\omega_p} = 3$  and c)  $\frac{\omega_c}{\omega_p} = 10$ . Plot d) shows the behaviour far from cutoff. Note that the horizontal scale differs from that of Figure 5.

As can be seen,  $\sigma_l$  is negative for all frequencies, irrespective of the strength of a background

field<sup>38</sup>. Thus this term acts to enhance the damping caused by the radiation reaction term  $\zeta_l$ . Note also that unless there is no background magnetic field, this term contains a turning point which corresponds to maximal damping. We examine this turning point in more detail below.

### Examination of the turning point

Repeating the procedure we used to examine the turning points of  $\sigma_r$  in the previous section, we once again obtain a twelfth order polynomial in  $\omega_0$ ;

$$\begin{aligned}
\frac{d\sigma_r}{d\omega_0} = & -136 \omega_c^7 \omega_p^2 \omega_0^3 + 344 \omega_c^7 \omega_0^5 + 112 \omega_c^6 \omega_p^4 \omega_0^2 - 496 \omega_c^6 \omega_p^2 \omega_0^4 + 712 \omega_c^6 \omega_0^6 - 42 \omega_c^5 \omega_p^6 \omega_0 \\
& + 245 \omega_c^5 \omega_p^4 \omega_0^3 - 452 \omega_c^5 \omega_p^2 \omega_0^5 + 632 \omega_c^5 \omega_0^7 + 6 \omega_c^4 \omega_p^8 - 40 \omega_c^4 \omega_p^6 \omega_0^2 - 45 \omega_c^4 \omega_p^4 \omega_0^4 \\
& + 420 \omega_c^4 \omega_p^2 \omega_0^6 + 40 \omega_c^4 \omega_0^8 + 59 \omega_c^3 \omega_p^6 \omega_0^3 - 440 \omega_c^3 \omega_p^4 \omega_0^5 + 1040 \omega_c^3 \omega_p^2 \omega_0^7 - 376 \omega_c^3 \omega_0^9 \\
& + 75 \omega_c^2 \omega_p^6 \omega_0^4 - 280 \omega_c^2 \omega_p^4 \omega_0^6 + 664 \omega_c^2 \omega_p^2 \omega_0^8 - 296 \omega_c^2 \omega_0^{10} + 18 \omega_c \omega_p^6 \omega_0^5 + 27 \omega_c \omega_p^4 \omega_0^7 \\
& + 124 \omega_c \omega_p^2 \omega_0^9 - 88 \omega_c \omega_0^{11} + 45 \omega_p^4 \omega_0^8 - 12 \omega_p^2 \omega_0^{10} - 8 \omega_0^{12} + 64 \omega_c^8 \omega_0^4. \tag{231}
\end{aligned}$$

While not able to solve this expression analytically, we are once again able to study the turning point in the limits  $\frac{\omega_c}{\omega_p} \ll 1$  and  $\frac{\omega_c}{\omega_p} \gg 1$ . Figure 9 examines the turning point in more detail.

---

<sup>38</sup>Unless the field is zero, in which case this term vanishes.

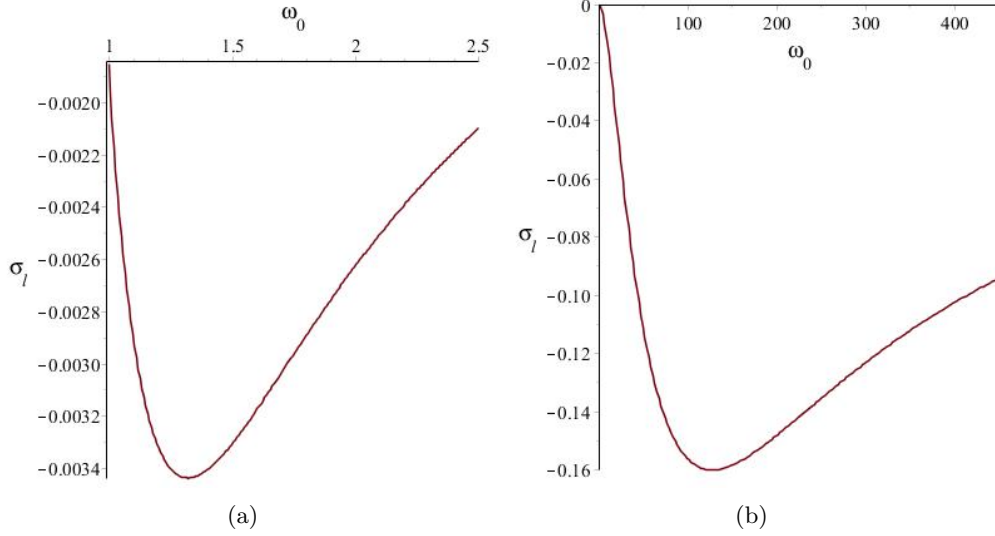


Figure 9: A closer examination of the turning point of  $\sigma_l(\omega_0)$ . In plot a)  $\omega_c = 0.01$  and  $\omega_p = 1$ , while in plot b)  $\omega_c = 100$  and  $\omega_p = 1$ .

From inspection of Figure 9(a), we see that when  $\frac{\omega_c}{\omega_p} \ll 1$ , the turning point occurs somewhere close to the point  $\omega_0 = \omega_p$ . Introducing  $\chi_l = \frac{\omega_0}{\omega_p}$  and  $\psi_l = \frac{\omega_c}{\omega_p}$ , we again recast  $\frac{d\sigma_l}{d\omega_0}$  in terms of  $\chi_l$  and  $\psi_l$ . Then, expanding as a series in  $\psi_l$  and discarding terms of  $\mathcal{O}(\psi)$  and higher we find

$$\omega_0 = 1.32 \omega_p. \quad (232)$$

Interestingly, the above result is identical to (222), the location of the turning point in the case of the R mode, though we must keep in mind that the above is simply an approximation.

Similarly, from inspection of Figure 9(b), we see that when  $\frac{\omega_c}{\omega_p} \gg 1$ , the turning point occurs somewhere close to the point  $\omega_0 = \omega_c$ . Introducing  $\hat{\chi}_l = \frac{\omega_0}{\omega_c}$  and  $\hat{\psi}_l = \frac{\omega_p}{\omega_c}$ , we again recast  $\frac{d\sigma_l}{d\omega_0}$  in terms of  $\hat{\chi}_l$  and  $\hat{\psi}_l$ . Then, expanding as a series in  $\hat{\psi}_l$  and discarding terms of  $\mathcal{O}(\hat{\psi})$  and higher we find

$$\omega_0 = 1.27 \omega_c. \quad (233)$$

Recall from the previous section that the turning point for  $\sigma_r$  occurred at  $\omega_0 = 1.32 \omega_c$ .

### 4.3 O Mode

The O mode is plane polarised, with the electric field parallel to the background magnetic field. In the cold, non-radiating plasma its dispersion relation is that of an electromagnetic wave in vacuum.

In a warm, radiating plasma it takes the form

$$\frac{k^2}{\omega^2} = \frac{\omega^2 - \omega_p^2}{\omega^2} + \frac{\theta \omega_p^2 (3\omega_c^2 - \omega^2 - 2\omega_p^2)}{2(\omega_c - \omega)(\omega_c + \omega)\omega^2} + i \frac{\omega_p^2}{\omega} \tau - \frac{i\omega_p^2 (\omega_c^4 - 3\omega_c^2 \omega^2 + 2\omega_p^2 \omega^2)}{(\omega_c - \omega)^2 (\omega_c + \omega)^2 \omega} \tau \theta. \quad (234)$$

Following the same procedure of the previous sections, we once again express  $k$  in terms of  $\omega_0$ , but this time with

$$k^2 = \omega_0^2 - \omega_p^2. \quad (235)$$

Once again, the full expression for  $\omega(\omega_0)$  can be obtained, and is included in Appendix C.

#### 4.3.1 Analysis of the Dispersion Relation

##### Frequency Shift

The warm fluid correction to the frequency shift of the O mode is

$$-\frac{\theta}{4} \frac{(3\omega_c^2 - 2\omega_p^2 - \omega_0^2) \omega_p^2}{\omega_0 (\omega_c - \omega_0) (\omega_c + \omega_0)}. \quad (236)$$

Note the presence of  $(\omega_c - \omega_0)$  in the denominator; we once again find singularities should  $\omega_0 = \omega_c$ , just as we did when examining the R mode in Section 4.1. To see if the singularity will occur for physical waves, we must again look to the cutoff frequency. For the O mode

$$\omega_{co} = \omega_p, \quad (237)$$

hence provided  $\omega_p > \omega_c$  the singularity will not occur for any physical wave.

Note that once again this limitation is not related to the warm fluid correction, or to radiation reaction, but to the cold, non-radiating dispersion relation the O mode obeys, as can be seen from

Table 2.

### Dominant Damping

In contrast to the modes that we have studied so far, the dominant damping term  $\zeta_o$  for the O mode takes the very simple form

$$\zeta_o = -\frac{1}{2} \omega_p^2. \quad (238)$$

Unlike in the cases of the L & R modes, this damping has no dependence on either the frequency of the wave or on the magnitude of the background magnetic field.

### Subdominant Damping

The subdominant damping term  $\sigma_o$  is given by

$$\sigma_o = \frac{1}{2} \omega_p^2 \frac{\omega_c^2 \omega_p^2 - 3 \omega_c^2 \omega_0^2 + \omega_c^4 - \omega_p^4 + 2 \omega_p^2 \omega_0^2}{(\omega_c + \omega_0)^2 (\omega_c - \omega_0)^2}. \quad (239)$$

Note that once again we encounter a singularity when  $\omega_0 = \omega_c$ , and hence must ensure that at no point does  $\omega_c$  exceed  $\omega_p$ . This term is plotted in Figure 10, and exhibits some familiar behaviour.

As we increase the strength of the magnetic field,  $\sigma_o$  develops a turning point. We saw this same behaviour occur in Figure 5 in Section 4.1, when studying the R mode. Due to the complicated nature of  $\sigma_r$ , we were unable to obtain an analytic expression for the location of this turning point. However,  $\sigma_o$  is significantly simpler, and hence a study of it may prove insightful.

Differentiating (239) with respect to  $\omega_0$  we find

$$\frac{d\sigma_o}{d\omega_0} = -\frac{\omega_p^2 \omega_0 (\omega_c^4 - 4 \omega_c^2 \omega_p^2 + 3 \omega_c^2 \omega_0^2 + 2 \omega_p^4 - 2 \omega_p^2 \omega_0^2)}{(\omega_c - \omega_0)^3 (\omega_c + \omega_0)^2}. \quad (240)$$

Setting the above to zero, and solving for  $\omega_0$  allows us to obtain an expression for the location of the turning point,

$$\omega_0 = \frac{\sqrt{(4 \omega_c^2 \omega_p^2 - \omega_c^4 - 2 \omega_p^4)}}{\sqrt{3 \omega_c^2 - 2 \omega_p^2}}. \quad (241)$$

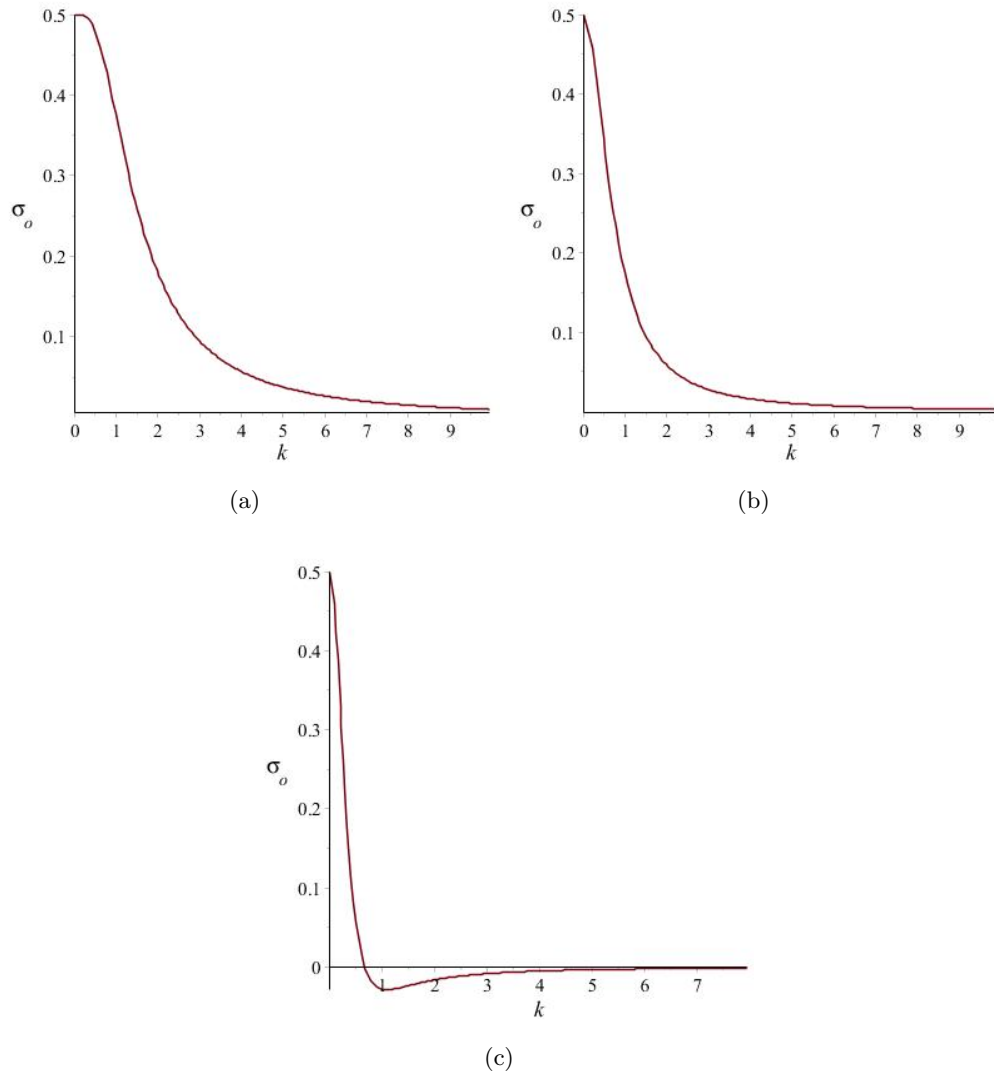


Figure 10: Plots of the subdominant damping term  $\sigma_o(\omega_0)$  vs  $k(\omega_0)$  for a)  $\frac{\omega_c}{\omega_p} = 0$ , b)  $\frac{\omega_c}{\omega_p} = 0.7$  and c)  $\frac{\omega_c}{\omega_p} = 0.85$ .

By definition,  $\omega_0$  is real and positive, hence the turning point will only exist when the right-hand side of (241) is real and positive. This can be shown to hold true when

$$(2 + \sqrt{2})\omega_p^2 \geq \omega_c^2 \geq \frac{2}{3}\omega_p^2. \quad (242)$$

Thus, for magnetic fields such that  $\omega_c$  lies outside of this range,  $\sigma_o$  will always be positive and will act to counter the effect of  $\zeta_o$ . However, for  $\omega_c$  within this range,  $\sigma_o$  will act to enhance the damping of  $\zeta_o$  for some frequencies.

#### 4.4 X Mode

The X mode is partly transverse, and partly parallel to the background magnetic field. It can be shown to satisfy a dispersion relation of the form

$$\frac{k^2}{\omega^2} = \frac{\omega_c^2 \omega^2 - \omega_p^4 + 2\omega_p^2 \omega^2 - \omega^4}{\omega^2 (\omega_c^2 + \omega_p^2 - \omega^2)} + \frac{\theta \omega_p^2 (\omega_c^2 \omega^2 + \omega_p^4 - 2\omega_p^2 \omega^2 + \omega^4)}{(\omega_p^2 - \omega^2 + \omega_c^2)^2 \omega^2} + i\tau \left[ \frac{(\omega_c^2 \omega^2 + \omega_p^4 - 2\omega_p^2 \omega^2 + \omega^4) \omega_p^2}{(\omega_p^2 - \omega^2 + \omega_c^2)^2 \omega} + \theta \frac{\omega_p^2 \omega_c^2 (3\omega^4 - 3\omega_p^2 \omega^2 + \omega_p^4 + \omega_c^2 \omega_p^2)}{(\omega_p^2 - \omega^2 + \omega_c^2)^3 \omega} \right]. \quad (243)$$

To proceed, we once again carry out the procedure outlined in Section 4.1, but this time with

$$k^2 = \frac{\omega_c^2 \omega_0^2 - \omega_p^4 + 2\omega_p^2 \omega_0^2 - \omega_0^4}{(\omega_c^2 + \omega_p^2 - \omega_0^2)}. \quad (244)$$

The full expression for  $\omega(\omega_0)$  can be found in Appendix C. We will examine its individual terms in detail below, but before we do so, we must introduce the concept of resonance.

Recall from Section 1.2.2, our discussion of the cutoff frequency  $\omega_{co}$ . A cutoff occurs at any point in a plasma where the index of refraction goes to zero; and hence where the wavelength of a wave becomes infinite. This is all that we have needed in our discussions so far, however to examine the dispersion relation of the X mode we must also discuss the resonant frequency.

A resonance occurs at any point in the plasma where the index of refraction becomes infinite, and hence the wavelength of a wave goes to zero. In general, waves are reflected at cutoffs and absorbed at resonances[32].

The R, L and O modes all have a cutoff frequency below which waves cannot propagate. The situation is slightly different for the X mode, which has two regions in which waves can propagate. In a cold, non radiating plasma it can be shown that a X mode with frequency  $\omega$  such that  $\omega_{co_r} < \omega < \infty$  can propagate freely, where

$$\omega_{co_r} = \frac{1}{2} \left( \sqrt{\omega_c^2 + 4\omega_p^2} + \omega_c \right) \quad (245)$$

is the cutoff frequency of the R mode.

Immediately below this frequency propagation is not possible, however as the frequency further decreases, it reaches a value known as the *upper hybrid* frequency  $\omega_h$ , where

$$\omega_h^2 = \omega_c^2 + \omega_p^2. \quad (246)$$

Waves with frequency below this value can also propagate, provided their frequency is not less than  $\omega_{\text{co}l}$ , where

$$\omega_{\text{co}l} = \frac{1}{2} \left( \sqrt{\omega_c^2 + 4\omega_p^2} - \omega_c \right), \quad (247)$$

is the cutoff frequency of the L mode.

Thus, the region  $\omega_{\text{co}l} < \omega < \omega_h$  is another region in which propagation is possible. Note that this behaviour only occurs if the plasma is magnetised; in an unmagnetised plasma  $\omega_{\text{co}l} = \omega_{\text{co}r} = \omega_h = \omega_p$  and hence the lower allowed region vanishes.

We will explore both of these regions in the remainder of the section.

#### 4.4.1 Analysis of the Dispersion Relation

##### Frequency Shift

The warm fluid correction to the frequency shift of the X mode is

$$\frac{\theta}{4} \frac{-\omega_c^2 \omega_p^2 \omega_0^2 - \omega_p^2 \omega_0^4 + 2\omega_p^4 \omega_0^2 - \omega_p^6}{(\omega_c^4 + 3\omega_c^2 \omega_p^2 - 2\omega_0^2 \omega_c^2 + \omega_p^4 + \omega_0^4 - 2\omega_p^2 \omega_0^2) \omega_0}. \quad (248)$$

As with the other modes, this term is independent of the effects of radiation reaction.

##### Dominant Damping

The dominant damping term  $\zeta_x$  for the case of the X mode is given by

$$\zeta_x = \frac{1}{2} \frac{-\omega_c^2 \omega_0^2 \omega_p^2 - \omega_p^6 - \omega_p^2 \omega_0^4 + 2\omega_0^2 \omega_p^4}{2\omega_c^4 + 3\omega_c^2 \omega_p^2 - 2\omega_0^2 \omega_c^2 + \omega_p^4 + \omega_0^4 - 2\omega_p^2 \omega_0^2}. \quad (249)$$

**In the Region**  $\omega_{\text{coI}} < \omega < \omega_h$

Let us first examine  $\zeta_r$  in the region  $\omega_{\text{coI}} < \omega < \omega_h$ . Note that there is little point examining the behaviour of this region in the limit  $\omega_c \ll \omega_p$ , since in this limit the region vanishes.

Close to  $\omega_{\text{coI}}$

$$\zeta_x \approx -\frac{\omega_p^2 \left( \omega_c^2 - \omega_c \sqrt{\omega_c^2 + 4\omega_p^2} + 2\omega_p^2 \right)}{\omega_c^2 + \omega_c \sqrt{\omega_c^2 + 4\omega_p^2} + 4\omega_p^2}, \quad (250)$$

which can be seen to be negligible when  $\omega_c \gg \omega_p$ .

Close to  $\omega_h$ ,

$$\zeta_x \approx -\left( \omega_c^2 + \frac{1}{2}\omega_p^2 \right). \quad (251)$$

Thus, frequencies close to  $\omega_{\text{coI}}$  will experience negligible damping, while the strength of the damping that higher frequencies will experience is dependent on the strength of the background magnetic field. This behaviour is plotted in Figure 11.

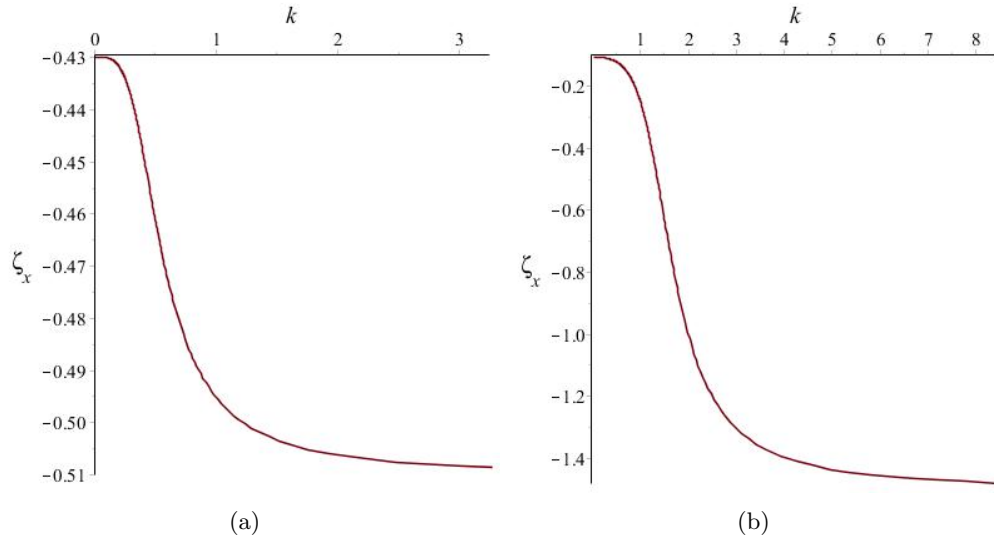


Figure 11: Plots of the dominant damping term  $\zeta_x(\omega_0)$  vs  $k(\omega_0)$  in the region  $\omega_{\text{coI}} < \omega_0 < \omega_h$  with a)  $\frac{\omega_c}{\omega_p} = 0.1$ , b)  $\frac{\omega_c}{\omega_p} = 1$ .

**In the Region**  $\omega_{\text{co},r} < \omega_0 < \infty$

Next we examine  $\zeta_x$  for frequencies in the region  $\omega_{\text{co},r} < \omega_0 < \infty$ . Close to  $\omega_{\text{co},r}$  we find

$$\zeta_x \approx -\frac{\omega_p^2 \left( \omega_c^2 + \omega_c \sqrt{\omega_c^2 + 4\omega_p^2} + 2\omega_p^2 \right)}{\omega_c^2 - \omega_c \sqrt{\omega_c^2 + 4\omega_p^2} + 4\omega_p^2}. \quad (252)$$

In the limit  $\omega_c \ll \omega_p$  this reduces to  $-\frac{1}{2}\omega_p^2$  as expected, while in the limit  $\omega_c \gg \omega_p$ ,

$$\zeta_x \approx -\omega_c^2. \quad (253)$$

Far from  $\omega_{\text{co},r}$  we find

$$\zeta_x \approx -\frac{1}{2}\omega_p^2, \quad (254)$$

which is independent of  $\omega_c$ .

Thus, high frequency waves will experience constant damping, while the damping experienced by those frequencies close to cutoff will depend on the strength of the background field<sup>39</sup>. Figure 12 shows this behaviour.

---

<sup>39</sup>Though the damping such frequencies experience cannot be less than  $|\frac{1}{2}\omega_p^2|$ .

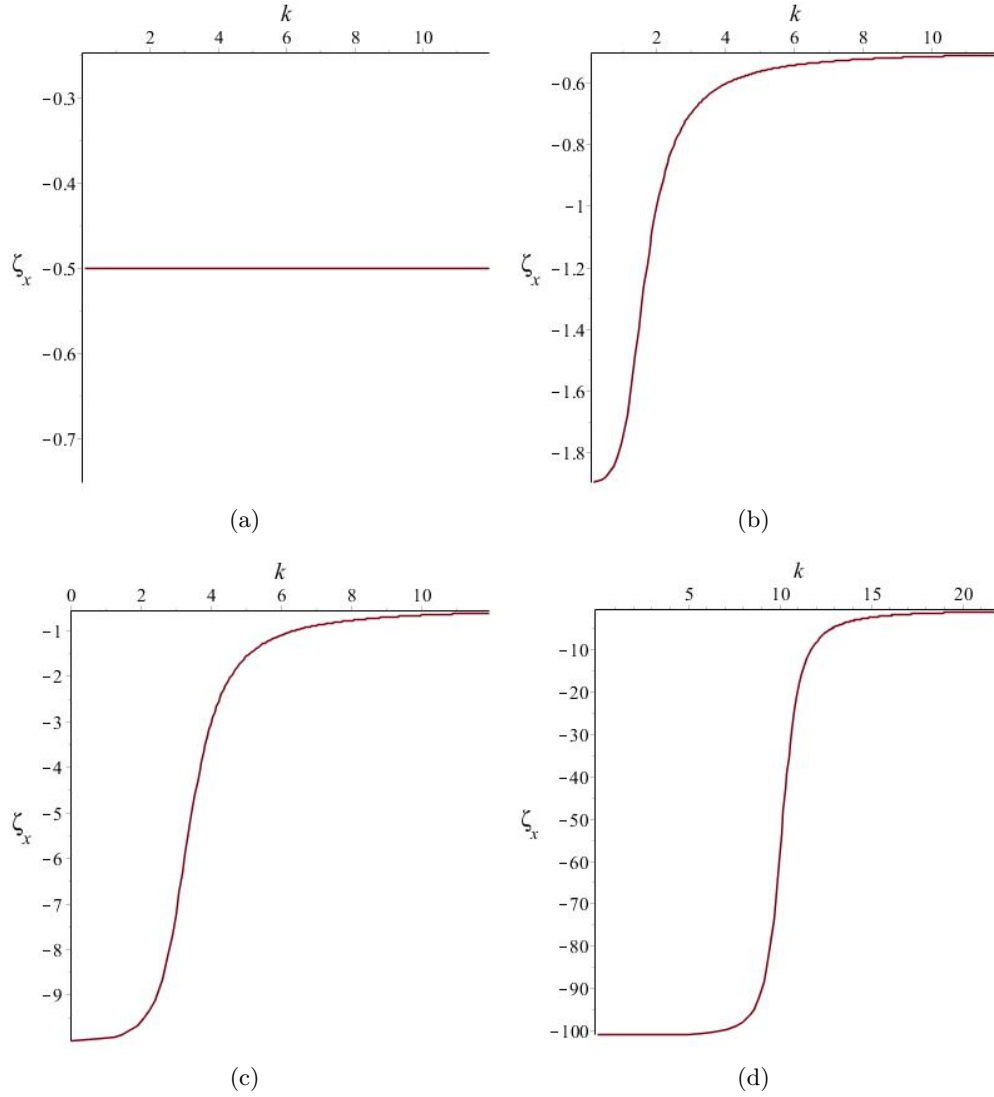


Figure 12: Plots of the dominant damping term  $\zeta_x(\omega_0)$  vs  $k(\omega_0)$  in the region  $\omega_0 > \omega_{co,r}$  with  $\frac{\omega_c}{\omega_p} = 0, 1, 3$  and  $10$  respectively.

Note that the profile of  $\zeta_x$  appears similar to that of  $\zeta_r$  in Figure 4.

## Subdominant Damping

**In the Region**  $\omega_{co,l} < \omega_0 < \omega_h$

We will again start by examining the subdominant damping term  $\sigma_x$  for frequencies in the region  $\omega_{co,l} < \omega_0 < \omega_h$ .

Close to  $\omega_{co_l}$

$$\sigma_x \approx -\frac{2\omega_p^6\omega_c\left(\omega_c+3\sqrt{\omega_c^2+4\omega_p^2}\right)}{\left(\omega_c^2+\omega_c\sqrt{\omega_c^2+4\omega_p^2}+4\omega_p^2\right)^3}, \quad (255)$$

and can be shown to vanish for  $\omega_c \gg \omega_p$ . Hence frequencies close to the lower cutoff  $\omega_{co_l}$  experience negligible damping, irrespective of the strength of the background field.

Close to  $\omega_h$

$$\sigma_x = \frac{1}{2}\omega_c^2, \quad (256)$$

and so the damping experienced by these frequencies is heavily dependent on the strength of the background field. Figure 13 shows that within these limits interesting behaviour occurs.

Once again, we see that the subdominant term contains a turning point. We see that for the lower frequency waves,  $\sigma_x$  acts to enhance the damping due to  $\zeta_x$ . However for higher frequency waves  $\sigma_x$  is positive, and thus acts to reduce the amount of damping the waves experience. Additionally, increasing the strength of the background magnetic field, acts not only to increase the magnitude of the damping, but also shifts the position of the peak, altering which frequencies are affected the most.

$\frac{d\sigma_x}{d\omega_0}$  is a twelfth order polynomial in  $\omega_0$ ,

$$\begin{aligned} \frac{d\sigma_x}{d\omega_0} = & \omega_c^{12} + 4\omega_c^{10}\omega_p^2 - \omega_c^8\omega_p^4 - 25\omega_c^6\omega_p^6 - 41\omega_c^4\omega_p^8 - 20\omega_c^2\omega_p^{10} + 3\omega_p^{12} \\ & + (4\omega_c^{10} + 34\omega_c^8\omega_p^2 + 110\omega_c^6\omega_p^4 + 160\omega_c^4\omega_p^6 + 76\omega_c^2\omega_p^8 - 18\omega_p^{10})\omega_0^2 \\ & + (-23\omega_c^8 - 120\omega_c^6\omega_p^2 - 210\omega_c^4\omega_p^4 - 104\omega_c^2\omega_p^6 + 45\omega_p^8)\omega_0^4 \\ & + (32\omega_c^6 + 104\omega_c^4\omega_p^2 + 56\omega_c^2\omega_p^4 - 60\omega_p^6)\omega_0^6 + (-13\omega_c^4 - 4\omega_c^2\omega_p^2 + 45\omega_p^4)\omega_0^8 \\ & + (-4\omega_c^2 - 18\omega_p^2)\omega_0^{10} + 3\omega_0^{12}, \end{aligned} \quad (257)$$

and so just like with the L and R modes we cannot obtain an analytic expression for the turning point<sup>40</sup>. We can however once again examine it in the limit  $\omega_c \gg \omega_p$ . Carrying out a procedure

---

<sup>40</sup>Though it only contains even powers of  $\omega_0$ .

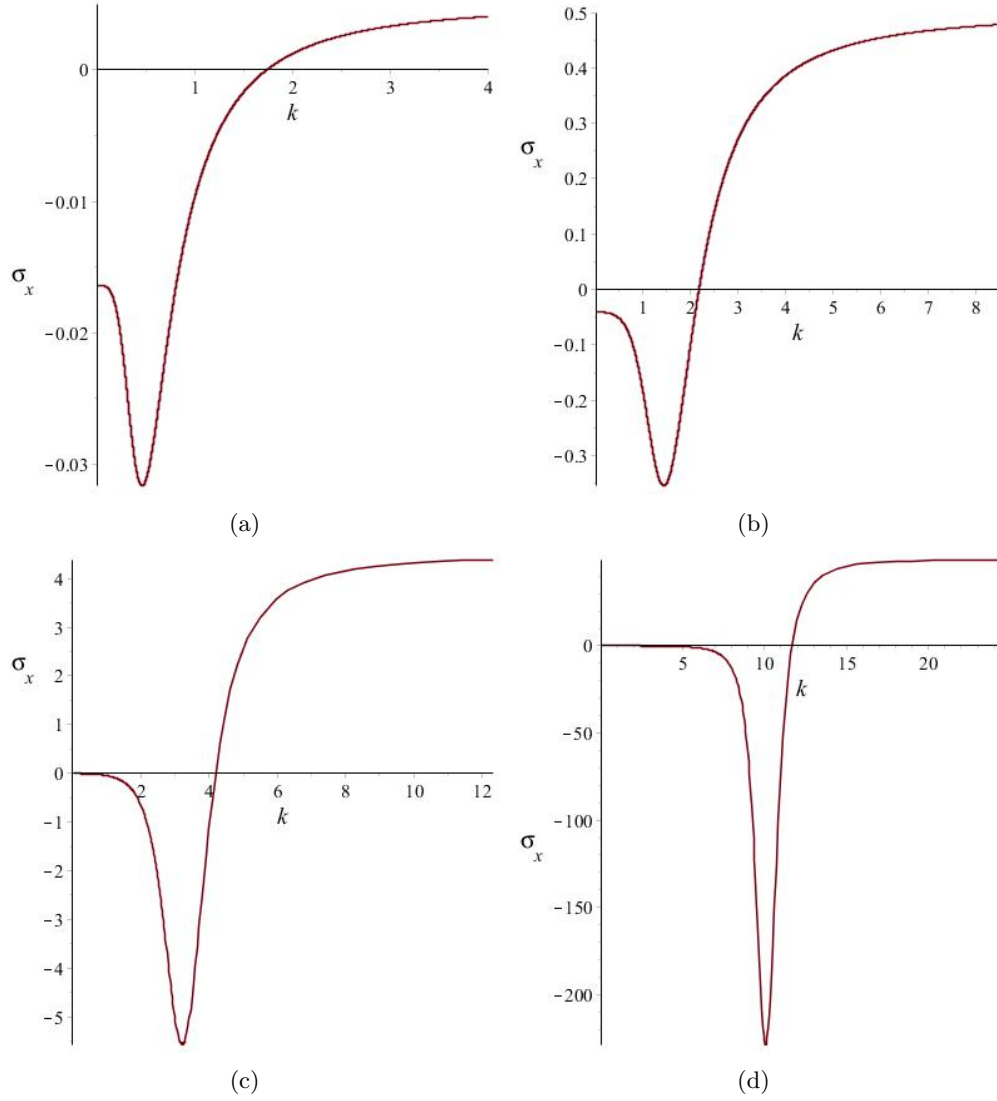


Figure 13: Plots of the subdominant damping term  $\sigma_x(\omega_0)$  vs  $k(\omega_0)$  in the region  $\omega_{co_l} < \omega_0 < \omega_h$  with a)  $\frac{\omega_c}{\omega_p} = 0.1$ , b)  $\frac{\omega_c}{\omega_p} = 1$ , c)  $\frac{\omega_c}{\omega_p} = 3$  and d)  $\frac{\omega_c}{\omega_p} = 10$ .

identical to that of Sections 4.1 and 4.2, we obtain the equation

$$(3\chi_x^4 + 8\chi_x^2 + 1)(\chi_x - 1)^4(\chi_x + 1)^4, \quad (258)$$

where  $\chi_x = \frac{\omega_0}{\omega_p}$ .

Solutions to the quartic equation have no real roots, thus the maximal damping occurs when  $\omega_0 = \omega_c$  (in the limit  $\omega_c \gg \omega_p$ ).

**In the Region**  $\omega_{\text{co},r} < \omega_0 < \infty$

Let us now examine frequencies in the region above  $\omega_{\text{co},r}$ . In this region, close to  $\omega_{\text{co},r}$

$$\sigma_x \approx -\frac{2\omega_p^6\omega_c\left(\omega_c - 3\sqrt{\omega_c^2 + 4\omega_p^2}\right)}{\left(\omega_c^2 - \omega_c\sqrt{\omega_c^2 + 4\omega_p^2} + 4\omega_p^2\right)^3}. \quad (259)$$

For  $\omega_c \ll \omega_p$  the subdominant term vanishes, however for  $\omega_c \gg \omega_p$

$$\sigma_x \approx \frac{1}{2}\omega_c^2. \quad (260)$$

Far from  $\omega_{\text{co},r}$ ,  $\sigma_x$  vanishes independently of the background magnetic field. However, we can see from Figure 14 that we once again find a turning point between these limits.

Our earlier calculation of the location of the turning point holds for this region. Hence the point still occurs at  $\omega_0 = \omega_c$ , however in this region  $\sigma_x$  is positive for all frequencies, thus acting in opposition to  $\zeta_x$ .

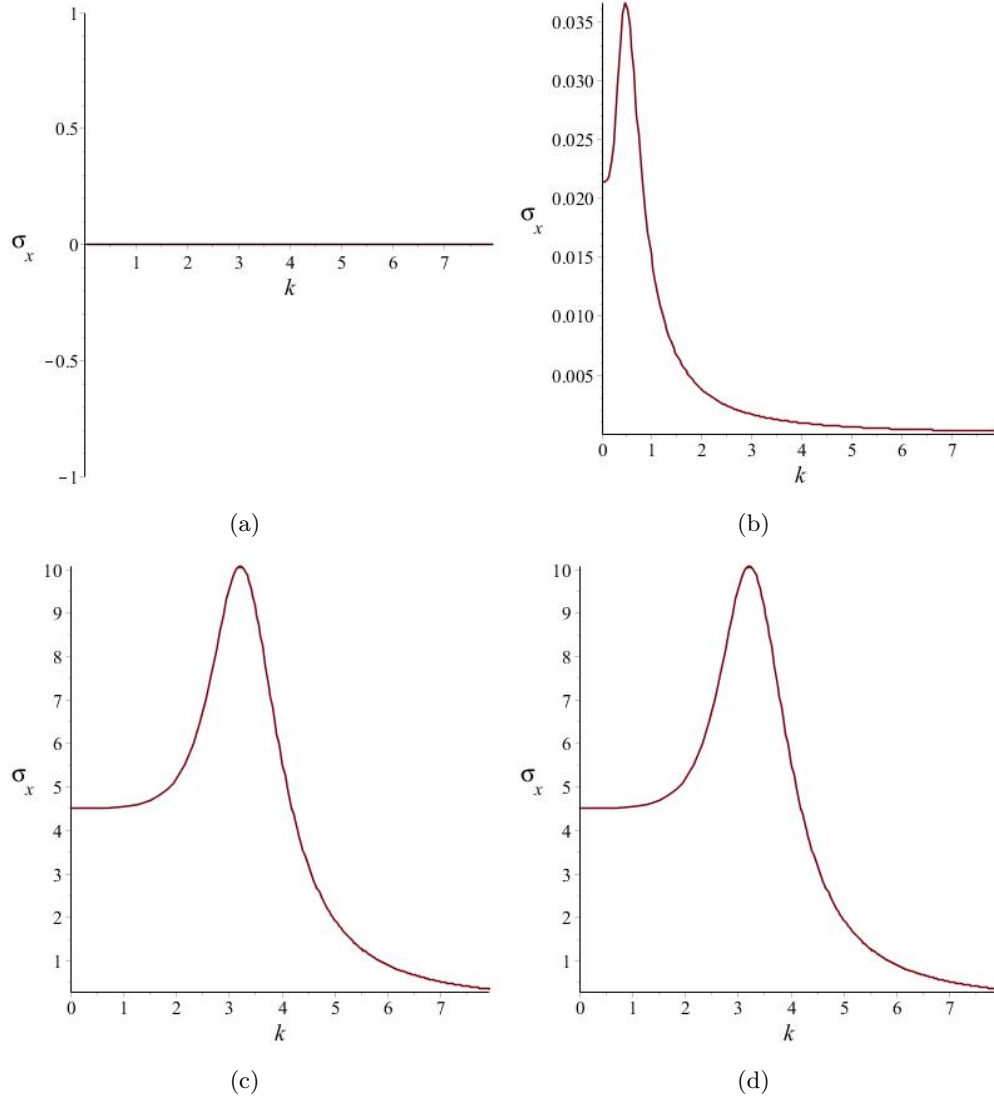


Figure 14: Plots of the subdominant damping term  $\sigma_x(\omega_0)$  vs  $k(\omega_0)$  in the region above  $\omega_{co_r}$  with a)  $\frac{\omega_c}{\omega_p} = 0$ , b)  $\frac{\omega_c}{\omega_p} = 0.1$ , c)  $\frac{\omega_c}{\omega_p} = 1$  and d)  $\frac{\omega_c}{\omega_p} = 3$ .

## 4.5 A Practical Application : Neutron Star Crusts

So far, we have examined the properties of the dispersion relations of various modes of an electromagnetic wave travelling through a plasma. We have split these dispersion relations up into four parts; the part found in cold, non-radiating plasmas, the part due to the warm fluid correction and the part due to the radiative correction (which itself has been split into the part neglecting the warm fluid approximation and the part that includes it). For convenience to the reader, these parts are now summarised in Table 3, which can be found at the end of this section.

Up to this point, we have been primarily concerned with the overall behaviour of the individual terms, and have not considered their application to a physical system, the goal of which is the focus of this section.

It is not immediately obvious however which physical system we should choose to apply our model to. We require a system that can be modelled as a single species electron plasma, that contains electromagnetic fields strong enough that the dominant and subdominant damping terms give measurable effects, yet not so high as to cause either term to become comparable to that of the cold, non-radiating term<sup>41</sup>.

To date, the strongest continuous magnetic field produced in the laboratory[49] is 45 T, which was achieved by Florida State University's 'National High Magnetic Field Laboratory'; however we do not expect radiation reaction effects to become significant at such field strengths. Larger magnetic fields can be created by utilising electromagnetic radiation. For example a typical laser wakefield accelerator will produce a laser pulse with a magnetic field strength[50] of  $\sim 10$  kT, while ELI hopes to produce even stronger pulses of  $\sim 1$  MT.

While one can expect radiation reaction to play a significant role in forthcoming ultra-high-intensity laser-based accelerators, they are not an appropriate system in which to apply the results of this section. Recall from (196) that we assumed the background magnetic field to be constant, which is clearly not the case for the oscillatory magnetic field of a laser pulse. By treating the oscillatory component of the fields as a perturbation to a constant background, we were able to

---

<sup>41</sup>Recall that throughout the previous chapters we have used a perturbative approach whereby we have assumed that the dominant damping term is small in comparison to the non-radiative term, and that the subdominant damping term is small in comparison to that of the dominant damping term.

uncover some of the implications of radiation reaction via dispersion relations. However, non-linearity plays an important role in laser wakefield accelerators and cannot be completely ignored. We will return to this point in section 5 and consider some of the implications of non-linearity there.

To find a physical system which satisfies our assumptions, in addition to producing a magnetic field strong enough for radiation reaction effects to become significant, we turn our attention to astrophysics, specifically, to the astrophysical bodies known as neutron stars.

#### 4.5.1 What is a Neutron Star?

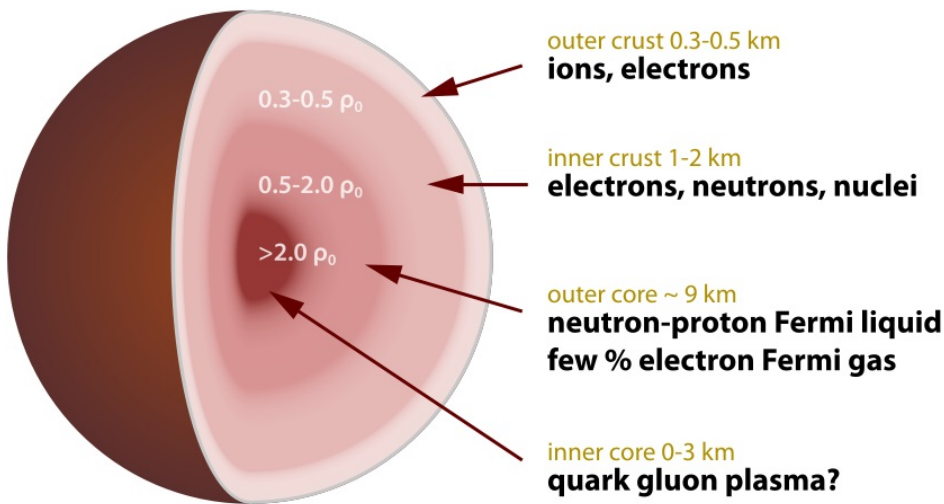


Figure 15: Cross-section of a neutron star<sup>42</sup>.

A neutron star is formed from the gravitational collapse of a massive star after a supernova[52]; some neutron stars rotate very rapidly, and are known as pulsars. Neutron stars have a radius of approximately 12 km -13 km whilst having a mass approximately twice that of our sun, making them the densest and smallest stars known to exist in the universe. Additionally, neutron stars have very strong magnetic fields, a typical pulsar can have a surface magnetic field of  $10^8$  T, and hence we can expect radiation reaction effects to play a significant role.

<sup>42</sup>This image has been created by Robert Schulze, using data from reference [51].

While not known precisely, it is estimated that the density within a neutron star's core is two to three times the average density of the nucleus of an atom[53],  $\rho_0$ . In the outer layer of a neutron star, known as the neutron star crust, the average density is less than  $\rho_0$  and hence this area is more amenable to modelling than the dense core<sup>43</sup>. Furthermore, one can consider the crust as a single species of atomic nuclei suspended in an electron gas[54], and thus make the same assumption that we made in Section 2.1.2 - that the atomic nuclei can be represented by a homogeneous background field included in the external source four-current.

#### 4.5.2 Our Fluid Model Applied to a Neutron Star Crust

Before we can substitute the parameters of a neutron star crust into our dispersion relations, we must first ensure that they are of the correct dimension. Recall in Section 1.1.1 that in order to simplify calculations we have used natural units where  $c = \epsilon_0 = \mu_0 = 1$ . Since, up to this point, we have been interested only in the overall properties of the dispersion relations, using such a unit system has been perfectly acceptable. However if we now wish to model a physical system we must reintroduce these variables where appropriate.

To do this, we must multiply our definition of the plasma frequency (68) by  $\frac{1}{\epsilon_0}$ ,  $\theta$  must be multiplied by a factor of  $\frac{1}{c^2}$ , and the right hand sides of our expressions for  $k(\omega_0)$  - (207), (223), (234) and (244) - must all be multiplied by a factor of  $\frac{1}{c^2}$ .

A typical neutron star crust [55] has an average electron number density  $n_e = 6.4 \times 10^{32} \text{ m}^{-3}$ , magnetic field  $B = 10^8 \text{ T}$  and temperature  $T = 10^6 \text{ K}$ . To find a suitable range over which to examine our dispersion relation, we must first compute the cutoff frequency of such a star.

Recall our expression (214) for the cutoff frequency of the R mode

$$\omega_{cor} = \frac{1}{2} \left( \sqrt{\omega_c^2 + 4\omega_p^2} + \omega_c \right). \quad (261)$$

Substituting the values given above into this we find  $\omega_{cor} = 1.77 \times 10^{19} \text{ rad s}^{-1}$ .

In Figure 16 below, we construct a log-log plot of the dominant and subdominant damping

---

<sup>43</sup>Note that such a large plasma density acts to reduce the size of  $\theta$  in comparison to its laboratory value (for the same temperature).

terms<sup>44</sup> of the R mode in the region  $\omega_{cor} \leq \omega_0 \leq 4 \times 10^{19} \text{ rad s}^{-1}$ .

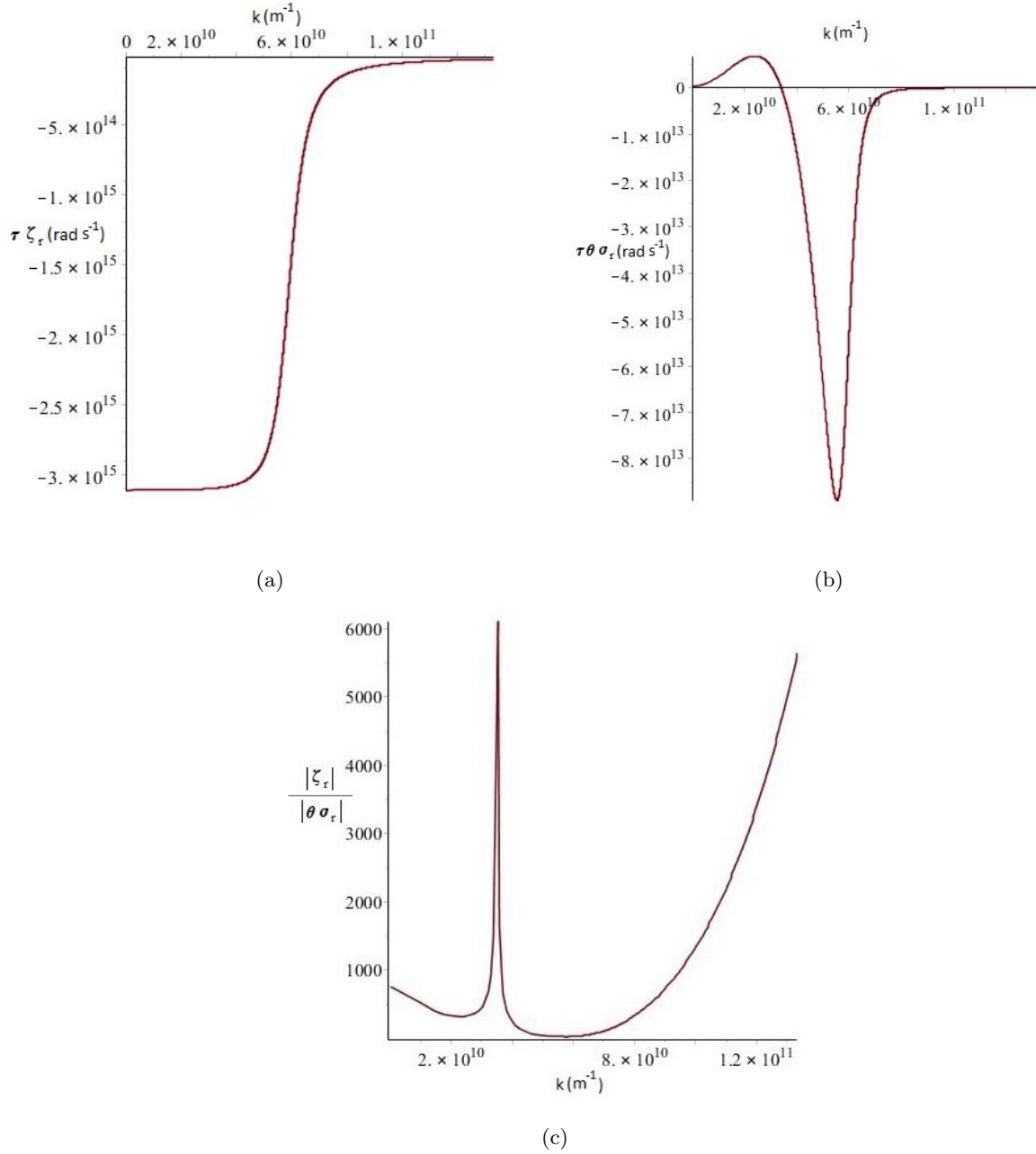


Figure 16: Plots of a)  $\tau \zeta_r(\omega_0)$  and b)  $\tau \theta \sigma_r(\omega_0)$ , vs  $k(\omega_0)$  in the region  $\omega_{cor} \leq \omega_0 \leq 4 \times 10^{19} \text{ rad s}^{-1}$ . Figure c) plots  $\frac{|\zeta_r|}{|\theta \sigma_r|}$  vs  $k(\omega_0)$ , showing the relative size of the two terms.

<sup>44</sup>Multiplied by their respective factors of  $\theta$  and  $\tau$ .

From Figure 16(c) we see that the correction to the damping rate due to the finite temperature of the plasma is small in comparison to that of the zero-temperature limit, and this result suggests that it is reasonable to neglect the temperature when calculating the damping due to radiation reaction of linear plasma waves in neutron star crusts.

However, we caution that the above analysis does not include important effects that can only be investigated using the full kinetic theory, such as Landau damping of longitudinal space charge waves. Further work is required to uncover the role of radiation reaction when such effects are taken into account.

Table 3: Summary of the dispersion relations for the R, L, O and X modes.

Mode	Frequency Shift	Dominant Damping ( $\zeta$ )	Subdominant Damping ( $\sigma$ )
R	$-\frac{\theta}{2} \frac{(3\omega_c^2\omega_0+2\omega_c\omega_p^2-4\omega_c\omega_0^2+\omega_0^3)\omega_p^2\omega_0}{(\omega_c-\omega_0)^2(2\omega_c^2\omega_0+\omega_c\omega_p^2-4\omega_c\omega_0^2+2\omega_0^3)}$	$-\frac{\omega_p^2\omega_0^3}{2\omega_0\omega_c^2-4\omega_0^2\omega_c+\omega_c\omega_p^2+2\omega_0^3}$	$-\frac{1}{2} \frac{\omega_0^2\omega_c\omega_p}{(2\omega_c^2\omega_0+\omega_c\omega_p^2-4\omega_c\omega_0^2+2\omega_0^3)^3(\omega_c-\omega_0)^2} \times$ $\left(32\omega_c^5\omega_0^3+56\omega_c^4\omega_p^2\omega_0^2-136\omega_c^4\omega_0^4+32\omega_c^3\omega_p^4\omega_0-160\omega_c^3\omega_p^2\omega_0^3\right.$ $+224\omega_c^3\omega_0^5+6\omega_c^2\omega_p^6-45\omega_c^2\omega_p^4\omega_0^2+148\omega_c^2\omega_p^2\omega_0^4-176\omega_c^2\omega_0^6$ $+4\omega_c\omega_p^4\omega_0^3-40\omega_c\omega_p^2\omega_0^5+64\omega_c\omega_0^7+9\omega_p^4\omega_0^4-4\omega_p^2\omega_0^6-8\omega_0^8)$
L	$-\frac{\theta}{2} \frac{(3\omega_c^2\omega_0-2\omega_c\omega_p^2+4\omega_c\omega_0^2+\omega_0^3)\omega_p^2\omega_0}{(\omega_c+\omega_0)^2(2\omega_c^2\omega_0-\omega_c\omega_p^2+4\omega_c\omega_0^2+2\omega_0^3)}$	$-\frac{\omega_p^2\omega_0^3}{2\omega_0\omega_c^2+4\omega_0^2\omega_c-\omega_c\omega_p^2+2\omega_0^3}$	$-\frac{1}{2} \frac{\omega_0^2\omega_c\omega_p}{(2\omega_c^2\omega_0-\omega_c\omega_p^2+4\omega_c\omega_0^2+2\omega_0^3)^3(\omega_c+\omega_0)^2} \times$ $\left(32\omega_c^5\omega_0^3-56\omega_c^4\omega_p^2\omega_0^2+136\omega_c^4\omega_0^4+32\omega_c^3\omega_p^4\omega_0-160\omega_c^3\omega_p^2\omega_0^3\right.$ $+224\omega_c^3\omega_0^5-6\omega_c^2\omega_p^6+45\omega_c^2\omega_p^4\omega_0^2-148\omega_c^2\omega_p^2\omega_0^4+176\omega_c^2\omega_0^6$ $+4\omega_c\omega_p^4\omega_0^3-40\omega_c\omega_p^2\omega_0^5+64\omega_c\omega_0^7-9\omega_p^4\omega_0^4+4\omega_p^2\omega_0^6+8\omega_0^8)$
O	$-\frac{\theta}{4} \frac{(3\omega_c^2-2\omega_p^2-\omega_0^2)\omega_p}{\omega_0(\omega_c-\omega_0)(\omega_c+\omega_0)}$	$-\frac{1}{2} \frac{\omega_p^2}{\omega_c^2}$	$\frac{1}{2} \frac{\omega_p^2(\omega_c^4+\omega_c^2\omega_p^2-3\omega_c^2\omega_0^2-\omega_p^4+2\omega_p^2\omega_0^2)}{(\omega_c-\omega_0)^2(\omega_c+\omega_0)^2}$
X	$-\frac{\theta}{4} \frac{(\omega_c^2\omega_0^2+\omega_p^4-2\omega_p^2\omega_0^2+\omega_0^4)\omega_p^2}{(\omega_c^4+3\omega_c^2\omega_p^2-2\omega_c^2\omega_0^2+\omega_p^4-2\omega_p^2\omega_0^2+\omega_0^4)\omega_0}$	$-\frac{1}{2} \frac{\omega_p^2(\omega_c^2\omega_0^2+\omega_p^4-2\omega_p^2\omega_0^2+\omega_0^4)}{\omega_c^4+3\omega_c^2\omega_p^2-2\omega_c^2\omega_0^2+\omega_p^4-2\omega_p^2\omega_0^2+\omega_0^4}$	$-\frac{1}{2} \frac{\omega_c^2\omega_p}{(\omega_c^4+3\omega_c^2\omega_p^2-2\omega_c^2\omega_0^2+\omega_p^4-2\omega_p^2\omega_0^2+\omega_0^4)^3} \times$ $\left(\omega_c^8\omega_0^2+\omega_c^6\omega_p^4+\omega_c^6\omega_p^2\omega_0^2+4\omega_c^4\omega_p^6-11\omega_c^4\omega_p^4\omega_0^2\right.$ $+13\omega_c^4\omega_p^2\omega_0^4-6\omega_c^4\omega_0^6+5\omega_c^2\omega_p^8-23\omega_c^2\omega_p^6\omega_0^2$ $+39\omega_c^2\omega_p^4\omega_0^4-29\omega_c^2\omega_p^2\omega_0^6+8\omega_c^2\omega_0^8+3\omega_p^{10}-15\omega_p^8\omega_0^2$ $+30\omega_p^6\omega_0^4-30\omega_p^4\omega_0^6+15\omega_p^2\omega_0^8-3\omega_0^{10})$

## 5 Radiation Reaction and Large Amplitude Waves

In the previous sections we have dealt with waves whose amplitude is small in comparison to the magnetic field of the plasma. However, plasma-based particle acceleration schemes exploit large amplitude fields that do not satisfy linear partial differential equations. The purpose of the present section is to illustrate the subtleties that immediately arise, even in the simplest of cases, when including radiation reaction in the analysis of large amplitude waves.

Let us choose our coordinate system such that the wave travels along the  $\hat{z}$  axis. If we introduce  $\xi = z - vt$  where  $v$  is the phase speed of the wave, the electromagnetic field tensor takes the form

$$F = E(\xi)dt \wedge dz, \quad (262)$$

where  $E(\xi)$  is the amplitude of the wave.

In the previous sections we employed a perturbative approach, whereby we assumed that the solutions we sought were those of the plasma in equilibrium, modified by a small correction term. This is not unreasonable when dealing with small amplitude external fields. In this section however we make no such assumption about the applied field, and hence we cannot use this approach. Instead, all we can say is that all the components of the centred moments depend solely on  $\xi$ , i.e.

$$\left[ R^{ab:\emptyset} \right] = \begin{bmatrix} R^{00:\emptyset}(\xi) & R^{01:\emptyset}(\xi) & R^{02:\emptyset}(\xi) & R^{03:\emptyset}(\xi) \\ R^{10:\emptyset}(\xi) & R^{11:\emptyset}(\xi) & R^{12:\emptyset}(\xi) & R^{13:\emptyset}(\xi) \\ R^{20:\emptyset}(\xi) & R^{21:\emptyset}(\xi) & R^{22:\emptyset}(\xi) & R^{23:\emptyset}(\xi) \\ R^{30:\emptyset}(\xi) & R^{31:\emptyset}(\xi) & R^{32:\emptyset}(\xi) & R^{33:\emptyset}(\xi) \end{bmatrix} \quad (263)$$

and similarly for  $R^{a:b\emptyset}$  and  $R^{\emptyset:ab}$ .

Note that even though we are considering arbitrarily strong fields, we are still working within the warm fluid approximation, and so we can still consider all centred moments of rank 3 or greater to be zero.

Furthermore, since the electric field  $E(\xi)$  is directed solely along  $\hat{z}$ , we set all spatial components

of  $U^a$ ,  $A^a$ ,  $R^{ab:\emptyset}$ ,  $R^{a:b}$  and  $R^{\emptyset:ab}$  orthogonal to  $\hat{\mathbf{z}}$  to zero. Thus the centred moments are given by

$$\left[ R^{ab:\emptyset} \right] = \begin{bmatrix} R^{00:\emptyset}(\xi) & 0 & 0 & R^{03:\emptyset}(\xi) \\ 0 & 0 & 0 & 0 \\ 0 & 0 & 0 & 0 \\ R^{30:\emptyset}(\xi) & 0 & 0 & R^{33:\emptyset}(\xi) \end{bmatrix}, \quad (264)$$

$$\left[ R^{a:b} \right] = \begin{bmatrix} R^{0:0}(\xi) & 0 & 0 & R^{0:3}(\xi) \\ 0 & 0 & 0 & 0 \\ 0 & 0 & 0 & 0 \\ R^{3:0}(\xi) & 0 & 0 & R^{3:3}(\xi) \end{bmatrix}, \quad (265)$$

and

$$\left[ R^{\emptyset:ab} \right] = \begin{bmatrix} R^{\emptyset:00}(\xi) & 0 & 0 & R^{\emptyset:03}(\xi) \\ 0 & 0 & 0 & 0 \\ 0 & 0 & 0 & 0 \\ R^{\emptyset:30}(\xi) & 0 & 0 & R^{\emptyset:33}(\xi) \end{bmatrix}. \quad (266)$$

Note that due to the symmetry of  $R^{ab:\emptyset}$  and  $R^{\emptyset:ab}$ ,  $R^{03:\emptyset} = R^{30:\emptyset}$  and  $R^{\emptyset:03} = R^{\emptyset:30}$ .

Substituting the above into the equations of motion (91 - 96), and coupling them to Maxwell's equations, we obtain a system of sixteen unique differential equations for the eleven fields, a sample of which is given below<sup>45</sup>.

$$\begin{aligned} -S^\emptyset A^0 &+ \frac{q}{m} E S^\emptyset U^3 + \tau \left( U^3 A^0 \dot{S}^\emptyset + S^\emptyset A^0 \dot{U}^3 + S^\emptyset U^3 \dot{A}^0 - U^0 A^0 \dot{S}^\emptyset v - S^\emptyset A^0 \dot{U}^0 v \right. \\ &- S^\emptyset U^0 \dot{A}^0 v - \dot{R}^{0:0} v + \dot{R}^{3:0} + S^\emptyset U^0 (A^0)^2 + U^0 R^{\emptyset:00} + 2A^0 R^{0:0} - S^\emptyset U^0 (A^3)^2 \\ &\left. - U^0 R^{\emptyset:33} - 2A^3 R^{0:3} \right) = 0, \end{aligned} \quad (267)$$

---

<sup>45</sup>For the full set of equations, see Appendix D.

$$\begin{aligned}
-S^\emptyset A^3 + \frac{q}{m} E S^\emptyset U^0 + \tau \left( S^\emptyset A^3 \dot{U}^3 + S^\emptyset U^3 \dot{A}^3 + \dot{R}^{3:3} + S^\emptyset U^3 (A^0)^2 + U^3 R^{\emptyset:30} \right. \\
+ 2 A^0 R^{3:0} - S^\emptyset U^3 (A^3)^2 - U^3 R^{\emptyset:33} - 2 A^3 R^{3:3} - U^0 A^3 \dot{S}^\emptyset v - S^\emptyset A^3 \dot{U}^0 \\
\left. - S^\emptyset U^0 \dot{A}^3 v - \dot{R}^{0:3} v + U^3 A^3 \dot{S}^\emptyset \right) = 0,
\end{aligned} \tag{268}$$

$$\text{.....} \tag{269}$$

Note that in the above we have omitted the argument  $\xi$  from the functions for clarity, and that the dots represent the remaining 14 equations. Additionally we have used  $\dot{X} = \frac{dX}{d\xi}$ .

From a visual inspection of (267 - 269), we see that only the first nine equations contain derivatives of the acceleration variables<sup>46</sup>, and that all of these derivatives are multiplied by a factor of  $\tau$ . Although we are now in the strong field regime, we still assume the corrections due to radiation reaction to be small in comparison to the remaining terms, and hence we can still discard terms  $\mathcal{O}(\tau^2)$  and higher. Thus, we need only solve for the derivatives of the acceleration variables to lowest order in  $\tau$ , greatly simplifying the calculation.

To do this, we create a subset of the sixteen equations (267 - 269) that consists of the set's first nine equations and set  $\tau$  to zero in each of them. These equations can then be algebraically manipulated such that we obtain 9 equations for the 9 acceleration variables  $\{A^0, A^3, R^{\emptyset:00}, R^{\emptyset:30}, R^{\emptyset:33}, R^{0:0}, R^{0:3}, R^{3:0}, R^{3:3}\}$ , yielding

$$A^0(\xi) = \frac{q}{m} U^3(\xi) E(\xi) + \mathcal{O}(\tau^2), \tag{270}$$

$$A^3(\xi) = \frac{q}{m} U^0(\xi) E(\xi) + \mathcal{O}(\tau^2), \tag{271}$$

$$R^{\emptyset:00}(\xi) = \frac{q^2}{m^2} E(\xi)^2 R^{33:\emptyset}(\xi) + \mathcal{O}(\tau^2), \tag{272}$$

$$R^{\emptyset:30}(\xi) = \frac{q^2}{m^2} E(\xi)^2 R^{30:\emptyset}(\xi) + \mathcal{O}(\tau^2), \tag{273}$$

$$R^{\emptyset:33}(\xi) = \frac{q^2}{m^2} E(\xi)^2 R^{00:\emptyset}(\xi) + \mathcal{O}(\tau^2), \tag{274}$$

$$R^{0:0} = \frac{q}{2m} R^{30:\emptyset}(\xi) E(\xi) + \mathcal{O}(\tau^2), \tag{275}$$

---

<sup>46</sup>By acceleration variables we mean the components of  $A^a$ ,  $R^{a:b}$  and  $R^{\emptyset:ab}$ .

$$R^{0:3} = \frac{q}{m} R^{00:\emptyset}(\xi) E(\xi) + \mathcal{O}(\tau^2), \quad (276)$$

$$R^{3:0} = \frac{q}{m} R^{33:\emptyset}(\xi) E(\xi) + \mathcal{O}(\tau^2), \quad (277)$$

$$R^{3:3} = \frac{q}{2m} R^{30:\emptyset}(\xi) E(\xi) + \mathcal{O}(\tau^2). \quad (278)$$

We then differentiate (270 - 278) with respect to  $\xi$ , and substitute the resulting differentials back into (267 - 269). If we now discard terms of  $\mathcal{O}(\tau^2)$ , all differentials of the acceleration variables vanish from the system.

What remains is a system of algebraic equations for the acceleration variables themselves. The best way to approach solving this system, however, is not clear. There are multiple roots for each of those variables, and we are concerned only with those that are well behaved as  $\tau \rightarrow 0$ . In principal one could solve for the acceleration variables first, and then inspect each root in turn; however such a method is computationally intensive.

Instead, we use a perturbative approach, whereby we assume that all the acceleration variables are of the form

$$A^0(\xi) = A_{(0)}^0(\xi) + \tau A_{(1)}^0(\xi), \quad (279)$$

where the zeroth order terms are given by (270 - 278).

To obtain solutions to the first order terms we substitute the above ansatz into (267 - 269) and solve for the coefficients of  $\tau$  for each of the first nine equations in turn. These solutions can then be substituted back into (267 - 269), resulting in 7 first order ordinary differential equations<sup>47</sup> for the remaining variables  $U^0$ ,  $U^3$ ,  $S^\emptyset$ ,  $R^{00:\emptyset}$ ,  $R^{03:\emptyset}$ ,  $R^{33:\emptyset}$  and  $E$ .

While again solvable in principal, we still run into problems due to resource limitations if we try to solve this system directly. At first sight it might appear that we cannot reduce the system any further; however recall from Section 2 that in addition to the equations of motion (91 - 96) of our model, we also have the constraints (98 - 103). Note however that many of the constraints contain terms involving the acceleration variables. Since we have just gone to some lengths to eliminate these it is necessary to confine our attention only to those constraints that do not involve

---

<sup>47</sup>These equations are very large, and so are not included in this thesis.

acceleration variables; (98) and (100). Of these five constraints, two are trivially satisfied. The remaining three yield

$$-U^0(\xi) R^{00:\emptyset}(\xi) + \frac{1}{2} U^3(\xi) R^{30:\emptyset}(\xi) = 0, \quad (280)$$

$$-\frac{1}{2} U^0(\xi) R^{30:\emptyset}(\xi) + U^3(\xi) R^{33:\emptyset}(\xi) = 0, \quad (281)$$

$$-R^{00:\emptyset}(\xi) + R^{33:\emptyset}(\xi) + S^\emptyset (-U^0(\xi)^2 + 1 + U^3(\xi)^2) = 0. \quad (282)$$

These constraints can then be rearranged to obtain expressions for the remaining centred moments in terms of  $U^0(\xi)$ ,  $U^3(\xi)$  and  $S^\emptyset$ :

$$R^{00:\emptyset}(\xi) = \frac{U^3(\xi)^2 S^\emptyset (U^0(\xi)^2 - U^3(\xi)^2 - 1)}{U^0(\xi)^2 - U^3(\xi)^2}, \quad (283)$$

$$R^{30:\emptyset}(\xi) = \frac{2 U^3(\xi) S^\emptyset U^0(\xi) (U^0(\xi)^2 - U^3(\xi)^2 - 1)}{U^0(\xi)^2 - U^3(\xi)^2}, \quad (284)$$

$$R^{33:\emptyset}(\xi) = \frac{S^\emptyset U^0(\xi)^2 (U^0(\xi)^2 - U^3(\xi)^2 - 1)}{U^0(\xi)^2 - U^3(\xi)^2}. \quad (285)$$

Substituting (283 - 285) back into the remaining seven equation system, and performing some algebraic manipulation, one is able to obtain 4 differential equations for  $U^0(\xi)$ ,  $U^3(\xi)$ ,  $E(\xi)$ , and  $S^\emptyset(\xi)$ , as well as 3 additional algebraic constraints on  $U^0(\xi)$ ,  $U^3(\xi)$ ,  $E^3(\xi)$ , and  $S^\emptyset(\xi)$ .

Solving the first algebraic constraint yields

$$S^\emptyset = -\frac{n_{\text{ion}} v}{U^3(\xi) - U^0(\xi)}, \quad (286)$$

where  $n_{\text{ion}}$  is the number density of the ions. Substitution of this solution back into the system of 7 equations, results in 6 equations for the three unknowns  $U^0(\xi)$ ,  $U^3(\xi)$ ,  $E(\xi)$ .

What we now have is an over-prescribed system; we have more equations than we need in order to solve for all the unknown variables. In general this is not a problem, provided you are working with a consistent system. However, if we were to choose subsets of these equations, comprised of different combinations of the 6 equation set, the solutions we would obtain would differ depending on which equations we chose to use. Clearly then, we do not have a consistent system. The reason

for this is that we have not yet completed our application of the warm fluid approximation. When working in this regime, one must continue to apply the approximation, reducing the number of equations one has until there are the same number of equations as unknowns.

In order to proceed then, we must introduce another parameter that can be used to determine which equations can be discarded in the warm fluid regime.

Let us assume that  $U^0(\xi)$  takes the form

$$U^0(\xi) = \sqrt{1 + U^3(\xi)^2} + \kappa(\xi). \quad (287)$$

The first term on the right-hand side of the above is the solution for  $U^0(\xi)$  in the cold fluid approximation, with  $\kappa(\xi)$  a small correction<sup>48</sup> of  $\mathcal{O}(\chi)$ . Note that if we set  $\kappa(\xi) = 0$  we obtain the solution to the cold fluid regime, whereas if we require  $\kappa(\xi)$  to be small, we obtain a solution close to, but not identical to that of the cold fluid. Hence  $\kappa(\xi)$  can be interpreted as a measure of how far the state of our plasma deviates from that of a cold plasma. Substituting (287) into the remaining two algebraic constraints, one finds that they vanish to order  $\mathcal{O}(\chi)$ , and hence can be discarded from our 6 equation system.

Thus, we arrive at a system of four differential equations for the three remaining unknowns  $E(\xi)$ ,  $U^3(\xi)$  and  $\kappa(\xi)$ .

In order to eliminate one more equation, it is necessary to carry out some simplification. A visual inspection of the remaining 4 equations shows that one of the equations is of the form

$$\frac{dU^3(\xi)}{d\xi} = \mathfrak{J}(U^3(\xi), E(\xi), \kappa(\xi)). \quad (288)$$

Substitution of the above back into the four-equation system allows us to simplify the system to a point whereby we can algebraically solve two of the equations for  $\kappa(\xi)$  independently. Comparison of these two solutions for  $\kappa(\xi)$  reveals them to be identical to  $\mathcal{O}(\chi)$ , and hence we can eliminate one from our system.

Hence we arrive at a system of three differential equations for the three unknowns  $E(\xi)$ ,  $U^3(\xi)$

---

<sup>48</sup>Recall from Section 4.1 that  $\tau$  and  $\theta$  are  $\mathcal{O}(\chi)$ , and  $\tau\theta$  is  $\mathcal{O}(\chi^2)$ .

and  $\kappa(\xi)$ . All that remains is to choose our initial conditions. We can choose  $E(\xi)$  and  $U^3(\xi)$  freely, but we must take care when choosing  $\kappa(\xi)$ , as it must be that  $|\kappa(\xi)| \ll \sqrt{1 + U^3(\xi)^2}$  or else we violate the warm fluid approximation<sup>49</sup>. From inspection of (287) it is clear that we can associate  $\kappa(\xi)$  with the deviation of the plasma's state from that of a cold plasma, or alternatively with the pressure tensor of the plasma. Hence to see what effect pressure has on the electric field it is helpful to examine plots with varying values of  $\kappa(0)$ . Figure 17 is composed<sup>50</sup> of such plots.

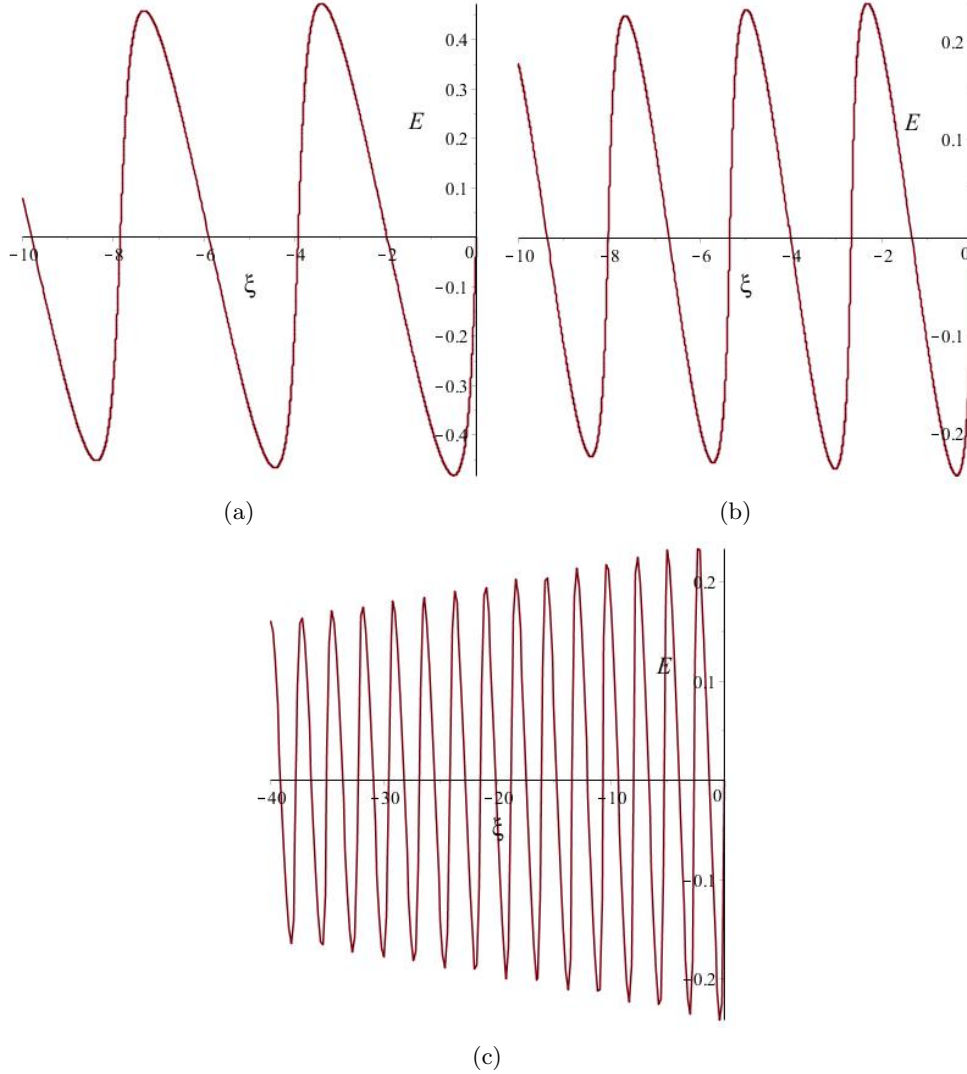


Figure 17: Plots of  $E(\xi)$  vs  $\xi$  for a)  $\kappa(0) = 0$  and b)  $\kappa(0) = 0.03$ . The range of plot c) is larger than that of a) and b), for perspective.

<sup>49</sup>Additionally we must ensure that  $|\kappa(\xi)|$  does not get much larger than its initial value.

<sup>50</sup>In order to generate the following figures we have set  $U^3(0) = 0.5$ ,  $E(0) = 0$ ,  $v = 0.6$  and  $q = m = n_e = 1$ .

Note the sawtooth profile of the wave. From inspection of the above we see that increasing the value of  $\kappa(0)$  has two effects. Firstly, the larger the value of  $\kappa(0)$  the lower the amplitude of the wave near  $\xi = 0$ , and secondly we see that as  $\kappa(0)$  increases, the wavelength of the wave decreases. This acts to increase the overall gradient of the wave, thus enhancing the sawtooth shape. Additionally, from Figure 17(c) we see that the amplitude of the wave decreases as  $\xi$  becomes more negative, as one would expect from a model that incorporates damping.

Recall that  $\xi$  is a coordinate that moves with the wave, and hence Figure 17 is a plot of the amplitude of the wave, as seen in the wave frame. While we can integrate from any point in the past of  $\xi$ , we cannot integrate arbitrarily far into the future of  $\xi$ . If we attempt to do so the numerical integrator breaks down, likely due to a singularity, and calculation is halted. Interestingly, increasing the value of  $\kappa$  reduces the distance into the future that we can integrate. This can be seen in Figure 18 below; initially we set  $\kappa$  to zero and numerical integration halts at approximately  $\xi = 16$ , while increasing  $\kappa$  to 0.01 causes the calculation to halt at  $\xi \approx 10$ .

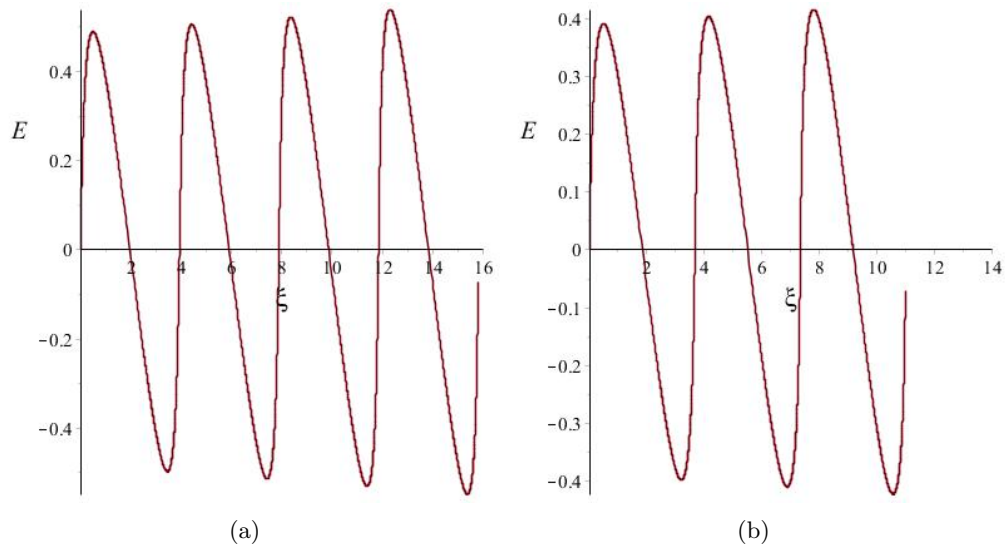


Figure 18: Plots of  $E(\xi)$  vs  $\xi$  for a)  $\kappa(0) = 0$  and b)  $\kappa(0) = 0.01$ .

Since this plot was obtained numerically, it is not clear exactly what is causing the singularity to occur. However the presence of a singularity for some future value of  $\xi$  is not unreasonable.

As we saw in Section 1.2.3, waves of the form (262) do not spontaneously generate in a plasma,

but rather are driven by a laser pulse that travels at speed  $v$  and overlaps the end of the wave. Our model is not valid in the region of the pulse, and hence a singularity is not unexpected.

## 6 Conclusion and Future Work

In this thesis we have generated a new model of a warm plasma that takes radiation reaction into account, and have examined some of its predictions for the behaviour of electric and electromagnetic waves propagating through plasma.

We first derived our model in Section 2, whereby we took moments of an already established kinetic description based upon the ALD equation. Later, in order to obtain solutions, we performed an approximation procedure similar to that used to generate the Landau-Lifshitz equation. Our new method has the advantage of generating a more compact set of moment equations than would be obtained from Landau-Lifshitz kinetic theory, thus simplifying implementation of the fluid theory in a symbolic algebra package.

Taking moments of a fluid description results in an infinite hierarchy of equations, that one must somehow close in order to obtain solutions. We used an approach inspired by models of warm fluids that do not take radiation reaction into account. Such a closure scheme allowed us to obtain a finite set of equations, while making no additional assumptions about the bulk properties of the plasma. However, there are other closure mechanisms one could apply, and this is certainly an area open to future study.

We then went on to use the techniques of perturbation theory to examine the behaviour of small amplitude electric waves, obtaining analytic descriptions of their dispersion relations. While models exist that examine electric waves in the warm fluid regime, and take radiation reaction into account, none so far have explored the properties of the  $\tau\theta$  correction in the warm fluid theory, and so these results are a new addition to the field. Additionally, we obtained analytic expressions for the bulk properties for the plasma<sup>51</sup>.

We subsequently examined small amplitude electromagnetic waves, deriving dispersion relations in a similar manner to those of the electric wave. We then went on to apply the dispersion relation we obtained for the R Mode to a physical system, that of neutron star crusts. Unfortunately, due to the complexity of the solutions we obtained, we were unable to derive expressions for the bulk properties of the plasma. This was simply due to computational limits, and perhaps in future, as

---

<sup>51</sup>i.e. the low rank centred moments of the 1-particle distribution function.

computational speeds increase, we can revisit this aspect of the work. However, we did find that it is not unreasonable to neglect the temperature when calculating the damping due to radiation reaction of linear plasma waves in neutron star crusts; the contribution to the damping due to the finite temperature is  $\sim 10^{-4} - 10^{-3}$  times that of the zero temperature limit.

In the final section, noting that plasma-based wakefield accelerators operate in a non-linear regime, we moved on from the perturbative approach and instead looked at an electric wave of arbitrary amplitude. A natural extension of this thesis would be to examine electromagnetic waves of arbitrary strength.

While we have only studied the effects of electromagnetic waves of infinite extent, experimental research that is being carried out in laser based particle acceleration invariably involves short pulses of electromagnetic waves. Hence, in order to compare the predictions of this model with those observed experimentally, it would be helpful to model such a pulse.

## A Derivation of the Moment Equations

We begin with the Vlasov Equation, given by (82) in Section 2.1.2 and reproduced below;

$$Lf + \frac{3}{\tau}f = 0. \quad (289)$$

Recall that  $L$  is the Liouville operator, and is given by

$$L = \dot{x}^a \frac{\partial}{\partial x^a} + a^\mu \frac{\partial}{\partial v^\mu} + \left[ \ddot{x}^a \dot{x}_a v^\mu + \frac{1}{\tau} \left( a^\mu + \frac{q}{m} F^\mu{}_a \dot{x}^a \right) \right] \frac{\partial}{\partial a^\mu}, \quad (290)$$

where  $v^\mu = \dot{x}^\mu$  and  $a^\mu = \ddot{x}^\mu$ .

Additionally,  $\dot{x}^a$  obeys the normalisation condition

$$\dot{x}^a \dot{x}_a = -1, \quad (291)$$

which can be differentiated to give

$$\ddot{x}^a \dot{x}_a = 0. \quad (292)$$

### A.1 Generation of the 1<sup>st</sup> Moment Equation

To begin, consider the expression<sup>52</sup>

$$\int \dot{x}^a \psi f d\omega, \quad (293)$$

where  $\psi = \psi(x^a, \dot{x}^a, \ddot{x}^a)$  is an arbitrary function and  $d\omega = \frac{d^3 v d^3 a}{1+v^2}$ . Differentiation with respect to  $x^a$  yields

$$\begin{aligned} \frac{\partial}{\partial x^a} \int \dot{x}^a \psi f d\omega &= \int \dot{x}^a \frac{\partial}{\partial x^a} (\psi f) d\omega \\ &= \int \dot{x}^a \frac{\partial \psi}{\partial x^a} f d\omega + \int \psi \dot{x}^a \frac{\partial f}{\partial x^a} d\omega. \end{aligned} \quad (294)$$

---

<sup>52</sup>Note that the measure  $d\omega$  has no relation to the frequencies  $\omega$  discussed throughout this thesis.

Rearranging (289) to obtain an expression for  $\dot{x}^a \frac{\partial f}{\partial x^a}$ , and substituting this into the above yields

$$\begin{aligned} \frac{\partial}{\partial x^a} \int \dot{x}^a \psi f d\omega &= \int \dot{x}^a \frac{\partial \psi}{\partial x^a} f d\omega - \int \psi a^\mu \frac{\partial f}{\partial v^\mu} d\omega \\ &\quad - \int \psi \left[ \ddot{x}^a \ddot{x}_a v^\mu + \frac{1}{\tau} \left( a^\mu + \frac{q}{m} F^\mu{}_a \dot{x}^a \right) \right] \frac{\partial f}{\partial a^\mu} d\omega - \int \psi \frac{3}{\tau} f d\omega. \end{aligned} \quad (295)$$

Applying integration by parts to the second and third terms we find,

$$\int \dot{x}^a \frac{\partial}{\partial x^a} (\psi f) d\omega = \int \left\{ \dot{x}^a \frac{\partial \psi}{\partial x^a} + a^\mu \frac{\partial \psi}{\partial v^\mu} + \left[ \ddot{x}^a \ddot{x}_a v^\mu + \frac{1}{\tau} \left( a^\mu + \frac{q}{m} F^\mu{}_a \dot{x}^a \right) \right] \frac{\partial \psi}{\partial a^\mu} \right\} f d\omega \quad (296)$$

$$+ \int \psi \left[ a^\mu \frac{\partial}{\partial v^\mu} \left( \frac{1}{1 + \mathbf{v}^2} \right) (1 + \mathbf{v}^2) + v^\mu \frac{\partial}{\partial a^\mu} (\ddot{x}^a \ddot{x}_a) \right] f d\omega, \quad (297)$$

where the  $1 + \mathbf{v}^2$  terms arise from within  $d\omega$ .

From (291) and (292), one can show

$$\ddot{x}^a \ddot{x}_a = -\frac{(v^\mu a_\mu)^2}{1 + \mathbf{v}^2} + \mathbf{a}^2. \quad (298)$$

Taking the derivative of (298) with respect to  $a^\nu$ , and contracting the resulting expression with  $v^\nu$ , we find

$$\begin{aligned} v^\mu \frac{\partial}{\partial a^\mu} (\ddot{x}^a \ddot{x}_a) &= \frac{2 a^\mu v_\mu}{1 + \mathbf{v}^2} \\ &= -a^\mu \frac{\partial}{\partial v^\mu} \left( \frac{1}{1 + \mathbf{v}^2} \right) (1 + \mathbf{v}^2), \end{aligned} \quad (299)$$

and hence the second integral of the right-hand side of (297) vanishes. Thus

$$\frac{\partial}{\partial x^a} \int \dot{x}^a \psi f d\omega = \int L \psi f d\omega. \quad (300)$$

Armed with (300) we are able to generate the first moment equation by setting  $\psi = 1$ ;

$$\frac{\partial}{\partial x^a} \int \dot{x}^a f d\omega = \partial_a S^{a:\emptyset} = 0. \quad (301)$$

## A.2 Generation of the 2<sup>nd</sup> Moment Equation

Setting  $\psi = \dot{x}^b$  in (300) yields

$$\frac{\partial}{\partial x^a} \int \dot{x}^a \dot{x}^b f d\omega = \int L \dot{x}^b f d\omega. \quad (302)$$

One can easily show that  $L\dot{x}^a = \ddot{x}^a$ , resulting in the second moment equation;

$$\frac{\partial}{\partial x^a} \int \dot{x}^a \dot{x}^b f d\omega = \int \ddot{x}^b f d\omega. \quad (303)$$

## A.3 Generation of the 3<sup>rd</sup> Moment Equation

Setting  $\psi = \ddot{x}^b$  in (300) yields

$$\frac{\partial}{\partial x^a} \int \dot{x}^a \ddot{x}^b f d\omega = \int L \ddot{x}^b f d\omega. \quad (304)$$

To proceed further we must evaluate  $L\ddot{x}^a$ . In order to simplify the calculation let us first look at the zeroth component,

$$\begin{aligned} L\ddot{x}^0 &= L \left( \frac{a^\beta v_\beta}{\sqrt{1 + \mathbf{v}^2}} \right) \\ &= a^\mu \frac{\partial}{\partial v^\mu} \left( \frac{a^\beta v_\beta}{\sqrt{1 + \mathbf{v}^2}} \right) + \left[ \ddot{x}^b \ddot{x}_b v^\mu + \frac{1}{\tau} \left( a^\mu + \frac{q}{m} F^\mu{}_\alpha \dot{x}^a \right) \right] \frac{\partial}{\partial a^\mu} \frac{a^\beta v_\beta}{\sqrt{1 + \mathbf{v}^2}}, \end{aligned} \quad (305)$$

where (292) has been used in the first step to eliminate  $\dot{x}^0$ .

Carrying out the differentiation we find,

$$\begin{aligned} L\ddot{x}^0 &= \frac{1}{\sqrt{1 + \mathbf{v}^2}} \left( \underbrace{a^2 - \frac{(a^\beta v_\beta)^2}{(1 + \mathbf{v}^2)}}_{=\dot{x}^a \dot{x}_a} + \ddot{x}^a \ddot{x}_a \mathbf{v}^2 \right) + \frac{1}{\tau} \left( \underbrace{\frac{a^\beta v_\beta}{\sqrt{1 + \mathbf{v}^2}}}_{=\dot{x}^0} + \frac{q}{m} F^\mu{}_\alpha \dot{x}^a \frac{v_\mu}{\sqrt{1 + \mathbf{v}^2}} \right) \\ &= \ddot{x}^a \dot{x}_a \left( \underbrace{\frac{1}{\sqrt{1 + \mathbf{v}^2}} + \frac{\mathbf{v}^2}{\sqrt{1 + \mathbf{v}^2}}}_{=\sqrt{1 + \mathbf{v}^2} = \dot{x}^0} \right) + \frac{1}{\tau} \left[ \dot{x}^0 + \frac{q}{m} (F^\mu{}_0 v_\mu + F^\mu{}_\alpha v^\alpha v_\mu) \right]. \end{aligned} \quad (306)$$

The last term in the above,  $F^\mu{}_\alpha v^\alpha v_\mu$ , vanishes due to symmetry. Thus

$$L\ddot{x}^0 = \ddot{x}^a \ddot{x}_a \dot{x}^0 + \frac{1}{\tau} \left( \ddot{x}^0 + \frac{q}{m} F^0{}_a \dot{x}^a \right). \quad (307)$$

If we next look at the spatial components;

$$\begin{aligned} L\ddot{x}^\alpha &= L a^\alpha \\ &= \left[ \dot{x}^b \ddot{x}_b v^\mu + \frac{1}{\tau} \left( a^\mu + \frac{q}{m} F^\mu{}_a \dot{x}^a \right) \right] \delta^\alpha_\mu \\ &= \dot{x}^b \ddot{x}_b \dot{x}^\alpha + \frac{1}{\tau} \left( \ddot{x}^\alpha + \frac{q}{m} F^\alpha{}_a \dot{x}^a \right). \end{aligned} \quad (308)$$

Combining (307) and (308) we find

$$L\ddot{x}^a = \dot{x}^b \ddot{x}_b \dot{x}^a + \frac{1}{\tau} \left( \ddot{x}^a + \frac{q}{m} F^a{}_b \dot{x}^b \right). \quad (309)$$

Substituting (309) into (304) yields

$$\frac{\partial}{\partial x^a} \int \dot{x}^a \ddot{x}^b f d\omega = \int \ddot{x}^c \ddot{x}_c \dot{x}^b + \frac{1}{\tau} \left( \ddot{x}^b + \frac{q}{m} F^b{}_a \dot{x}^a \right) f d\omega, \quad (310)$$

the third moment equation.

All other moment equations are generated in a similar manner.

## B Centred Moment Expansions

We begin with the definition of the centred moments

$$R^{a_1 \dots a_l : b_1 \dots b_n} = \int (\dot{x}^{a_1} - U^{a_1}) \dots (\dot{x}^{a_l} - U^{a_l}) \times (\ddot{x}^{b_1} - A^{b_1}) \dots (\ddot{x}^{b_n} - A^{b_n}) \times f d\omega, \quad (311)$$

where  $d\omega = \frac{d^3 v d^3 a}{1+v^2}$ .

From this definition we can express all  $n$ th order centred moments in terms of  $(n-1)$ th centred moments and a single  $n$ th order natural moment by expanding the brackets, as follows:

$$R^{ab:\emptyset} = S^{ab:\emptyset} - S^\emptyset U^a U^b, \quad (312)$$

$$R^{a:b} = S^{a:b} - S^\emptyset U^a A^b, \quad (313)$$

$$R^{\emptyset:ab} = S^{\emptyset:ab} - S^\emptyset A^a A^b, \quad (314)$$

$$R^{abc:\emptyset} = S^{abc:\emptyset} - U^a R^{bc:\emptyset} - U^b R^{ac:\emptyset} - U^c R^{ab:\emptyset} - S^\emptyset U^a U^b U^c, \quad (315)$$

$$R^{ab:c} = S^{ab:c} - U^a R^{b:c} - U^b R^{a:c} - A^c R^{ab:\emptyset} - S^\emptyset U^a U^b A^c, \quad (316)$$

$$R^{a:bc} = S^{a:bc} - U^a R^{\emptyset:bc} - A^b R^{a:c} - A^c R^{a:b} - S^\emptyset U^a A^b A^c, \quad (317)$$

$$R^{\emptyset:abc} = S^{\emptyset:abc} - A^a R^{\emptyset:bc} - A^b R^{\emptyset:ac} - A^c R^{\emptyset:ab} - S^\emptyset A^a A^b A^c, \quad (318)$$

and similarly for the centred moments of higher rank.

## C Electromagnetic Electron Wave Dispersion Relations

Here we list the four dispersion relations, in full, for the R, L, O and X modes of an electromagnetic wave travelling through a magnetised plasma, with radiation reaction taken into account.

### R Mode

$$\begin{aligned}
 \omega(\omega_0) = & \omega_0 - \frac{\theta}{2} \frac{(3\omega_c^2\omega_0 + 2\omega_c\omega_p^2 - 4\omega_c\omega_0^2 + \omega_0^3)\omega_p^2\omega_0}{(\omega_c - \omega_0)^2(2\omega_c^2\omega_0 + \omega_c\omega_p^2 - 4\omega_c\omega_0^2 + 2\omega_0^3)} \\
 & -i\tau \left[ \frac{\omega_p^2\omega_0^3}{2\omega_c^2\omega_0 + \omega_c\omega_p^2 - 4\omega_c\omega_0^2 + 2\omega_0^3} + \frac{1}{2} \frac{\theta\omega_0^2\omega_c\omega_p^2}{(2\omega_c^2\omega_0 + \omega_c\omega_p^2 - 4\omega_c\omega_0^2 + 2\omega_0^3)^3(\omega_c - \omega_0)^2} \right. \\
 & \times \left( 32\omega_c^5\omega_0^3 + 56\omega_c^4\omega_p^2\omega_0^2 - 136\omega_c^4\omega_0^4 + 32\omega_c^3\omega_p^4\omega_0 - 160\omega_c^3\omega_p^2\omega_0^3 + 224\omega_c^3\omega_0^5 \right. \\
 & + 6\omega_c^2\omega_p^6 - 45\omega_c^2\omega_p^4\omega_0^2 + 148\omega_c^2\omega_p^2\omega_0^4 - 176\omega_c^2\omega_0^6 + 4\omega_c\omega_p^4\omega_0^3 - 40\omega_c\omega_p^2\omega_0^5 + 64\omega_c\omega_0^7 \\
 & \left. \left. + 9\omega_p^4\omega_0^4 - 4\omega_p^2\omega_0^6 - 8\omega_0^8 \right) \right].
 \end{aligned}$$

### L Mode

$$\begin{aligned}
 \omega(\omega_0) = & \omega_0 - \frac{\theta}{2} \frac{(3\omega_c^2\omega_0 - 2\omega_c\omega_p^2 + 4\omega_c\omega_0^2 + \omega_0^3)\omega_p^2\omega_0}{(\omega_c + \omega_0)^2(2\omega_c^2\omega_0 - \omega_c\omega_p^2 + 4\omega_c\omega_0^2 + 2\omega_0^3)} \\
 & -i\tau \left[ \frac{\omega_p^2\omega_0^3}{2\omega_c^2\omega_0 - \omega_c\omega_p^2 + 4\omega_c\omega_0^2 + 2\omega_0^3} + \frac{1}{2} \frac{\theta\omega_0^2\omega_c\omega_p^2}{(2\omega_c^2\omega_0 - \omega_c\omega_p^2 + 4\omega_c\omega_0^2 + 2\omega_0^3)^3(\omega_c + \omega_0)^2} \right. \\
 & \times \left( 32\omega_c^5\omega_0^3 - 56\omega_c^4\omega_p^2\omega_0^2 + 136\omega_c^4\omega_0^4 + 32\omega_c^3\omega_p^4\omega_0 - 160\omega_c^3\omega_p^2\omega_0^3 + 224\omega_c^3\omega_0^5 \right. \\
 & - 6\omega_c^2\omega_p^6 + 45\omega_c^2\omega_p^4\omega_0^2 - 148\omega_c^2\omega_p^2\omega_0^4 + 176\omega_c^2\omega_0^6 + 4\omega_c\omega_p^4\omega_0^3 - 40\omega_c\omega_p^2\omega_0^5 + 64\omega_c\omega_0^7 \\
 & \left. \left. - 9\omega_p^4\omega_0^4 + 4\omega_p^2\omega_0^6 + 8\omega_0^8 \right) \right].
 \end{aligned}$$

## O Mode

$$\begin{aligned} \omega(\omega_0) = & \omega_0 - \frac{\theta}{4} \frac{(3\omega_c^2 - 2\omega_p^2 - \omega_0^2) \omega_p^2}{\omega_0 (\omega_c - \omega_0) (\omega_c + \omega_0)} - \frac{i\tau}{2} \omega_p^2 \\ & + \frac{i\tau\theta}{2} \frac{\omega_p^2 (\omega_c^4 + \omega_c^2 \omega_p^2 - 3\omega_c^2 \omega_0^2 - \omega_p^4 + 2\omega_p^2 \omega_0^2)}{(\omega_c - \omega_0)^2 (\omega_c + \omega_0)^2}. \end{aligned}$$

## X Mode

$$\begin{aligned} \omega(\omega_0) = & \omega_0 - \frac{\theta}{4} \frac{(\omega_c^2 \omega_0^2 + \omega_p^4 - 2\omega_p^2 \omega_0^2 + \omega_0^4) \omega_p^2}{(\omega_c^4 + 3\omega_c^2 \omega_p^2 - 2\omega_c^2 \omega_0^2 + \omega_p^4 - 2\omega_p^2 \omega_0^2 + \omega_0^4) \omega_0} \\ & - \frac{i\tau}{2} \left[ \frac{\omega_p^2 (\omega_c^2 \omega_0^2 + \omega_p^4 - 2\omega_p^2 \omega_0^2 + \omega_0^4)}{\omega_c^4 + 3\omega_c^2 \omega_p^2 - 2\omega_c^2 \omega_0^2 + \omega_p^4 - 2\omega_p^2 \omega_0^2 + \omega_0^4} \right. \\ & + \frac{\theta \omega_c^2 \omega_p^2}{(\omega_c^4 + 3\omega_c^2 \omega_p^2 - 2\omega_c^2 \omega_0^2 + \omega_p^4 - 2\omega_p^2 \omega_0^2 + \omega_0^4)^3} \times \left( \omega_c^8 \omega_0^2 + \omega_c^6 \omega_p^4 \right. \\ & + \omega_c^6 \omega_p^2 \omega_0^2 + 4\omega_c^4 \omega_p^6 - 11\omega_c^4 \omega_p^4 \omega_0^2 + 13\omega_c^4 \omega_p^2 \omega_0^4 - 6\omega_c^4 \omega_0^6 + 5\omega_c^2 \omega_p^8 \\ & - 23\omega_c^2 \omega_p^6 \omega_0^2 + 39\omega_c^2 \omega_p^4 \omega_0^4 - 29\omega_c^2 \omega_p^2 \omega_0^6 + 8\omega_c^2 \omega_0^8 + 3\omega_p^{10} - 15\omega_p^8 \omega_0^2 \\ & \left. \left. + 30\omega_p^6 \omega_0^4 - 30\omega_p^4 \omega_0^6 + 15\omega_p^2 \omega_0^8 - 3\omega_0^{10} \right) \right]. \end{aligned}$$

## D The System of Equations Describing a Non-Linear Wave

In Section 5, for convenience, we listed only a sample of the full system<sup>53</sup> of equations that we obtained. Here we list the system of sixteen equations in full. As in Section 5, we have omitted the argument  $\xi$  of the fields for clarity.

$$\begin{aligned}
& \tau \left( -U^0 A^0 \dot{S}^\theta v - S^\theta A^0 \dot{U}^0 v - S^\theta U^0 \dot{A}^0 v - \dot{R}^{0:0} v + U^3 A^0 \dot{S}^\theta + S^\theta A^0 \dot{U}^3 \right. \\
& + S^\theta U^3 \dot{A}^0 + \dot{R}^{3:0} + S^\theta U^0 (A^0)^2 + U^0 R^{0:00} + 2 A^0 R^{0:0} - S^\theta U^0 (A^3)^2 - U^0 R^{\theta:33} \\
& \left. - 2 A^3 R^{0:3} \right) - S^\theta A^0 + \frac{q}{m} E S^\theta U^3 = 0, \tag{319}
\end{aligned}$$

$$\begin{aligned}
& \tau \left( -U^0 A^3 \dot{S}^\theta v - S^\theta A^3 \dot{U}^0 v - S^\theta U^0 \dot{A}^3 v - \dot{R}^{0:3} v + U^3 A^3 \dot{S}^\theta + S^\theta A^3 \dot{U}^3 \right. \\
& + S^\theta U^3 \dot{A}^3 + \dot{R}^{3:3} + S^\theta U^3 (A^0)^2 + U^3 R^{0:00} + 2 A^0 R^{3:0} - S^\theta U^3 (A^3)^2 - U^3 R^{\theta:33} \\
& \left. - 2 A^3 R^{3:3} \right) - S^\theta A^3 + \frac{q}{m} E S^\theta U^0 = 0, \tag{320}
\end{aligned}$$

$$\begin{aligned}
& \tau \left( -R^{\theta:00} \dot{U}^0 v - U^0 \dot{R}^{\theta:00} v - 2 R^{0:0} \dot{A}^0 v - 2 A^0 \dot{R}^{0:0} v + U^3 (A^0)^2 \dot{S}^\theta \right. \\
& + S^\theta (A^0)^2 \dot{U}^3 - U^0 (A^0)^2 \dot{S}^\theta v - S^\theta (A^0)^2 \dot{U}^0 v + 2 S^\theta U^3 A^0 \dot{A}^0 - 2 S^\theta U^0 A^0 (A^3)^2 \\
& + R^{\theta:00} \dot{U}^3 + U^3 \dot{R}^{\theta:00} + 2 R^{3:0} \dot{A}^0 + 2 A^0 \dot{R}^{3:0} - 2 (A^3)^2 R^{0:0} + 6 (A^0)^2 R^{0:0} \\
& - 2 U^0 A^0 R^{\theta:33} - 4 A^0 A^3 R^{0:3} - 2 U^0 A^3 R^{\theta:30} + 2 S^\theta U^0 (A^0)^3 + 6 U^0 A^0 R^{\theta:00} \\
& \left. - 2 S^\theta U^0 A^0 \dot{A}^0 v \right) - 2 S^\theta (A^0)^2 - 2 R^{\theta:00} + 2 \frac{q}{m} E \left( S^\theta U^3 A^0 + R^{3:0} \right) = 0, \tag{321}
\end{aligned}$$

---

<sup>53</sup>Given by (262 - 269).

$$\begin{aligned}
& \tau \left( 2 S^\emptyset U^3 (A^0)^2 A^3 - U^0 \dot{R}^{\emptyset:33} v - 2 R^{0:3} \dot{\Lambda}^3 v - 2 A^3 \dot{R}^{0:3} v + U^3 (A^3)^2 \dot{S}^\emptyset \right. \\
& + S^\emptyset (A^3)^2 \dot{U}^3 - R^{\emptyset:33} \dot{U}^0 v - 6 (A^3)^2 R^{3:3} + 2 (A^0)^2 R^{3:3} - 2 S^\emptyset U^3 (A^3)^3 \\
& - 6 U^3 A^3 R^{\emptyset:33} + 4 A^0 A^3 R^{3:0} + 2 U^3 A^0 R^{\emptyset:30} + 2 U^3 A^3 R^{\emptyset:00} + 2 A^3 \dot{R}^{3:3} + R^{\emptyset:33} \dot{U}^3 \\
& + U^3 \dot{R}^{\emptyset:33} + 2 R^{3:3} \dot{\Lambda}^3 - S^\emptyset (A^3)^2 \dot{U}^0 v + 2 S^\emptyset U^3 A^3 \dot{\Lambda}^3 - U^0 (A^3)^2 \dot{S}^\emptyset v \\
& \left. - 2 S^\emptyset U^0 A^3 \dot{\Lambda}^3 v \right) - 2 S^\emptyset (A^3)^2 - 2 R^{\emptyset:33} + 2 \frac{q}{m} E \left( S^\emptyset U^0 A^3 + R^{0:3} \right) = 0, \quad (322)
\end{aligned}$$

$$\begin{aligned}
& \tau \left( - 2 R^{0:0} \dot{U}^0 v - 2 U^0 \dot{R}^{0:0} v - R^{00:\emptyset} \dot{\Lambda}^0 v - A^0 \dot{R}^{00:\emptyset} v - (U^0)^2 R^{\emptyset:33} \right. \\
& - (A^3)^2 R^{00:\emptyset} - S^\emptyset (U^0)^2 (A^3)^2 - 4 U^0 A^3 R^{0:3} + S^\emptyset (U^0)^2 (A^0)^2 \\
& + 4 U^0 A^0 R^{0:0} + (U^0)^2 R^{\emptyset:00} + (A^0)^2 R^{00:\emptyset} - 2 S^\emptyset U^0 A^0 \dot{U}^0 v - S^\emptyset (A^0)^2 \\
& - R^{\emptyset:00} + U^0 U^3 A^0 \dot{S}^\emptyset + S^\emptyset U^3 A^0 \dot{U}^0 + S^\emptyset U^0 A^0 \dot{U}^3 + S^\emptyset U^0 U^3 \dot{\Lambda}^0 \\
& - (U^0)^2 A^0 \dot{S}^\emptyset v - S^\emptyset (U^0)^2 \dot{\Lambda}^0 v + R^{3:0} \dot{U}^0 + U^0 \dot{R}^{3:0} + R^{0:0} \dot{U}^3 + U^3 \dot{R}^{0:0} \\
& \left. + \frac{1}{2} R^{30:\emptyset} \dot{\Lambda}^0 + \frac{1}{2} A^0 \dot{R}^{30:\emptyset} \right) - S^\emptyset U^0 A^0 - R^{0:0} + \frac{q}{m} E \left( S^\emptyset U^0 U^3 + \frac{1}{2} R^{30:\emptyset} \right) = 0, \quad (323)
\end{aligned}$$

$$\begin{aligned}
& \tau \left( - R^{3:3} \dot{U}^0 v - U^0 \dot{R}^{3:3} v - R^{0:3} \dot{U}^3 v - U^3 \dot{R}^{0:3} v - \frac{1}{2} R^{30:\emptyset} \dot{\Lambda}^3 v \right. \\
& - \frac{1}{2} A^3 \dot{R}^{30:\emptyset} v + (U^3)^2 A^3 \dot{S}^\emptyset + S^\emptyset (U^3)^2 \dot{\Lambda}^3 + 2 S^\emptyset U^3 A^3 \dot{U}^3 + S^\emptyset (U^3)^2 (A^0)^2 \\
& + 4 U^3 A^0 R^{3:0} - S^\emptyset (A^3)^2 - R^{\emptyset:33} + 2 R^{3:3} \dot{U}^3 + 2 U^3 \dot{R}^{3:3} + R^{33:\emptyset} \dot{\Lambda}^3 \\
& + A^3 \dot{R}^{33:\emptyset} - (U^3)^2 R^{\emptyset:33} - (A^3)^2 R^{33:\emptyset} + (U^3)^2 R^{\emptyset:00} + (A^0)^2 R^{33:\emptyset} \\
& - S^\emptyset (U^3)^2 (A^3)^2 - 4 U^3 A^3 R^{3:3} - U^0 U^3 A^3 \dot{S}^\emptyset v - S^\emptyset U^3 A^3 \dot{U}^0 v - S^\emptyset U^0 A^3 \dot{U}^3 v \\
& \left. - S^\emptyset U^0 U^3 \dot{\Lambda}^3 v \right) - S^\emptyset U^3 A^3 - R^{3:3} + \frac{q}{m} E \left( S^\emptyset U^0 U^3 + \frac{1}{2} R^{30:\emptyset} \right) = 0, \quad (324)
\end{aligned}$$

$$\begin{aligned}
& \tau \left( -S^\emptyset U^0 U^3 (A^3)^2 + U^0 U^3 R^{\emptyset:00} + 2U^0 A^0 R^{3:0} + 2U^3 A^0 R^{0:0} \right. \\
& - U^0 U^3 R^{\emptyset:33} - 2U^0 A^3 R^{3:3} - 2U^3 A^3 R^{0:3} - 2R^{0:3} \dot{U}^0 v - 2U^0 \dot{R}^{0:3} v - R^{00:\emptyset} \dot{\lambda}^3 v \\
& - A^3 \dot{R}^{00:\emptyset} v + S^\emptyset U^0 U^3 (A^0)^2 + \frac{1}{2} (A^0)^2 R^{30:\emptyset} - 2S^\emptyset U^0 A^3 \dot{U}^0 v - S^\emptyset A^0 A^3 \\
& - \frac{1}{2} R^{\emptyset:30} - (U^0)^2 A^3 \dot{S}^\emptyset v - S^\emptyset (U^0)^2 \dot{A}^3 v + U^0 U^3 A^3 \dot{S}^\emptyset + S^\emptyset U^3 A^3 \dot{U}^0 \\
& + S^\emptyset U^0 A^3 \dot{U}^3 + S^\emptyset U^0 U^3 \dot{A}^3 + R^{3:3} \dot{U}^0 + U^0 \dot{R}^{3:3} + R^{0:3} \dot{U}^3 + U^3 \dot{R}^{0:3} + \frac{1}{2} R^{30:\emptyset} \dot{\lambda}^3 \\
& \left. + \frac{1}{2} A^3 \dot{R}^{30:\emptyset} - \frac{1}{2} (A^3)^2 R^{30:\emptyset} \right) - S^\emptyset U^0 A^3 - R^{0:3} + \frac{q}{m} E \left( S^\emptyset (U^0)^2 + R^{00:\emptyset} \right) = 0, \quad (325)
\end{aligned}$$

$$\begin{aligned}
& \tau \left( -U^0 U^3 A^0 \dot{S}^\emptyset v - S^\emptyset U^3 A^0 \dot{U}^0 v - S^\emptyset U^0 A^0 \dot{U}^3 v - S^\emptyset U^0 U^3 \dot{A}^0 v - \frac{1}{2} R^{30:\emptyset} \dot{\lambda}^0 v \right. \\
& - S^\emptyset U^0 U^3 (A^3)^2 + U^0 U^3 R^{\emptyset:00} + 2U^0 A^0 R^{3:0} + 2U^3 A^0 R^{0:0} - U^0 U^3 R^{\emptyset:33} - 2U^0 A^3 R^{3:3} \\
& - 2U^3 A^3 R^{0:3} + S^\emptyset U^0 U^3 (A^0)^2 + \frac{1}{2} (A^0)^2 R^{30:\emptyset} - S^\emptyset A^0 A^3 - \frac{1}{2} R^{\emptyset:30} + 2S^\emptyset U^3 A^0 \dot{U}^3 \\
& + (U^3)^2 A^0 \dot{S}^\emptyset + S^\emptyset (U^3)^2 \dot{A}^0 - R^{3:0} \dot{U}^0 v - U^0 \dot{R}^{3:0} v - R^{0:0} \dot{U}^3 v - U^3 \dot{R}^{0:0} v \\
& - \frac{1}{2} A^0 \dot{R}^{30:\emptyset} v + A^0 \dot{R}^{33:\emptyset} + 2U^3 \dot{R}^{3:0} + R^{33:\emptyset} \dot{\lambda}^0 + 2R^{3:0} \dot{U}^3 - \frac{1}{2} (A^3)^2 R^{30:\emptyset} \\
& \left. - S^\emptyset U^3 A^0 - R^{3:0} + \frac{q}{m} E \left( S^\emptyset (U^3)^2 + R^{33:\emptyset} \right) = 0, \quad (326)
\right.
\end{aligned}$$

$$\begin{aligned}
& \tau \left( -S^\emptyset U^3 A^0 (A^3)^2 + \frac{1}{2} R^{\emptyset:30} \dot{U}^3 + \frac{1}{2} U^3 \dot{R}^{\emptyset:30} + R^{3:3} \dot{A}^0 + A^0 \dot{R}^{3:3} + R^{3:0} \dot{\lambda}^3 \right. \\
& + A^3 \dot{R}^{3:0} + S^\emptyset U^0 (A^0)^2 A^3 - (A^3)^2 R^{3:0} + 3U^3 A^0 R^{\emptyset:00} + (A^0)^2 R^{0:3} - \frac{1}{2} R^{\emptyset:30} \dot{U}^0 v \\
& + 3(A^0)^2 R^{3:0} - 3(A^3)^2 R^{0:3} - U^3 A^0 R^{\emptyset:33} - 2A^0 A^3 R^{3:3} - U^3 A^3 R^{\emptyset:30} + S^\emptyset U^3 (A^0)^3 \\
& - R^{0:3} \dot{A}^0 v - A^0 \dot{R}^{0:3} v - R^{0:0} \dot{A}^3 v - A^3 \dot{R}^{0:0} v - S^\emptyset U^0 (A^3)^3 - 3U^0 A^3 R^{\emptyset:33} + U^0 A^3 R^{\emptyset:00} \\
& + 2A^0 A^3 R^{0:0} + U^0 A^0 R^{\emptyset:30} + U^3 A^0 A^3 \dot{S}^\emptyset + S^\emptyset A^0 A^3 \dot{U}^3 + S^\emptyset U^3 A^3 \dot{A}^0 + S^\emptyset U^3 A^0 \dot{\lambda}^3 \\
& - S^\emptyset U^0 A^0 \dot{A}^3 v - U^0 A^0 A^3 \dot{S}^\emptyset v - S^\emptyset A^0 A^3 \dot{U}^0 v - S^\emptyset U^0 A^3 \dot{A}^0 v - \frac{1}{2} U^0 \dot{R}^{\emptyset:30} v \\
& \left. - 2S^\emptyset A^0 A^3 - R^{\emptyset:30} + \frac{q}{m} E \left( S^\emptyset U^3 A^3 + R^{3:3} + S^\emptyset U^0 A^0 + R^{0:0} \right) = 0, \quad (327)
\right.
\end{aligned}$$

$$\begin{aligned}
& - (U^0)^2 \dot{S}^\emptyset v - 2 S^\emptyset U^0 \dot{U}^0 v - \dot{R}^{00:\emptyset} v + U^0 U^3 \dot{S}^\emptyset \\
& + S^\emptyset U^3 \dot{U}^0 + S^\emptyset U^0 \dot{U}^3 + \frac{1}{2} \dot{R}^{30:\emptyset} - S^\emptyset A^0 = 0,
\end{aligned} \tag{328}$$

$$\begin{aligned}
& -U^0 U^3 \dot{S}^\emptyset v - S^\emptyset U^3 \dot{U}^0 v - S^\emptyset U^0 \dot{U}^3 v - \frac{1}{2} \dot{R}^{30:\emptyset} v + (U^3)^2 \dot{S}^\emptyset \\
& + 2 S^\emptyset U^3 \dot{U}^3 + \dot{R}^{33:\emptyset} - S^\emptyset A^3 = 0,
\end{aligned} \tag{329}$$

$$\begin{aligned}
& - (U^0)^3 \dot{S}^\emptyset v - 3 S^\emptyset (U^0)^2 \dot{U}^0 v - 3 R^{00:\emptyset} \dot{U}^0 v - 3 U^0 \dot{R}^{00:\emptyset} v \\
& + (U^0)^2 U^3 \dot{S}^\emptyset + 2 S^\emptyset U^0 U^3 \dot{U}^0 + S^\emptyset (U^0)^2 \dot{U}^3 + R^{30:\emptyset} \dot{U}^0 + U^0 \dot{R}^{30:\emptyset} \\
& + R^{00:\emptyset} \dot{U}^3 + U^3 \dot{R}^{00:\emptyset} - 2 S^\emptyset U^0 A^0 - 2 R^{0:0} = 0,
\end{aligned} \tag{330}$$

$$\begin{aligned}
& -U^0 (U^3)^2 \dot{S}^\emptyset v - S^\emptyset (U^3)^2 \dot{U}^0 v - 2 S^\emptyset U^0 U^3 \dot{U}^3 v - R^{33:\emptyset} \dot{U}^0 v \\
& -U^0 \dot{R}^{33:\emptyset} v - R^{30:\emptyset} \dot{U}^3 v - U^3 \dot{R}^{30:\emptyset} v + (U^3)^3 \dot{S}^\emptyset + 3 S^\emptyset (U^3)^2 \dot{U}^3 \\
& + 3 R^{33:\emptyset} \dot{U}^3 + 3 U^3 \dot{R}^{33:\emptyset} - 2 S^\emptyset U^3 A^3 - 2 R^{3:3} = 0,
\end{aligned} \tag{331}$$

$$\begin{aligned}
& - (U^0)^2 U^3 \dot{S}^\emptyset v - 2 S^\emptyset U^0 U^3 \dot{U}^0 v - S^\emptyset (U^0)^2 \dot{U}^3 v - R^{30:\emptyset} \dot{U}^0 v - U^0 \dot{R}^{30:\emptyset} v \\
& - R^{00:\emptyset} \dot{U}^3 v - U^3 \dot{R}^{00:\emptyset} v + U^0 (U^3)^2 \dot{S}^\emptyset + S^\emptyset (U^3)^2 \dot{U}^0 + 2 S^\emptyset U^0 U^3 \dot{U}^3 \\
& + R^{33:\emptyset} \dot{U}^0 + U^0 \dot{R}^{33:\emptyset} + R^{30:\emptyset} \dot{U}^3 + U^3 \dot{R}^{30:\emptyset} - S^\emptyset U^0 A^3 - R^{0:3} \\
& - S^\emptyset U^3 A^0 - R^{3:0} = 0,
\end{aligned} \tag{332}$$

$$-\dot{E} + q S^\emptyset U^0 - q n_{\text{ion}} = 0, \tag{333}$$

$$-\dot{E} v + q S^\emptyset U^3 = 0. \tag{334}$$

## References

- [1] D. Burton, A. Carr, J. Gratus, A. Noble, “The radiative self-force and charged fluids”. Proc. SPIE 8779 1Y (2013).
- [2] P. J. Nahin, “Oliver Heaviside: The life, work, and times of an electrical genius of the Victorian age”, Johns Hopkins University Press, ISBN 0801869099.
- [3] D. J. Griffiths “Introduction to Electrodynamics”, Pearson, ISBN 0139199608.
- [4] A. Einstein “Die Grundlage der allgemeinen Relativittstheorie” (1916). Reprinted in ADP (2005) Vol. 14(S1), pp. 517-571.
- [5] J. C. Maxwell “A Dynamical Theory of the Electromagnetic Field” Proc. Roy. Soc. Lon. (1863-1864), Vol. 13, pp. 531-536.
- [6] J. D. Jackson, “Classical Electrodynamics”, 3rd Ed, John Wiley & Sons Inc. ISBN 8126510943.
- [7] M. Spivak “A Comprehensive Introduction to Differential Geometry Vol.1 ”, Publish or Perish, ISBN 0914098843.
- [8] J. Larmor, Proc. 5th Int. Congress of Mathematics 1, p 197 (1913). Reprinted; J. H. Poynting, “Poyntings Collected Scientific Papers” Cambridge University Press (1920), p. 426.
- [9] M. Abraham, Ann. Phys. 10, pp 105-179.
- [10] P. I. M. Dirac, “Classical Theory of radiating electrons”, Proc. Roy. Soc. of Lon. A, Mathematical and Physical Sciences, Vol. 167(929) (1938), pp.148-169.
- [11] T. Fulton, F. Rohrlich “Classical radiation from a uniformly accelerated charge”, Annals of Phys. Vol. 9(4), pp. 499-517.
- [12] D. Sciama, P. Candelas “Is there a quantum equivalence principle”. Phys. Rev. D, 1983, Vol.27(8), pp. 1715-1721.

- [13] G. Plass, “Classical Electrodynamics Equations of Motion with Radiative Reaction” *Rev. Mod. Phys.* Vol. 33(1) (1961), pp. 37-62.
- [14] C. J. Eliezer, “On the Classical theory of particles”, *Proc. R. Soc. Lon. A*, Vol. 194(1039), pp. 543-555.
- [15] G. W. Ford, R. F. O’Connell, “Radiation reaction in electrodynamics and the elimination of runaway solutions”, *Phys. Lett. A*, Vol. 157(4-5) (1991), pp. 217-220.
- [16] G. W. Ford, R. F. O’Connell, “Relativistic form of radiation reaction”, *Phys. Lett. A*, Vol. 174(3) (1993), pp. 182-184.
- [17] R. F. O’Connell, “Radiation Reaction: General approach and applications, especially to electrodynamics”, *Contemp. Phys.* 53(4) (2012), pp. 301-313.
- [18] T. C. Mo and C. H. Papas, “New equation of motion for classical charged particles”, *Phys. Rev. D*, Vol. 4(12) (1971), pp. 3566-3571.
- [19] W. B. Bonnor, “A new equation of motion for a radiating charged particle”, *Proc. R. Soc. Lond. A*, Vol. 337(1611) (1974), pp. 591-598.
- [20] I. V. Sokolov, “Renormalization of the Lorentz-Abraham-Dirac equation for radiation reaction force in classical electrodynamics”, *J. Exp. Theor. Phys.* Vol. 109(2) (2009), pp.207-212.
- [21] D. A. Burton, A Noble, “Aspects of electromagnetic radiation reaction in strong fields”, *Contemp. Phys*, 55(2) (2014), pp. 110-121.
- [22] L. D. Landau and E.M. Lifshitz, “The Classical Theory of Fields”, 4th Ed. Butterworth-Heinemann (1980), ISBN 0080250726.
- [23] H. Spohn “The Critical Manifold of the Lorentz-Dirac Equation”, *EPL*, Vol. 50(3) (200), pp. 287-292.
- [24] A. Piazza, “Exact Solution of the Landau-Lifshitz Equation in a plane wave”. *Lett. Math. Phys.* Vol. 83(3) (2008), pp. 305 - 313.

- [25] C. Harvey, T. Heinzl, M. Marklund, “Symmetry breaking from radiation reaction in ultra-intense laser fields”, *Phys. Rev. D* Vol. 84(116005) (2011).
- [26] A. Noble, D.A. Burton, J. Gratus and D.A. Jaroszynski, “A kinetic model of radiating electrons”, *J. Math. Phys.* Vol. 54(043101) (2013).
- [27] J. Puerta, P. Martin, “Plasma Physics: Proceedings of the 1997 Latin American Workshop”, Springer (2012), ISBN 0792355274.
- [28] M. Wakatani, K. Nishikawa, “Plasma Physics: Basic Theory with Fusion Applications”, Springer (2010), ISBN 978-3642084652.
- [29] W. Baumjohann, R. Treumann, “Basic Space Plasma Physics”, Imperial College Press (1996), ISBN 1860940798.
- [30] V. I. Berezhiani, R. D. Hazeltine, S. M. Mahajan, “Radiation reaction and relativistic hydrodynamics”, *Phys. Rev. E*, Vol. 69(5) (2004), pp. 056406.
- [31] P. Madau, C. Thompson. “Relativistic Winds from Compact Gamma-ray Sources: Radiative Acceleration in the Klein-Nishina Regime” *The Astrophysical Journal*, Vol. 534(1) (2000), pp.239-247.
- [32] F. F. Chen, “Introduction to Plasma Physics and Controlled Fusion”, Springer (2006), ISBN 0306413329.
- [33] T. Tajima, J. M. Dawson, “Laser electron accelerator”, *Phys. Rev. Lett.* Vol. 43(4) (1979), pp. 267-270.
- [34] <http://lhc-machine-outreach.web.cern.ch/lhc-machine-outreach/lhc-machine-outreach-faq.htm>
- [35] R Assmann et al “Proton-driven plasma wakefield acceleration: a path to the future of high-energy particle physics” *Plas. Phys. Con. Fus.* Vol 56(8) (2014), pp. 084013.

- [36] E. Esarey, P. Sprangle, J. Krall, A. Ting “Overview of plasma based accelerator concepts”, IEEE Transactions on Plasma Science, Vol.24(2) (1996), pp.252-288.
- [37] A. Modena, Z. Najmudin et. al. “Electron acceleration from the breaking of relativistic plasma waves”, Nature, 1995, Vol.377(6550), p. 606.
- [38] L. Lyu, “Elementary Space Plasma Physics”, Airiti Press (2010), ISBN 9868270954.
- [39] Y. L. Klimontovich “The Kinetic Theory of Electromagnetic Processes”, Springer, ISBN 3642818242
- [40] R. Fitzpatrick, “Plasma Physics: An Introduction”, CRC Press (2014), ISBN 1466594265.
- [41] R. C. Davidson , “Physics of Intense Charged Particle Beams in High Energy Accelerators”, Imperial College Press (2002), ISBN 1860943012.
- [42] T. O’Neil, F. Coroniti, “The collisionless nature of high temperature plasmas”, Rev. Mod. Phys. Vol. 71(2) (1999), pp. S404-S410.
- [43] A. Noble, J. Gratus, D. Burton *et al.*, “Kinetic treatment of radiation reaction effects”, Proc. SPIE 8079 0L (2011).
- [44] P. Amendt, “Plasma wave equations of state”, Phys. Fluids, Vol. 29(5) (1986), pp. 1458.
- [45] H. Weitzner, “Relativistic fluid dynamics”, Lecture Notes in Mathematics, Vol. 1385(4) (1989).
- [46] M. Atiyah, “Introduction to Commutative Algebra”, Westview Press (1994), ISBN 0201407515.
- [47] P.C. Clemmow and A.J. Willson, “The Dispersion Equation in Plasma Oscillations”, Proc. R. Soc. Lon. A, Vol. 237(1208) (1956).
- [48] R. Burman, “Effect of radiation reaction on plasma waves”, Phys. Lett A, Vol. 30(7) (1969), pp. 431.
- [49] Obtained from the official website of the National High Magnetic Field Laboratory; <https://nationalmaglab.org/user-facilities/dc-field/instruments-dcfield/resistive-magnets/138>

- [50] S. P. D. Mangles et al. “Monoenergetic beams of relativistic electrons from intense laser-plasma interactions”, *Nature*, 2004, Vol. 431(7008), p.535
- [51] P. Haensel, A. Y. Potekhin, D. G. Yakovlev. “Neutron Stars 1: Equation of State and Structure”, Springer (2007 ed), ISBN 0387335439.
- [52] S. L. Shapiro, S. A. Teuolsky. “Black Holes, White Dwarfs, and Neutron Stars: The Physics of Compact Objects”, Wiley, ISBN 0471873167.
- [53] N. Chamel. “Physics of Neutron Star Crusts”, *Liv. Rev. Relativity*, 11, (2008), 10.
- [54] D. Blaschke, N. K. Glendenning, A. Sedrakian “Physics of Neutron Star Interiors (Lecture Notes in Physics)”, Springer, ISBN 3642076145.
- [55] D. A Diver, A. A. da Costa, E. W. Laing, C. R. Stark, L. F. A. Teodoro, “On the Surface Extraction of Electrons in a Pulsar”, *Mon. Not. R. Astron. Soc.* Vol. 401, pp 613-620 (2010).